Functional characterisation of VAV-interacting Krüppel-like factor (VIK) in breast cancer

Catherine Lenihan

A thesis submitted in partial fulfilment of the requirements for the degree of Doctor of Philosophy

July 2016

Statement of originality

I, Catherine Lenihan, confirm that the research included within this thesis is my own work or that where it has been carried out in collaboration with, or supported by others, that this is duly acknowledged below and my contribution indicated. Previously published material is also acknowledged below.

I attest that I have exercised reasonable care to ensure that the work is original, and does not to the best of my knowledge break any UK law, infringe any third party's copyright or other Intellectual Property Right, or contain any confidential material.

I accept that the College has the right to use plagiarism detection software to check the electronic version of the thesis.

I confirm that this thesis has not been previously submitted for the award of a degree by this or any other university.

Signature: Catherine Lenihan

Date: 22.07.16

Abstract

Background. VAV interacting Krüppel-like factor (VIK) is a novel transcription factor. Previously our lab reported a series of breast cancer tumour samples where VIK methylation was associated with an increased risk of recurrence in tamoxifen-treated patients, indicating a role for VIK in ER positive breast cancer and endocrine resistance. Additionally VIK has been shown to be involved in cell cycle regulation, interacting with CDK4 and VAV1. The cyclin D-CDK4/6-Rb pathway is frequently dysregulated in ER positive breast cancer. Combined treatment of palbociclib, a highly selective CDK4/6 inhibitor, with endocrine therapy substantially improved outcome of patients with ER positive metastatic breast cancer. Increasing clinical use means acquired resistance to palbociclib is emerging as a major clinical challenge.

Results. VIK was confirmed to be subject to regulation by DNA methylation in breast cancer. VIK methylation correlated to transcriptional silencing of mRNA in both cancer cell lines and primary tumours. To determine the functional significance of loss of VIK expression, VIK was knocked down in unmethylated breast cancer cell lines and a normal breast epithelial cell line. Knockdown resulted in cell death via induction of apoptosis. VIK knockdown altered cell cycle progression from G1 to S phase. Expression of multiple regulatory cell cycle proteins was altered, differentially in normal and tumour cells. Treatment with the CDK4/6 inhibitor, palbociclib, in cells with reduced VIK expression resulted in decreased sensitivity to the drug, inducing a shift in IC50 value towards resistance. In a model of acquired resistance, T47D cells were cultured long-term with palbociclib generating resistant clones. VIK was significantly downregulated in all resistant clones to barely detectable mRNA levels, suggesting a role for VIK in resistance to CDK4/6 inhibition.

Conclusion. This PhD has confirmed VIK is a novel epigenetically regulated gene in breast cancer. VIK expression is essential to both normal and tumour breast cell survival and is involved in the regulation of the G1/S phase transition in the cell cycle. Loss of VIK expression potentially contributes to the development of acquired resistance to CDK4/6 inhibitors.

Acknowledgements

I would first like to acknowledge Breast Cancer Campaign for providing the funding for this research.

I would like to thank Prof. Peter Schmid, for giving me the opportunity to work in his lab and for his supervision throughout this PhD. Thank you to all members of the Schmid lab, from both the Sussex years and the BCI years, for all of their help and advice. In particular to Alice Shia, for all of your guidance and direction.

Of course I must mention everyone in the office, who made every day enjoyable. Thank you to all of you: Katy for always being there, especially for all the support and also quite literally, meaning those late nights/weekends/18 hour days were not lonely! Alex for the lab hugs and unique encouragement, Juliette for being awesome, Joe for making me laugh no matter how horribly wrong I felt things were going, Ketan for often reminding me there is a life outside of the lab and Hannah for all the positivity. Thank you also to Hefin for help and advice on statistics.

And to my friends and family, I cannot thank you all enough for all your patience and encouragement. Especially my mum and my sister, who deserve their own PhD for their unending love, support and just generally putting up with me though the many highs and lows of these PhD years.

Finally, this thesis is dedicated to my Dad, the reason I am interested in science in the first place.

Table of Contents

List of Figures

List of tables

List of Abbreviations

A	Adenosine
AF	Activation Function
ANOVA	Analysis of variance
AP1	Activator Protein 1
AZA	5-aza-deoxycytidine
BAD	Bcl-2-associated death promoter
BAK	Bcl-2 homologous antagonist killer
BAX	Bcl-2-Associated X Protein
BCA	Bicinchoninic acid
BCL-2	B-cell lymphoma 2
BCL-X	Bcl-2 like
BCP	1-Bromo-3-chloropropane
BH3	Bcl-2 homology 3
BIK	Bcl-2cinteracting killer
BSA	Bovine serum albumin
C	Cytosine
CDK	Cyclin Dependent Kinase
CH	Calponin homology domain
ChIP-seq	Chromatin Immunoprecipitation sequencing
Cip	CDK interacting protein
cmv	Cytomegalovirus
CO_2	Carbon dioxide
CoA	Co-activator
cqn	conditional quantile normalisation
C_T	Cycle threshold
Ct	Control
DAPI	4',6-Diamidino-2-Phenylindole
DBD	DNA-binding domain
DCIS	Ductal Carcinoma In Situ

DH	Dbl-homology
DMEM	Dulbecco's Modified Eagle Medium
DMSO	Dimethyl sulfoxide
DNA	Deoxyribonucleic acid
DNMT	DNA methyl transferase
DSS	Double Stripped Serum
E1	Estrone
E2	Estradiol
E2F	E2F Transcription Factor
E3	Estriol
EGF	Endothelial Growth Factor
EGFP	Enhanced Green Fluorescent protein
EMT	Epithelial-Mesenchymal Transition
ER	Estrogen receptor
ERE	Endocrine Response element
ERK	Extracellular signal regulated kinase
FBS	Fetal Bovine Serum
FFPE	Formalin Fixed Paraffin Embedded
FISH	Fluorescence in situ hybridisation
FOX	Forkhead box
FOXP1	Forkhead box protein P1
G	Guanine
G0	Gap 0 phase
G1	Gap 1 phase
G2	Gap 2 phase
GDP	Guanosine diphosphate
GEF	Guanine Nucleotide exchange factor
GFP	Green Fluorescent protein
GTP	Guanosine triphosphate
HAT	Histone acetyltransferase
HCL	Hydrochloric Acid
HDAC	Histone Deacetylase

HEK	Human Embryonic Kidney
HER2	Human Epidermal Growth Factor Receptor-2
IC_{50}	50% Inhibitory Concentration
IGF-1	Insulin Growth Factor-1
IGFR	Insulin-like growth factor receptor
IgG	Immunoglobulin G
INK	Inhibitor of CDK
IP	immunoprecipitation
kDa	Kilodalton
Kip	Kinase inhibitory protein
KLD	Kinase, ligase, dpnI
KLF	Krüppel-like Factor
KRAB	Krüppel-associated box
LDH	Lactate Dehydrogenase
LIMMA	Linear models for microarray data
MAPK	Mitogen-activated protein kinase
MCS	Multiple cloning site
mM	millimolar
µM	micromolar
miRNA	microRNA
mRNA	Messenger RNA
MSP	Methylation specific PCR
mTOR	Mammalian target of rapamycin
MTT	3-(4,5-Dimethylthiazol-2-yl)-2,5-Diphenyltetrazolium Bromide
NaCl	Sodium Chloride
ncRNA	Non-coding RNA
NLS	Nuclear Localisation signal
nM	nanomolar
NTC	No-Template Control
O/N	Overnight
OD	Optical Density
P/S	Penicillin-Streptomycin

PAGE	Poly-Acrylamide Gel Electrophoresis
PARP	Poly (ADP-ribose) polymerase
PBS	Phosphate Buffered Saline
PBS-T	Phosphate Buffered Saline-Tween
PCR	Polymerase Chain Reaction
PDVF	Polyvinylidene fluoride
PFA	Paraformaldehyde
PH	Pleckstrin-homology
PI3K	Phosphatidylinositol-4,5-bisphosphate 3-kinase
PR	Progesterone Receptor
pRb	Phosphorylated Rb
Pro	Proline-rich
PS	Phosphatidyl serine
q-RT-PCR	Quantitative real time PCR
R	Restriction point
Rb	retinoblastoma protein
RIPA	Radioimmunoprecipitation assay buffer
RNA	Ribonucleic acid
RNAseq	RNA sequencing
RPLPO	Large Ribosomal Protein
rpm	Revolutions per minute
RPKM	Reads per kilobase per million mapped reads
RPMI	Roswell Park Memorial Institute
RSEM	RNA-seq by expectation maximisation
RT	Room Temperature
RTK	Receptor Tyrosine Kinase
S phase	Synthesis phase
SD	Standard Deviation
SDS	Sodium Dodecyl Sulphate
SERM	selective estrogen receptor modulator
SFIH	serum-free medium plus insulin and hydrocortisone
SH	Src homology

shRNA	Short hairpin RNA
siRNA	Small interfering RNA
SP1	Specificity protein 1
STAT	Signal transducer and activator of transcription
T	Thymidine
TAIP	TTV apoptosis inducing protein
TBE	Tris/Borate/EDTA
TBS-T	Tris-Buffered Saline- Tween
TCGA	The Cancer Genome Atlas
TCR	T-cell receptor
TDLU	terminal duct lobular unit
TEMED	Tetramethylethylenediamine
TF	Transcription Factor
TGF	Transforming growth factor
TSA	Trichostatin A
UTR	Untranslated Region
VEGF	Vascular Endothelial Growth Factor
VIK	Vav-interacting Krüppel-like
VO	Vector only
ZNF	Zinc finger
piRNA	Piwi-interacting RNA
RISC	RNA induced silencing Complex

1. Introduction

1.1 Breast Cancer

Breast cancer is a leading cause of death by cancer in women of the Western world. Breast cancer has a yearly incidence of over 1.3 million, this accounts for 23% of all malignancies (3). In the UK alone, every year nearly 55,000 people are diagnosed with breast cancer. Women have a 1 in 8 chance of being diagnosed with breast cancer in their lifetime, and nearly 12,000 people die of breast cancer each year (4).

As with the majority of cancers, breast cancer is a complex disease and presents a multifactorial aetiology. There are a wide range of risk factors from age, lifestyle, and diet to family history and genetic and epigenetic alterations in the genome. The nature of the cancer significantly influences prognosis and risk of recurrence (5).

1.1.1 Breast Cancer development

The normal breast is made up of a system of branched epithelial tubes, called ducts, which connect the lobules to the nipple where milk is secreted (Figure 1.1A). The lobules contain secretory units called acini. The lobules and the distal end of the duct form the terminal duct lobular unit (TDLU). The ducts of the breast are lined by a single layer of epithelial cells, surrounded by a layer of myoepithelial cells or basal cells, which are encircled by a basement membrane made up of laminin and collagen. This whole structure is surrounded by connective tissue and embedded into adipose tissue (6).

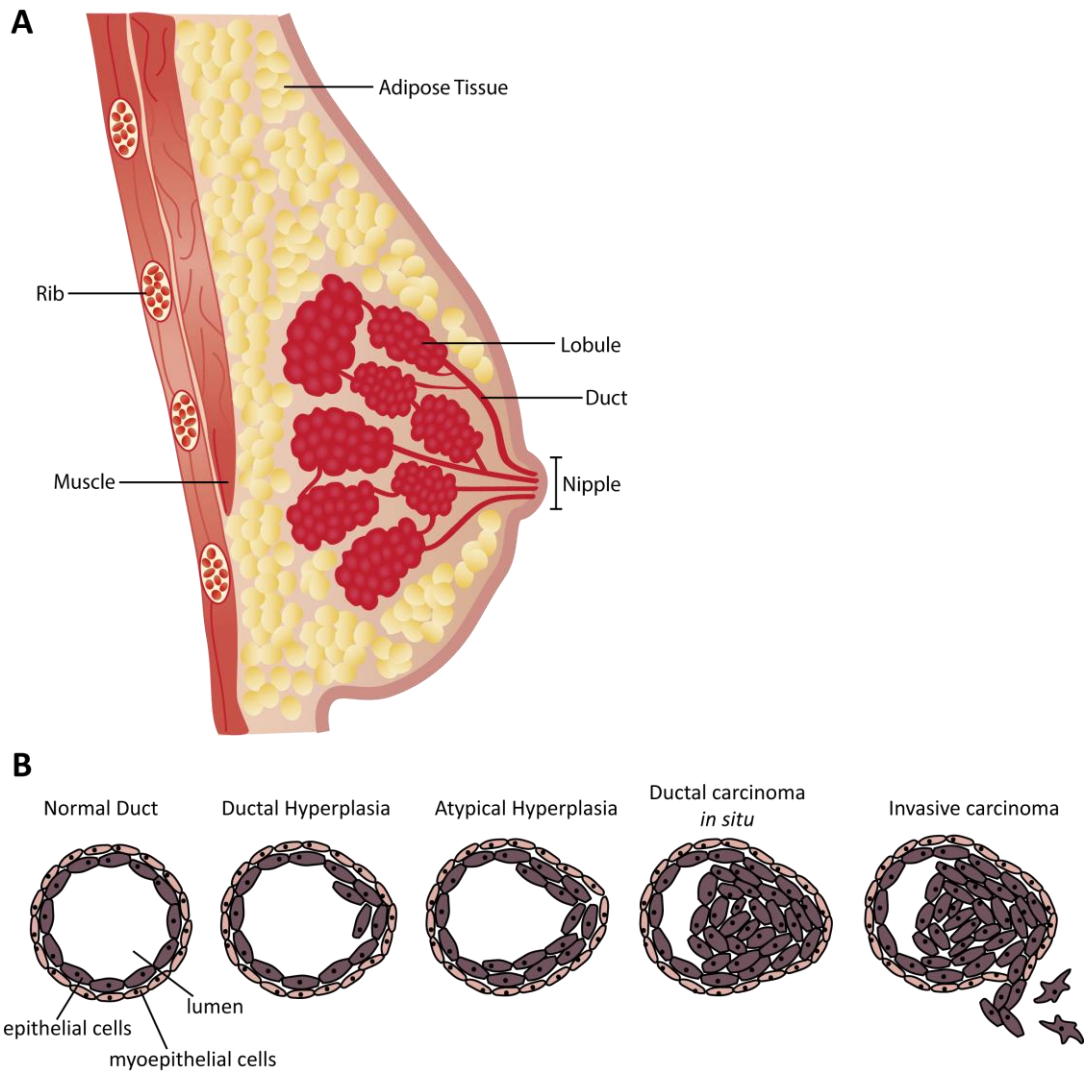

Figure 1.1. Anatomy of the human breast and breast cancer development. A) Each mammary gland contains 15-20 lobes, which contain a series of branched ducts that drain into the nipple. B) The normal duct consists of a layer of epithelial cells surrounded by myoepithelial cells. Ductal carcinoma starts as a benign epithelial lesion defined by an abnormal structure of the duct, which develops into atypical hyperplasia with an additional layer within the lumen. The hyperplasia proliferates into *in situ* carcinoma, which develops into invasive carcinoma.

Breast carcinoma arises from the mammary epithelium and most commonly the epithelial cells of the TDLU (Figure 1.1B). Breast cancer development is thought to begin with a benign epithelial lesion characterised by abnormal structure of the breast duct or lobule. This evolves into atypical hyperplasia where an extra cell layer grows within the lumen. These cells grow and proliferate into an early stage in situ carcinoma. This develops into invasive breast cancer, with cells reaching towards the nearest blood vessels and then lymph vessels to cause metastatic spread (7, 8).

1.1.2 Breast Cancer Classification

Breast cancer diagnosis is based on clinical examination of the breast and lymph nodes, followed by a mammogram and a core biopsy or fine-needle aspiration. Breast cancer is widely considered as a highly heterogeneous disease. Different types of breast carcinoma vary in histopathological and biological features, different clinical outcome and response to therapies. Therefore, clinically, breast cancer cannot be treated as one single disease and is instead classified into more homogenous subgroups. A variety of clinical and pathological factors are routinely used to categorise breast cancer to assess prognosis and guide treatment strategy. These include patient age, tumour size, histological features and lymphovascular migration (9).

Breast cancer can be broadly divided into *in situ* carcinoma and invasive carcinoma. *In situ* carcinoma is a benign disease, characterised by localised uncontrolled proliferation of cells into the lumen of the ducts or lobules, but with no invasion into the surrounding breast tissue. *In situ* carcinoma is further sub-classified as either Ductal Carcinoma *in situ* (DCIS) or lobular carcinoma *in situ*, based on the cells of origin within the TDLU (10). Ductal carcinoma is considerably more common than lobular carcinoma, accounting for 80% and

15% of *in situ* carcinomas respectively (11). DCIS are classified into histological grades based on degree of cell differentiation. Grade 1 (low) is characterised by small, undifferentiated cells with small nuclei and absence of necrosis. Grade 3 (high) comprised highly atypical and differentiated cells with multiple nuclei and a high proliferative rate and presence of necrosis. Grade 2 represents an intermediate group (12). Ductal carcinoma in itself is not life threatening, but is often seen as a precursor to invasive carcinoma (13, 14).

Invasive breast carcinoma describes a group of heterogeneous malignant cancers, which have invaded into the surrounding breast tissue and have the potential to metastasise. Histological classification is not sufficient to fully describe the heterogeneity of invasive breast cancers, however advances in molecular understanding along with gene expression profiling has helped refine breast cancer classification. Such classification is especially relevant when considering the treatment for invasive and metastatic breast cancers. Molecular biomarkers have been utilised to determine breast cancer subtypes. The predominant markers are the hormone receptors, estrogen receptor (ER) and progesterone receptor (PR) and the human epidermal growth factor receptor 2 (HER2/neu) (15). During histological examination, samples are routinely evaluated for presence of these markers by immunohistochemistry and/or fluorescence in situ hybridisation (FISH). Based on the presence or absence of these markers, breast cancer can be divided into three main groups: Triple Negative, negative for all three markers, hormone receptor positive, expressing ER and/or PR and HER-2 enriched, where HER2 is amplified (16). Further to this, gene expression profiling and many studies evaluating patterns of gene expression support 4 main intrinsic breast cancer subtypes that have prognostic relevance; luminal A, luminal B, HER2+ and basal-like (17-19).

The luminal subtypes share expression of the estrogen receptor and/or progesterone receptor and have better overall survival than the HER2 and basal-like subtypes. Luminal A breast cancers, account for approximately 40% of breast cancers, are characterised by high estrogen receptor signalling and under-expression of HER2. These cancers tend to be associated with a more favourable prognosis (20). Luminal B, corresponding to approximately 20% of cases, tends to have lower ER regulation, a higher proliferation rate and correlates with a worse prognosis and higher tendency to relapse (21, 22). HER2+ represents 20-30% of all diagnosed breast cancers, and exhibit over expression of HER2, with under-expression of luminal-associated genes (23). Basal-like tumours account for up to 15% of all breast cancers. These tumours primarily exhibit no expression of ER, PR or HER2, but are a highly heterogeneous sub-group of breast cancers (24, 25) and have been sub divided in up to 6 separate subtypes (26). The highly diverse nature of breast cancer, and increasing understanding of molecular markers and genetic profiling, means subtyping and classification is subject to changes and adjustments all of the time.

1.1.3 Estrogen receptor positive breast cancer

Estrogen is essential to normal female physiology, reproduction and behaviour. Sustained exposure to endogenous or exogenous estrogen is a well-established cause of breast cancer (27, 28).

ER expressing breast cancers represent the majority of breast cancers, approximately 60-70% of all breast cancers (29). Estrogen plays a key role in the initiation and progression of these carcinomas. The action of estrogen is mediated by two estrogen receptors, ER-α and ER-β. The two receptors are encoded by separate genes located on different chromosomes. ESR1, encoding ER-α, and ESR2, encoding ER-β, are located on chromosome

6 and chromosome 14 respectively (30, 31). They have an overall similar structure, consisting of a central DNA-binding domain, flanked by two transcriptional activation domains. An N-terminal AF1 domain and a C-terminal ligand binding region containing an AF2 domain. This AF2 domain also mediates interactions with co-activators that increase ER transcriptional activity (32, 33).

ER are members of the nuclear hormone receptor family and function as ligand-dependent transcription factors (34). ER signalling regulates a diverse range of cellular functions including proliferation, apoptosis, invasion and angiogenesis. ER-α is responsible for many of the actions of estrogen on both normal and cancerous tissue, through ligand activated transcriptional regulation (genomic actions) and by acting as a component of membrane and cytoplasmic signalling cascades (non-genomic actions) (35). The ER is activated by estrogen, which exists in three forms estrone (E1), estradiol (E2) and estriol (E3). E2 is the most potent ER activating ligand (36). ERα comprises an N-terminal AF1 domain, a DNA binding domain, and a C-terminal ligand binding region that contains an AF2 domain (37).

The classical mechanism of ER action is via its genomic actions. This involves binding of estrogen, upon which the receptor dimerises and translocates to the nucleus, binds to endocrine response elements in the regulatory region of the target genes and stimulates gene transcription. Emerging evidence indicates ER signalling is complex, and includes multiple co-regulatory proteins, and involves a number of pathways beyond the classical genomic signalling (38) (Figure 1.2).

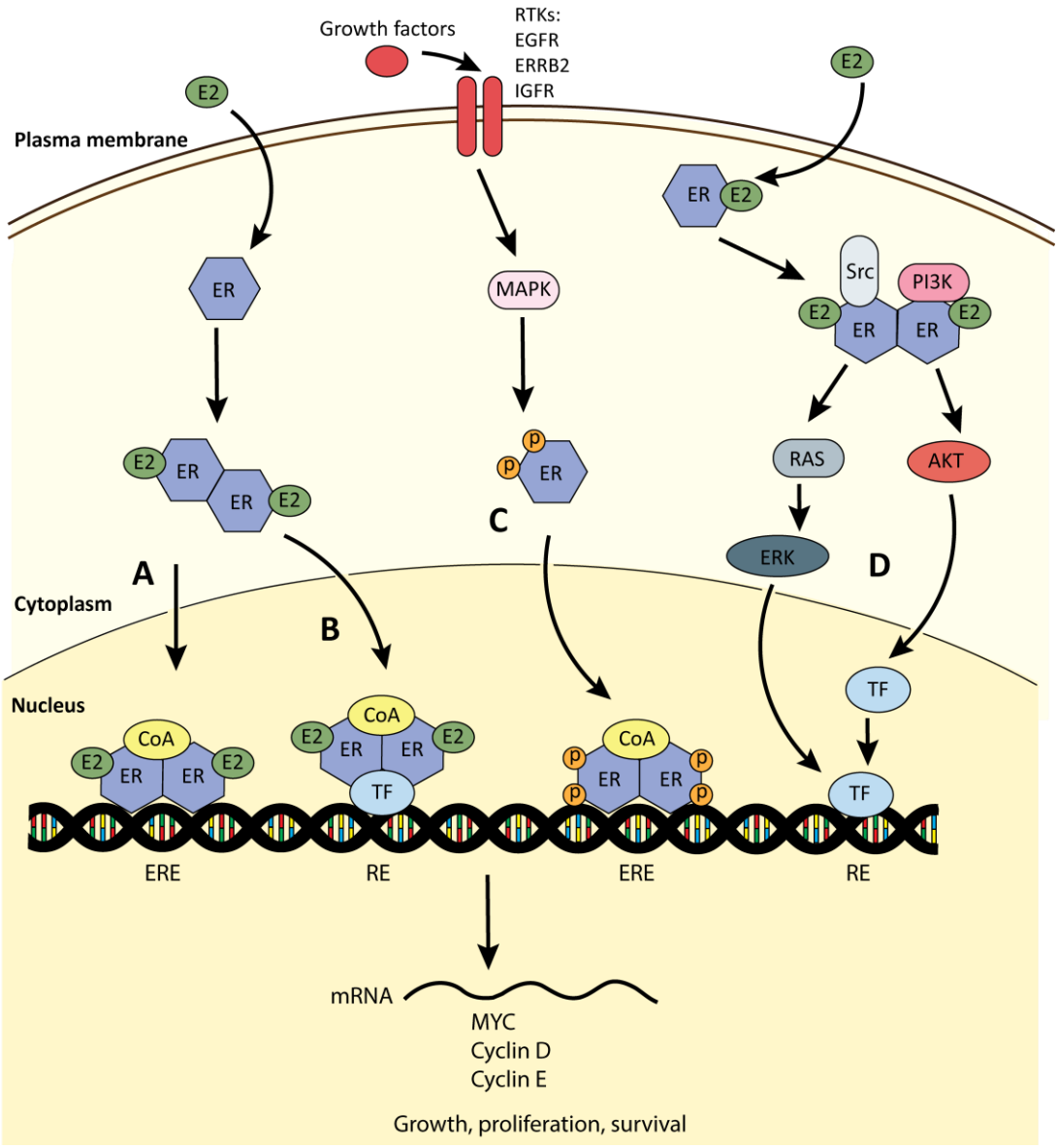

Figure 1.2 Estrogen Receptor signalling pathways. Four different signalling pathways have been recognised in which ER leads to cell proliferation and survival (38). Pathway A is the classical genomic pathway. When estradiol binds, ER dimerises and relocates to the nucleus where it binds to EREs and recruits co-activators that will activate transcription of target genes. Pathway B is the non-classical genomic pathway, involving interaction of ER with other transcription factors such as AP-1. Pathway C is estradiol independent, whereby growth factors activate ER via phosphorylation. Pathway D is a non-genomic pathway involving estrogen receptors that are located close to the cell membrane. ER activates Akt, MAPK signalling via recruitment of kinases such as Src and PI3K. (ER: Estrogen Receptor. ERE: Estrogen Response Element. RE: Response Element. TF: Transcription Factor. p: phosphorylation site. RTK: Receptor Tyrosine Kinase. E2: Estradiol. CoA: Co-activator)

1.1.3.1 Hormone therapies for treatment of ER positive breast cancer

In the first instance breast cancer is normally treated by surgery to remove the tumour. Adjuvant therapies such as radiation or endocrine therapy may be considered before surgery to reduce the tumour mass for operation and/or after surgery to reduce risk of recurrence and metastasis.

Interfering with the action of estrogen is been the mainstay of treatment for ER+ breast cancer and the treatment methods most commonly used in the clinic for ER positive cancers are hormone therapies. Current endocrine strategies either target the ER itself, with selective estrogen receptor modulators (SERMS), or suppress the amount of available estrogen. This would be via gonadal suppression in premenopausal women e.g. luteinising hormone releasing agonists, or with aromatase inhibitors in postmenopausal women.

SERMS such as tamoxifen and fulvestrant, bind to ER, inhibiting estrogen from binding and initiating oncogene expression and cellular proliferation. Tamoxifen is the most established SERM, and has significant effect on breast cancer proliferation. Adjuvant therapy with tamoxifen almost halves the rate of disease recurrence and reduces the annual breast cancer death rate by a third (39). Fulvestrant, however, in addition to blocking the estrogen receptor, also downregulates the receptor (40). Aromatase inhibitors, such as anastrozole and letrozole, block estrogen synthesis via inhibition of aromatase, the enzyme that converts androgens to estrogens (41).

Due to their proven efficacy and generally favourable side effects, these endocrine therapies are widely used for both early-stage, recurrent and metastatic breast cancer. However, despite their effectiveness, 50% of patients will relapse. Not all patients respond

to first line endocrine therapy, due to *de novo* resistance, whereas others develop acquired resistance and eventually relapse despite the initial response (42). One third of all women treated with tamoxifen for 5 years will develop recurrent disease within 15 years (39).

1.1.3.2 Resistance to hormone therapies

Of all breast cancer patients 30-40% fail to respond to initial therapy and exhibit intrinsic resistance to such therapies (43). The primary mechanism of such *de novo* or intrinsic resistance to endocrine therapy is lack of ER-α expression. Additionally, approximately 8% of all Caucasian women have inactive alleles of cytochrome P450 2D6. These patients are less sensitive to tamoxifen, as they are unable to covert the drug to its active metabolite, endoxifen (44, 45).

The majority of patients acquire resistance to endocrine therapy over the course of treatment. Many processes have been proposed to mediate this acquired resistance following prolonged treatment with endocrine therapies. Deregulation of various aspects of estrogen signalling is a common mechanism. Additionally tumour cells can develop mechanisms that provide an alternative, ER independent pathways for proliferation and survival. Such adaptive mechanisms can result from genetic or epigenetic changes within the tumour that drive hormone-independent mitogenic pathways (46, 47).

ER can regulate gene expression though protein-protein interactions with other transcription factors such as activator protein 1 (AP1), specificity protein 1 (SP1) and nuclear factor-κB (NF-κB). Increased transcriptional activity of these is associated with endocrine resistance (48, 49).

Anti-estrogen treatments act as cytotoxic agents but also have cytostatic properties, decreasing proliferation and leading to specific G1 phase cell cycle arrest (50). Therefore atypical expression of estrogen dependent and independent cell cycle regulators can confer endocrine resistance. For example c-myc is implicated in endocrine resistance (51) through driving estrogen independent cell proliferation, mimicking the estrogen stimulated activation of CDK2/cyclin E (51, 52). Amplification of both cyclin D (53-55) and cyclin E (56, 57) has been connected to tamoxifen resistance. Over-expression of cyclin D1b specifically has been shown to overcome the effect of anti-estrogen therapy (58). Tamoxifen is known to alter both p27 and p21 expression, and loss of these inhibitors is implicated in anti-estrogen resistance (59). There is transcriptional repression of p21 (60), this loss of p21 releases the inhibitory effect on cyclin E-CDK2, driving cell cycle progression independent of ER. There is also data that suggests in endocrine resistant cancers, pathways such as HER2 and AKT/PI3K can enhance CDK4/6-cyclin D signalling independent of ER (61, 62).

Upregulation of growth factors is widely considered a key resistance mechanism. Increased expression of EGFR, HER2 and IGF1 can confer tamoxifen resistance, along with members of their downstream signalling, particularly ERK and PI3K (63-65). In fact, overexpression of HER2 is one of the best characterised mechanisms of endocrine resistance. Loss of transcriptional repressors i.e. FOXP3 (66), GATA4 (67) and PAX2 (68) as well as gene amplification might be responsible for increased HER2 receptor expression.

The PI3K-Akt-mTOR pathway, a complex pathway activated in response to tyrosine kinase receptors and growth factors, is an essential cell survival pathway. Activation of this pathway, through either overexpression of fibroblast growth factor receptor or HER2, is considered to be involved in endocrine resistance (69, 70). Increased signalling through this

pathway can drive cell proliferation and anti-apoptotic responses. Additionally inhibition of mTOR has been shown to restore response to tamoxifen (64). A hallmark of resistance to drug treatment is the upregulation of pro-survival mechanisms and inhibition of apoptotic pathways. There is accumulating evidence for increased expression of anti-apoptotic molecules in endocrine resistance, for example BCL-2 and BCL-XL, coordinated with decreased expression of pro-apoptotic molecules BAK, BIK and caspase 9 (71). Although, this is potentially a consequence of activation of proliferation signalling through the PI3K-Akt pathway. Inhibition of the PI3K/mTOR pathway has received much attention in recent years for use either alone or in combination with hormone therapies in both primary disease and advanced cancers. Multiple compounds have been developed to inhibit various aspects and are in preclinical development or clinical trials already (72, 73).

Increased understanding of resistance mechanisms provides avenues for new treatment strategies to overcome resistance. Identification of novel therapies for use as a single agent or in combination with endocrine therapies is essential for patients who have relapsed following endocrine treatment.

1.2 Epigenetics

Epigenetics describes heritable changes in gene expression that are not due to alteration in the DNA sequence. The main features of epigenetic regulation involve chemical modifications to DNA or to the proteins associated with DNA, such as histones, which form the cores of chromatin packaging i.e. DNA methylation or histone modifications (Figure 1.3). A prominent role for non-coding RNAs is also emerging (74). Either by DNA methylation or histone modifications, epigenetic changes play a crucial role in the regulation of gene expression.

Diverse biological properties can be affected by epigenetic mechanisms. Epigenetic changes are crucial for the development and differentiation of the various cell types in an organism (75), as well as for normal cellular processes such as X-chromosome inactivation in female mammals. However, epigenetic states can become disrupted by environmental changes. Epigenetic defects can develop over time and are inherited by the daughter cells (76). Therefore the importance of epigenetic changes in the development of cancer and the potential for use as therapy and prognostic biomarkers is increasingly being appreciated.

1.2.1 Non-coding RNAs

Non-coding RNAs (ncRNAs) refer to RNAs that are transcribed from DNA but do not encode a protein. However, lack of an encoded protein does not directly mean these RNAs do not hold information or have a biological function. These ncRNAS can be separated into short ncRNAs (<30 nucleotides) and long ncRNAs (>200 nucleotides) (77).

Long ncRNAs are a diverse group of transcribed RNA molecules, thought to encompass nearly 30,000 human transcripts (78). Long ncRNAs have been described to have a range of functions including regulation of alternate splicing (79), directing imprinting (80, 81) and may serve as precursors to short ncRNAs (82). Increasing evidence suggests a role in epigenetic modulation, via an ability to complex with chromatin modifying proteins and recruiting their catalytic activity to specific regions within the genome. Long ncRNAs have been shown to bind to both chromatin repressing (83-85) and enhancing (86-88) complexes, thereby modulating chromatin states and altering gene expression (89).

Short ncRNAs are best known to function in regulating mRNA transcripts and include PIWI interacting RNAs (piRNAs), microRNAs (miRNAs), and small interfering siRNAs (siRNAs). piRNAs are single stranded RNAs produced in clusters and cleaved to individual units. They then bind to PIWI proteins, a subset of the Argonaute proteins, inducing epigenetic regulation and transposon control (90). miRNA are single stranded RNAs produced via transcription or through splicing, which fold into hairpin loop structures. These are then processed by the RNAse III endoribonuclease, Dicer, before being denatured. One of the RNA strands assembles with Argonaute proteins into the RNA induced silencing complex (RISC), which then targets specific mRNA containing the complementary sequence to the miRNA, to induce either cleavage or degradation, inhibiting translation of the protein (91). siRNAs are produced as double stranded RNAs, that can enter the post-transcriptional gene silencing pathway which via RISC, leads to mRNA degradation, or can enter the transcription gene silencing pathway involved in chromatin modification (92).

The majority of ncRNAs do not yet have a described function and potentially these RNAs still have roles in epigenetic mechanisms that are not yet completely understood (93).

1.2.2 Histone modifications

Histones are the small proteins that pack and order the DNA into nucleosomes. Each nucleosome contains two subunits of each histone H2A, H2B, H3 and H4. Together they form a structure around which the DNA is coiled, forming the nucleosome. H1 and H5 function as linkers. A flexible N-terminal tail on each histone protrudes from the core (94). Multiple different types of modification of the histone tail have been described such as histone acetylation, methylation, phosphorylation and ubiquitination. Such modifications

of the histone tail can dynamically modify the chromatin structure, altering activation or repression of gene transcription (95).

Histone acetylation is the most widely studied and most common modification. Histone acetyltransferases (HAT) and histone deacetylases (HDACs) regulate acetylation of histone tails. Lysine residues within H3 and H4 are preferential targets for histone acetylation. Acetylation is largely targeted to promoter regions. Presence of an acetyl group on the histone tail is associated with an open chromatin structure and therefore correlates with active gene transcription. Whereas deacetylation causes the chromatin to adopt a closed structure, silencing transcription (96, 97). Therefore histone modifications are one of the key mechanisms in regulating gene expression and consequently have been found to be disturbed in multiple disease types, including cancer.

Histone modification and DNA methylation may be closely related. Methylation of DNA may lead to modification of histones, which would cause the chromatin to assume a closed condensed form, thereby preventing transcription of the gene at that site (98).

1.2.3 DNA methylation

DNA methylation is a modification of the 5^{th} position of the pyrimidine ring in a cytosine that precedes a guanine nucleotide. DNA methylation occurs by addition of a methyl group at the 5' carbon of the cytosine ring, resulting in 5-methylcytosine. The addition of a methyl group is carried out by DNA methyl transferases (DNMTs), a family of enzymes including DNMT1, DNMT3a and DNMT3b. DNMT1 appears to be responsible to maintaining inherited patterns of methylation, whilst DNMT3a and DNMT3b mediate establishment of new, *de novo*, methylation patterns (99). In mammalian DNA, 5-methylcytosine is found in

approximately 5% of genomic DNA, primarily at cytosines that precede guanines in the nucleotide sequence (100). A cytosine next to a guanine in the DNA sequence is called a CpG dinucleotide or CpG site. Such CpG dinucleotides tend to be grouped together in small regions of DNA rich in CpG sites, known as CpG islands. These CpG islands have a G+C content of greater than 50% and account for 1-2% of the genome (101-103). Typically CpG islands are found spanning the 5' regulatory region of genes, where transcription is initiated (104). In fact, CpG islands overlap the promoter regions of 60-75% of all human genes (105). DNA hyper-methylation of these CpG islands is associated with transcriptional silencing of genes and thereby loss of gene function, as well as genomic instability through silencing of DNA repair genes. DNA methylation silences gene expression via two main mechanisms; the methyl group projects into the major groove of the DNA and actively inhibits transcription, by either blocking transcription factor binding through steric hindrance or recruiting additional proteins to block transcriptional activation (106).

1.2.3.1 DNA methylation in breast cancer

Methylation plays an important role in normal cells as well as cancer development. DNA methylation contributes to chromatin organisation and tissue-specific gene expression. In normal cells, DNA methylation is essential in genomic imprinting i.e. the mechanism by which mammals express genes inherited through the paternal or maternal chromosome only. The selective gene expression is achieved through differential methylation of DNA regions of specific genes on the appropriate chromosome (107).

In normal cells CpG dinucleotides tend to be unmethylated within the promoter region and methylated across the rest of the genome. The reverse is generally seen in cancer cells (108). Such alterations in the methylation of promoter regions in cancer cells are an

important mechanism in carcinogenesis, where methylation can switch off genes that would otherwise suppress tumorigenesis. When CpG islands that are normally hypo-methylated become hyper-methylated important genes such as tumour suppressor genes, DNA repair genes or inhibitors of angiogenesis or cell adhesion may be transcriptionally repressed. In fact epigenetic gene inactivation is thought to be at least as common, if not more frequent than genetic mutation in cancer development (109-112).

Many studies have established hyper-methylated genes in breast cancer and whole genome approaches have attempted to identify methylation signatures of breast cancer cells (113-116). In fact *de novo* methyl transferase DNMT3b is overexpressed in breast tumours (117) suggesting involvement of methylation alterations in tumourigenesis. DNA methylation of the hormone receptors, ER and PR has been proposed as a mechanism for hormone receptor negative tumours and implicated in resistance to hormone therapies (118-121). Among other methylated genes are those involved in cell cycle and proliferation, such as the cell cycle inhibitors p16 (122, 123) and 14-3-3-σ (124), methylation dependent silencing of these genes would override regulation of growth signals. DNA methylation has been implicated in promoting epithelial-mesenchymal transition (EMT) and metastasis through the inhibition of metastasis suppressing genes such as CREB3L1 (125), SDPR (126) and TES (127). DNA methylation in the promoter region has been detected in genes involved in DNA damage repair such as BRCA1 (128-130), MGMT (131) and mismatch repair genes hMLH1 and hMSH2 (132). Silencing of these genes could increase frequency of sporadic mutations, a hallmark of cancer. Hyper-methylation of such DNA damage response genes has been associated with simultaneous hypo-methylation of anti-apoptotic/pro-survival genes such as DR4, FLIP and RNF8 (133) promoting cell growth and survival.

DNA methylation has been implicated in multiple processes promoting breast cancer development, tumour cell proliferation and metastasis. Understanding the epigenetic changes in breast cancer is important to comprehend the mechanics of breast tumourigenesis but could also assist in diagnosis, prognosis and treatment of breast cancers.

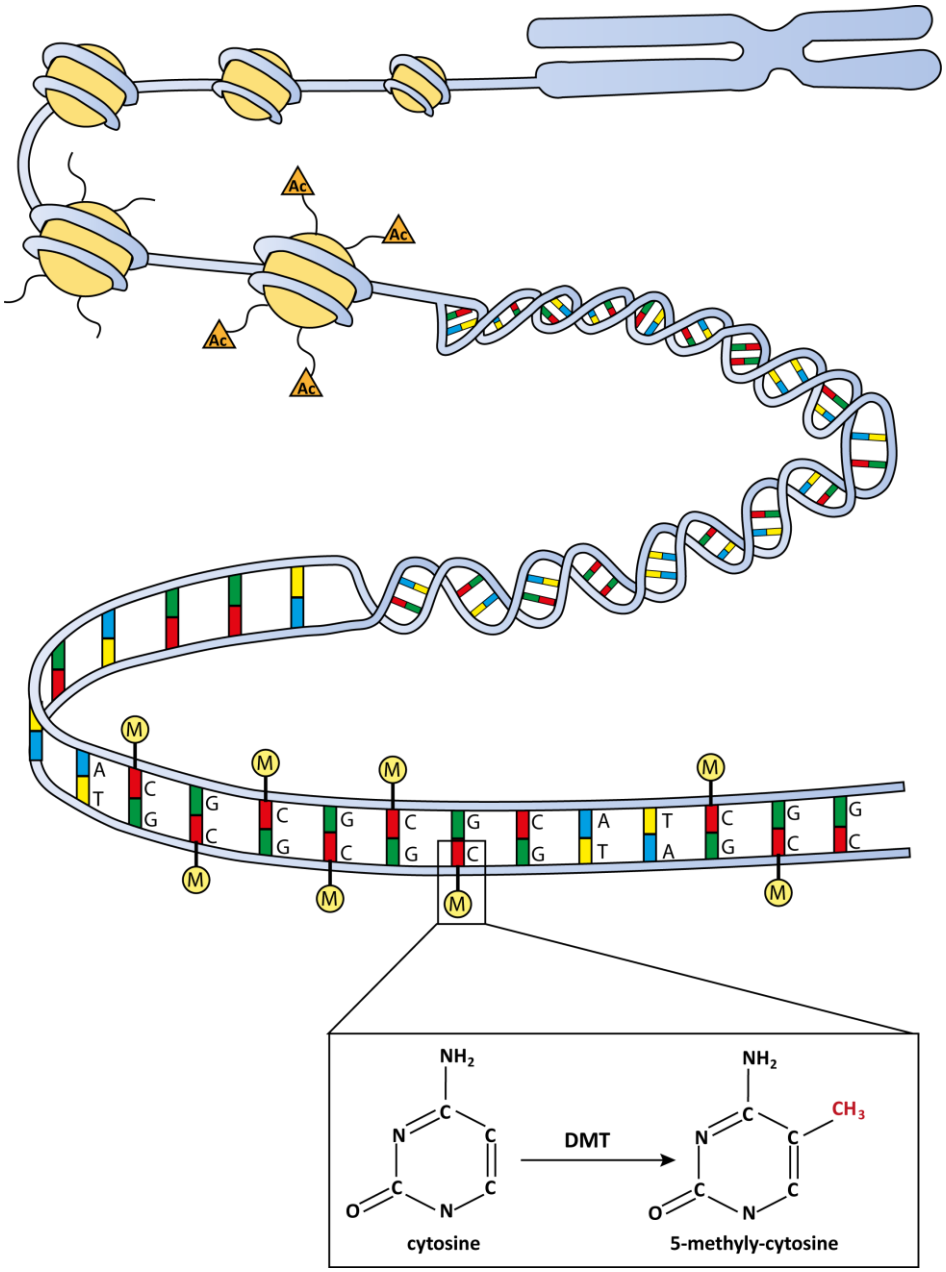

Figure 1.3 Schematic representation of epigenetic regulation. DNA is organised by wrapping around histones to form nucleosomes. Histone modifications such as acetylation, are post-translational modifications that occur to the histone tail, altering the chromatin structure and accessibility of the DNA to the transcription machinery. DNA methylation is the covalent attachment of a methyl group by DNA methyltransferases (DMT) to a cytosine that precedes a guanine, thereby leading to transcriptional silencing (M: methyl group Ac: Acetyl group).

1.3 The Cell Cycle

1.3.1 Regulation of the cell cycle

The cell cycle comprises a series of tightly controlled events that drive the replication of DNA and cell division. It is divided into several phases; G1 in which cells prepare the machinery for replication, S phase involving duplication of the DNA, G2 a secondary gap phase and M phase in which the mitosis and cytokinesis takes place, and therefore proliferation. Cells then start a new cycle or remain in G0 state, quiescence, a distinct state from which cells can re-enter the cell cycle. The restriction point (R) is defined as the point of no return in G1, after which the cell is committed to enter the cell cycle (134). In the normal cell, several checkpoints throughout the different phases are controlled by activation and inactivation of a complex system of modulators (Figure 1.4). This ensures orderly execution through each of the cell cycle events. Cancer cells have acquired features that allow them to override these checkpoints leading to uncontrolled proliferation (135).

The transitions between the cell cycle phases are controlled by a small number of protein kinases. Cyclin dependent kinases (CDKs) are a family of serine/threonine kinases that are activated at specific points of the cell cycle and require binding of cyclins for full activity. Members of the CDK family are characterised by an ATP-binding pocket, a PSTAIRE helix, which acts as a cyclin binding domain, and an activating T-loop motif. Activation of the CDK involves binding of the appropriate cyclin causing a conformational change which displaces the T-loop and exposes the substrate binding interface (136, 137). In total, at least 9 CDKs and 16 cyclins have been described in the literature (138). Different members of the CDK family, in association with particular cyclins, control key events throughout the cell cycle. CDK1 controls progression from G2 to mitosis and CDK2/CDK4/CDK6 control G1 to S phase.

CDK4 and CDK6 are structurally related proteins with many biological and biochemical similarities, within the cell cycle they are functional homologues (137). In addition to these there are regulatory CDKs such as CDK7 and transcriptional CDKs, including CDK8 and CDK9 (139).

The cyclins are a more diverse family of proteins and are divided into four classes, type A, B, D, and E cyclins. Cyclins are characterised by the presence of a cyclin box, required for binding to CDKs (140). The cyclins act as regulatory subunits to the CDKs and provide specificity of function at precise times during the cell cycle. CDK proteins remain at stable levels throughout the cell cycle, whilst the cyclin levels undergo phase dependent fluctuations. The sequential accumulation of different cyclins allows the formation of specific cyclin–CDK complexes that control progression through the cell-cycle phases (141). On the other hand, targeted degradation of partner cyclins inactivates CDKs when they are no longer required. For example, cyclin B is actively degraded by proteolysis mediated by the ubiquitin ligase, anaphase promoting complex (APC) (142). Cyclin D is particularly unstable, with a half life of less than 30 minutes, and shuttles to the nucleus during G1 phase and is exported to the cytoplasm during S-phase (143). Phosphorylation of threonine 286 by glycogen synthase kinase-3beta (GSK-3beta) actively promotes export of the protein and rapid degradation via ubiquitination (144, 145).

Two distinct families of CDK inhibitors have been identified, INK4 and Cip/Kip, which can counteract CDK activity. These proteins inhibit CDK catalytic activity by allosteric competition with their cyclin binding partners. The INK4 family includes p15, p16 and p18. These specifically bind to CDK4 and CDK6. The INK4 proteins weaken the binding of cyclin D with CDK4 and CDK6 and interact with the catalytic domain of the kinases to effectively

suppress kinase activity (146). In this way CDK4 and CDK6 can be inactivated when INK4 proteins are induced by anti proliferative signals, such as TGFβ (p15) (147), senescence (p16) (148) and terminal differentiation (p18) (149, 150). INK4 proteins can interact with both cyclin bound CDKs and monomeric CDKs. In the case that the CDK-cyclin D complex is already formed, the INK4 can inhibit without dissociating the cyclin. When binding to individual CDK subunits, INK4 binding interferes with subsequent CDK-cyclin complex formation (148), via competing with Cdc37, a chaperone protein required for the assembly of the CDK4/6-cyclin D complex (151, 152).

The Cip/Kip family including p21, p27 and p57 interact with a broader spectrum of CDKs and can bind to CDK2, CDK4 or CDK6 (153, 154). In response to inhibitory signals such as TGF-β, DNA damage or senescence, these cell cycle inhibitors are rapidly upregulated to inhibit cell cycle progression (155, 156) via negative regulation of CDKs. However, in proliferating cells, Cip/Kip family members can positively regulate CDK4/6 by facilitating their complex formation with cyclin D in early G1 (157). For example, in response to inhibitory signals including TGFβ (156) and drug treatment (158), p27 will bind to and inactivate CDK2, inducing cell cycle arrest. However, in proliferating cells, phosphorylation at tyrosine residues 88 and 89, within the CDK interacting domain, alters p27 to a noninhibitor (157). In this state, p27 can bind to and is sequestered by active CDK4-cyclin D complexes, freeing CDK2 from inhibition via p27. In turn p27 is then phosphorylated at threonine 187 by active CDK2-cyclin E, targeting the protein for degradation (159, 160). Therefore p27 balances cell proliferation and arrest via association with CDK4 or CDK2 respectively (161).

In addition to CDK inhibitors, and degradation of partner cyclins, CDKs can also be reversibly inactivated by phosphorylation of crucial tyrosine and threonine residues within the ATP binding loop (162, 163). Most CDKs have both inhibitory and activating phosphorylation sites. Phosphorylation within the ATP-binding site by inhibitory kinases interferes with ATP alignment, thereby inhibiting kinase activity (164). Conversely, phosphorylation within the T-loop by CDK activating kinases (CAK) will enhance substrate binding and stability of the complex, allowing for full CDK activation (165). Cdc25 is a family of 3 phosphatases (Cdc25 A,B,C) that contribute to cell cycle control via dephosphorylation of CDKs allowing for sequential activation. CDK2 phosphorylation at tyrosine 15 and threonine 14 residues blocks cells in G1, but dephosphorylation by Cdc25A enables entry into S-phase (166). CDK1 is phosphorylated by Wee1 (167), and unless CDK1 is dephosphorylated at tyrosine 15 by Cdc25C cells will arrest at the G1/M transition (168).

All of these regulatory elements come together to ensure orderly progression through the cell cycle phases. G1 is an intermediate phase occupying the time between cell division in mitosis and the DNA replication in S-phase. During G1 cells grow in preparation for DNA replication and intracellular components, such as centrosomes, undergo replication. In G1 the retinoblastoma protein (Rb) directly binds to the transactivation domain of E2F, and recruits chromatin modifying enzymes, actively repressing E2F mediated transcription (169). Upon mitogenic signalling, D-type cyclins (D1, D2, D3) are synthesised and form a complex with CDK4 and CDK6. CDK4/6-cyclin D complexes phosphorylate Rb, which becomes partly inactive, lifting its repression of E2F. Free E2F is active and induces transcription of S phase specific genes, including cyclin E gene transcription (170). This provides a positive feedback loop, whereby cyclin E forms a complex with CDK2, which further phosphorylates and inactivates Rb. This leads to complete dissociation of E2F1,

initiating further transcription of S phase genes (171). At this point, so called the restriction point, cells are committed irreversibly to undergo transition from G1 to S phase. This progression from G1 to S phase is a crucial checkpoint in protecting cells from abnormal replication. Cells may be halted at this checkpoint to repair any damage. For example, in response to DNA damage p53 stimulates transcription of several genes, including p21, which inhibits both CDK2 and CDK4/6, halting cells in G1 (172).

CDK2 is further activated by cyclin A2 to progress through S-phase, where the cell duplicates its chromosomes. Autoregulatory negative feedback loops subsequently suppress transcription of G1-S phase genes once cells have advanced into S-phase (173). Phosphorylation of E2F transcription factors by CDK2-cyclin A results in their release from target promoters, inactivating transcription (174), and E2F proteins are targeted for degradation via ubiquitination (175, 176). As well as proteins necessary for completion of S-phase, CKD2-cyclin A complexes phosphorylate numerous proteins involved in transcription and DNA replication and repair (177). Once the DNA is replicated the cells enter a second gap phase. G2 is the interval between completion of DNA replication and onset of mitosis, and acts as a checkpoint to ensure DNA replication has been completed without mistake or damage. In response to DNA damage, cells can be halted at this checkpoint to complete DNA replication or repair damaged DNA (178). DNA damage is associated with many cellular events, including activation of Chk1 (Checkpoint kinase 1). Chk1 inactivates the phosphatase Cdc25C, maintaining CDK1 in an inactive state and thus causing G2-M arrest (163, 179).

Finally CDK1 associates with cyclins A and B to control progression from G2 and onset of mitosis. Cyclin A is accumulated during G2 and mediates entry into mitosis. At the end of

interphase, CDK1 is activated by A-type cyclins, enabling progression from G2 and onset of mitosis. Once the nuclear envelope has broken down, type A cyclins are degraded by ubiquitin-mediated proteolysis. Cyclin B proteins are actively synthesised and associate with CDK1 to drive cells through mitosis. CDK1-cyclin B complexes are activated by release from inhibitory phosphorylation within the active site. Cyclin B-CDK1 complexes have numerous substrates and are known to associate with centrosomes during prophase (180) and facilitate in centrosome separation and chromosome condensation (181). At this point CDK1 mediated phosphorylation of the origin of recognition complex (ORC) inhibits activation of pre-replication complexes (PRC), thus preventing DNA replication until mitosis is completed and the nuclear envelope is assembled (182). Rapid degradation B cyclins at the onset of anaphase mediates exit from mitosis. The subsequent drop in CDK1 activity towards the completion of M phase allows PRC to bind to specific DNA chromosomal sites, in preparation for initiation of replication in the next cycle (183).

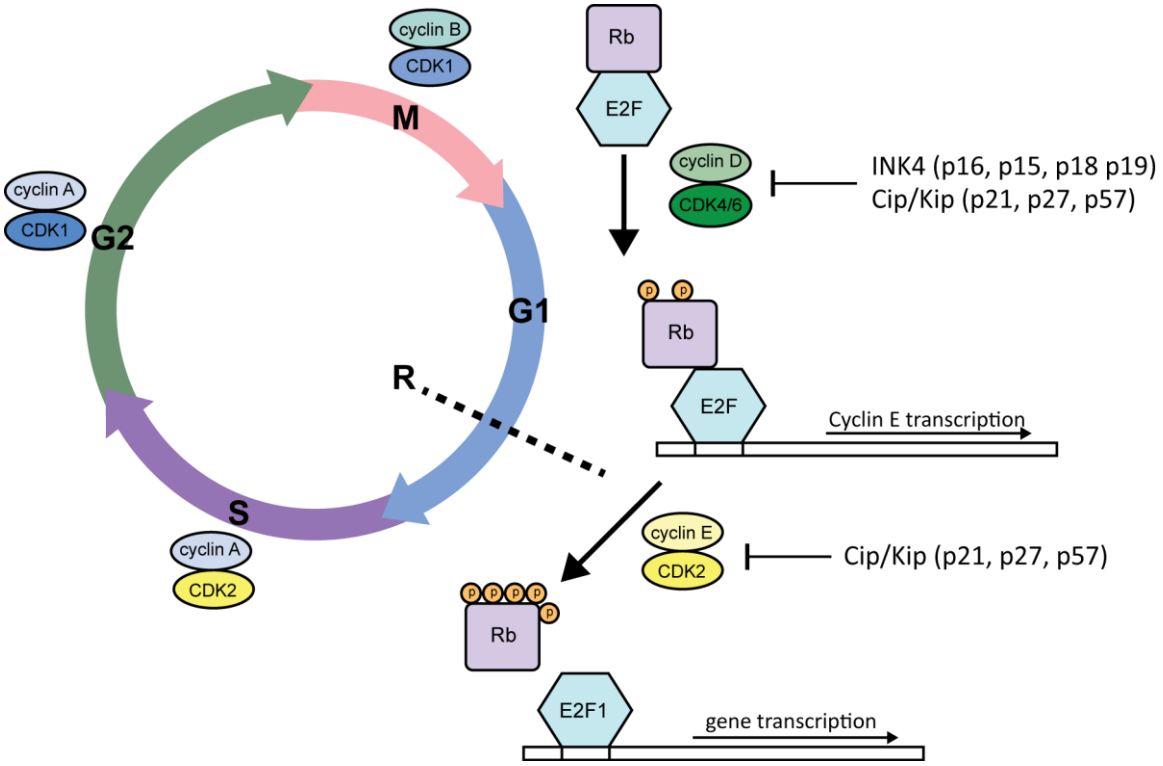

Figure 1.4. Structure of the cell cycle and regulation of the G1 to S phase transition. The cell cycle can be divided into four successive phases. G1 followed by S phase (DNA synthesis), G2 and M phase (Mitosis). The G1 to S phase transition is a major restriction point (R), once crossed cells are committed to complete the cell cycle. Transition between each phase in controlled by specific cyclin-CDK (cyclin dependent kinases) complexes. CDK activity is suppressed by two families of inhibitors, the INK family is specific for CDK4 and CDK6, whilst the Kip family also inhibits CDK2.

1.3.2 The cell cycle and breast cancer

Alterations in the mechanisms controlling cell cycle progression are considered a hallmark of cancer due to the resulting uncontrolled proliferation. The G1-S phase transition encompasses many events that are specifically altered in breast cancer, with dysregulation of the cyclin D-CDK4/6-Rb axis occurring in a substantial proportion of breast cancers.

Loss of pRb function has been described in 20-35% of breast cancers (184). Inactivation of Rb protein is more common than deletion or mutation of the RB1 gene. Those cancers with loss of pRb function tend to have a more invasive phenotype as Rb inactivation facilitates loss of proliferative control and therefore tumour progression (185). In estrogen receptor positive breast cancer loss of Rb is associated with poor prognosis (186).

In cancers with intact Rb, the process of phosphorylating Rb and driving G1 progression forward is rate limited by cyclin D. Cyclin D is essential for both normal breast development and breast cancer progression (186). Cyclin D is overexpressed in breast cancer either through gene amplification or translocations of the CCND locus on chromosome 11q13 (187). Additionally, signalling via the RAS/RAF/MAPK pathway can increase production of cyclin D (188). Over expression of cyclin D is more common than amplification of the corresponding gene (189). Amplification of the cyclin D gene (CCND1) has been identified in up to 20% of breast cancers (187, 190, 191) and a higher percentage, between 35-40%, show overexpression of the protein (192, 193).

The prognostic implications of cyclin D amplification is currently unclear. CDK4 and cyclin D are not required for normal breast cell development, but in mice models CDK4 and cyclin D are required for induction of breast tumour growth (194, 195). Some studies suggest cyclin D is a dominant oncogene associated with poor outcome (196-198). Specific isoforms of

cyclin D might have particular roles. For example, Cyclin D 1a levels have been shown to inversely correlate with proliferation and Ki67 levels, however they were not prognostic. Whilst, in contrast, cyclin D1b increase was associated with increased recurrence and metastases (199).

Studies suggest Cyclin D might be more specifically associated with ER positive breast cancers. As outlined earlier, in ER positive breast cancer cells are dependent on estrogen signalling for proliferation and survival, and multiple alterations in cell cycle regulators are associated with endocrine resistance. Estrogen can induce cells from G0 to enter the cell cycle and increase progression from G1 to S phase (200). Cyclin D is essential for regulation of breast epithelial division. ERα directly drives cyclin D transcription and cyclin D can also independently activate ERα, driving transcription and cell division (61). Treatment with endocrine therapy reduces complex formation of CDKs and cyclins therefore inducing cell cycle arrest. Evidence suggests that breast cancer cells that have already developed resistance to endocrine therapy remain dependent on cyclin D/CDK4 to promote proliferation (201). This suggests a role for CDK4/6-cyclin D signalling in ER independent growth of breast cancers.

Alterations in CDK inhibitors have also been reported in breast cancers. Inactivation of CDKN2A, the gene encoding p16, through methylation, gene deletion and point mutation has been reported in up to 50% of invasive breast cancers (202). p16 inactivation allows uncontrolled cell division and increased proliferation (203). CDKN1B, the gene encoding p27, is rarely mutated or deleted, but p27 is frequently reduced in expression or degraded by accelerated proteolysis (204-206). Additionally, absence of p27 has been linked to poor prognosis in breast cancer (207).

The alterations in this checkpoint of the cell cycle in breast cancer suggest it as a good target, with a therapeutic role for CDK4/6 inhibitors.

1.3.3 Targeting the cell cycle for cancer therapy

Over recent years the cell cycle as a therapeutic target in cancer has been evolving with CDKs considered a promising target. Numerous small molecule inhibitors of CDKs have been developed. The first generation consisted of pan-CDK inhibitors, with little specificity for individual CDKs, such as flavopiridol (Sanofi-Aventis) (208). Whilst, roscovitine (Seliciclib, Cyclacel) was initially considered a specific inhibitor of CDK1, 2 and 5, it was later discovered to also inhibit CDK7 and CDK9 (209).

Flavopiridol was the most well studied of these first generation inhibitors. A synthetic favone derived from a natural product found in the plant *Dysoxylum binectariferum*, shown to inhibit CDK1,2,4,6,7 and 9 (210). Preclinical evidence showed potent effects in breast cancer cell lines. Flavopiridol was shown to induce cell cycle arrest and inhibited cell proliferation by 50% at nM concentrations (211). The drug also inhibits angiogenesis, induces apoptosis and potentiates the effects of chemotherapy (212, 213). Whilst pre-clinical studies showed the broad spectrum nature of this drug was promising, this was not the case in patients. Phase II clinical trials across different solid tumours; renal cancer (214), liver cancer (215), ovarian (216), pancreatic (217) and prostate (218), did not show flavopiridol to be particularly effective. In metastatic breast cancer particularly, flavopiridol was associated with severe toxicity, especially high rates of neutropenia (219).

Following from the pan-CDK inhibitors further inhibitors were developed aiming for increased selectivity for CDK1 and CDK2. For example, Dinaciclib was specifically developed as a potent inhibitor of CDK1,2,5 and 9 (IC_{50} 1-4nM) with less activity for CDK4,6 and 7 (IC_{50}

60-100nM) (220). Compared to flavopiridol, dinaciclib exhibited greater activity. In cell based assays, dinaciclib suppressed phosphorylation of Rb in over 100 cell lines or multiple tumour types and *in vivo* induced regression of established solid tumours in a range of mouse models. However, dinaciclib treatment in combination with chemotherapy in triple negative breast cancer was associated with substantial toxicity (221). A randomised trial in advanced breast cancer comparing dinaciclib to the chemotherapeutic agent capecitabine, was discontinued after only 30 patients had enrolled as interim analysis indicated the time to disease progression was inferior with dinaciclib treatment (222).

The failure of non-selective CDK inhibitors can be attributed to lack of understanding of the mechanism of action. With low specificity it is hard to differentiate which CDKs are inhibited in pre-clinical models and corresponding to the therapeutic effect. The majority of clinical studies were conducted in unstratified patient cohorts. The lack of appropriate patient selection and lack of predictive biomarkers to select for the most sensitive patient population could contribute to the initial clinical failures. It was thought that specific CDK inhibitors might be better suited for cancer with different drivers, such CDK2 inhibition might be better to target tumours driven by cyclin E amplification (223, 224). Alternatively, specific CDK inhibition might be synergistic with a particular co-treatment, such as CDK1 inhibitors seem to cooperate with poly(ADP-ribose) polymerase (PARP) inhibitors (223, 224). This therefore suggested improved selectivity for specific CDKs would be more advantageous as a therapeutic strategy.

1.3.3.1 Specific CDK4/6 inhibitors

Further understanding of mechanism of CDK4 and CDK6 dysregulation in cancer led to the understanding that targeting these CDKs should specifically lead to cytostatic arrest in G1 phase, and directly suppress Rb initiated gene expression and cell proliferation.

It was identified that pyrido[2,3-*d*]pyrimidin-7-one compounds with a 2-aminipyridine side chain at the C2 position acted as inhibitors with a high selectivity for CDK4 and CDK6 compared to other CDKs (225). Subsequent screening and optimisation resulted in the compound PD-0332991, now called palbociclib (developed by Pfizer). Drug discovery programmes from Novartis and Eli Lilly led to development of LEE011 (Ribociclib) and LY-2835219 (Abemaciclib) respectively. All three CDK4/6 inhibitors are structurally distinct from the un-specific pan-CDK inhibitors. Palbociclib and LEE011 are structurally similar, whilst abemaciclib differs in its structure. It is hypothesised these drugs bind to the ATP-binding pocket of CDK4 and CDK6, with specific interaction with residues within the ATP binding cleft (226). Notably, abemaciclib is thought to have a slightly different mechanism of action, with a higher selectivity against CDK4 over CDK6 (227).

Palbociclib is the CDK4/6 inhibitor the most advanced along clinical development. Palbociclib is an orally available small-molecule inhibitor of CDK4 and CDK6, with a high level of specificity for these over other CDKs and other protein kinases (Figure 1.5).

Protein kinase	IC_{50} (μmol/L)
Cdk4/cyclin D1	0.011
Cdk4/cyclin D3	0.009
Cdk6/cyclin D2	0.015
Cdk2/cyclin E2	>10
Cdk2/cyclin A	>10
Cdk1/cyclin B	>10
Cdk5/p25	>10
Epidermal growth factor receptor	>10
Fibroblast growth factor receptor	>10
Platelet-derived growth factor receptor	>10
Insulin receptor	>10
Lymphocyte kinase	>10
Vascular endothelial growth factor receptor	>10
AMP-activated protein kinase	>10
Checkpoint kinase-1	>10
Casein kinase-1	>10
Casein kinase-2	>10
c-Src kinase	>10

Figure 1.5. Inhibitory activity of Palbociclib against a panel of protein kinases, concentration of drug required to inhibit 50% of activity. Palbociclib is highly selective for CDK4/6–cyclin D complexes over other targets (1).

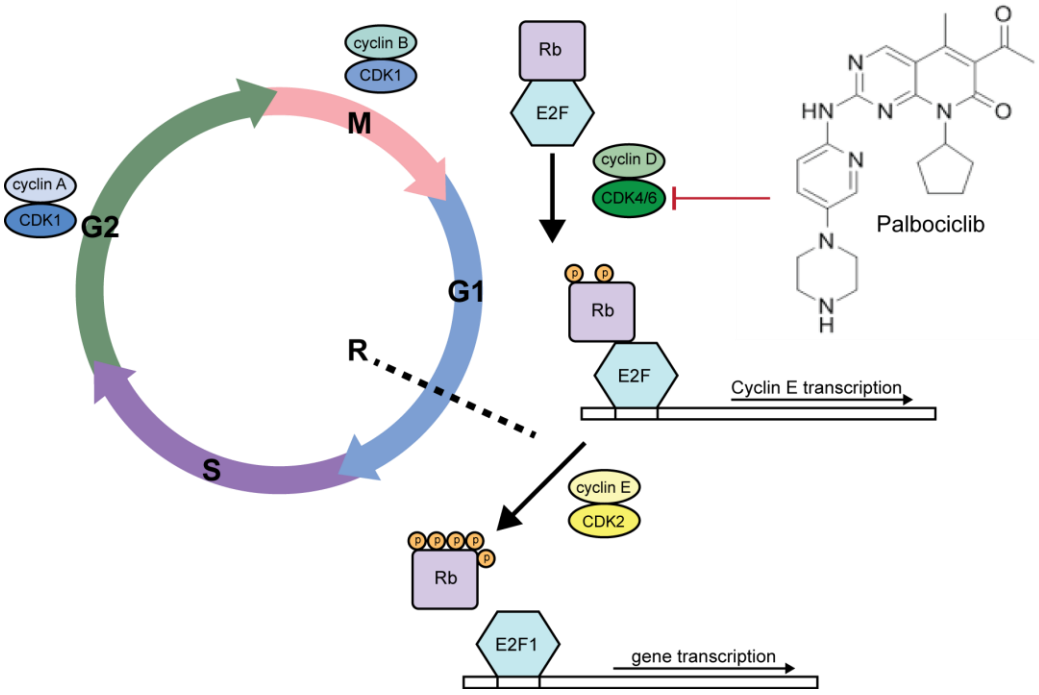

Figure 1.6 Palbociclib is a small molecule inhibitor of CDK4/6, blocking the phosphorylation of Rb inducing cell cycle arrest and preventing cell proliferation.

Treatment at low nanomolar concentrations results in effective G1 arrest though an inhibition of Rb phosphorylation in cancer cell lines (228). This inhibition causes downstream loss of expression of S phase cyclins, nucleotide biosynthesis, DNA replication machinery and cell cycle regulatory genes (229). *In vivo* a significant anti-tumour effect was demonstrated in breast cancer xenografts, with almost complete suppression of tumour growth (228). As expected, there is no effect in Rb deficient cells (228, 230).

Across a panel of breast cancer cell lines, it was observed that ER positive cell lines are particularly sensitive to growth inhibition following palbociclib treatment (1). A synergistic effect of palbociclib was observed with endocrine therapies in ER positive tumours and cell lines. Palbociclib treatment was also able to resensitise tamoxifen resistant cells to endocrine therapy. Additionally, it has been shown that resistance to endocrine therapy is associated with dysregulation of genes that are controlled by the CDK4/6-pRb-E2F pathway. Following from this, CDK4/6 inhibition has been shown to be effective in models of acquired resistance to endocrine therapy and treatment is able to induce stable cell cycle arrest completely distinct from treatment with ER antagonists (201).

A phase II study of palbociclib in women with advanced breast cancer showed palbociclib treatment was well tolerated and response or prolonged stable disease was demonstrated using palbociclib as a single agent (231), whilst a phase I study demonstrated combination of palbociclib and letrozole was generally well tolerated and encouraging anti-tumour activity was demonstrated (232). Whilst palbociclib is furthest in development, the CDK4/6 inhibitor from Novartis (LEE011) is also in advanced development, and has been demonstrated to be well tolerated in patients with preliminary clinical activity (233). Phase II and phase III trials are still ongoing to evaluate LEE011 in combination with endocrine

therapy in advanced breast cancer, and also with the addition of the PI3K inhibitor BYL719. Abemaciclib has also entered into clinical trials. A small phase I study of solid tumours, including 47 breast cancer patients, indicates the potential efficacy of abemaciclib as a single agent, with 61% of ER positive breast cancer patients achieving stable disease lasting longer than 6 months (234).

Early trials have defined the key clinical hallmarks upon CDK4/6 inhibition in patients. Primarily, neutropenia is the principal dose-limiting toxicity of both palbociclib and LEE011. However, this is a reversible effect, indicating the drugs have a cytotoxic effect on neutrophil precursors within the bone marrow. To account for this, the drugs have a treatment regime with intermittent breaks to allow for haematological recovery (226). Abemaciclib has a different toxicity profile, with the dose-limiting toxicity being fatigue, allowing for a continuous dosing schedule (234).

A number of phase II studies have moved forward with combined palbociclib treatment with endocrine therapy. The PALOMA-1 trial, a randomised phase II trial in 165 postmenopausal women with advanced ER positive breast cancer showed significant increase in median progression free survival in dual letrozole and palbociclib treatment compared to single agent letrozole therapy, 20.2 months compared to 10.2 months respectively (235). Subsequently, palbociclib was given Breakthrough Therapy designation by the US Food and Drug Administration in April 2015. The further PALOMA-3 trial, a double blind phase III trial of 521 breast cancer patients whose cancer had relapsed or progressed on prior endocrine therapy, palbociclib combined with fulvestrant improved progression free survival from 4.6 months to 9.5 months compared to fulvestrant only (236, 237). A longer follow up time is still required to determine the effect of palbociclib on

overall patient survival. Another phase III trial (PALOMA-2) is ongoing, to explore the efficacy of palbociclib in combination with letrozole for advanced breast cancer, not previously treated with hormone therapy.

Results from trials thus far reveal palbociclib in combination with endocrine therapy to be well tolerated and associated with significant and consistently improved progression free survival. Development of palbociclib offers a class of treatment for advanced hormone-receptor positive breast cancer and is likely to be increasingly introduced as standard treatment in clinic. However, due to the adaptive nature of cancer, as with endocrine therapies, development of resistance to palbociclib can be expected. Therefore with the increasing clinical use, acquired resistance to palbociclib is likely to emerge as a new major clinical challenge and understanding of resistance mechanisms will become crucial.

1.4 Krüppel-like Factors

Krüppel-like factors (KLFs) are a diverse family of homologous genes. All KLFs are DNA binding transcriptional regulators that control essential cellular processes including proliferation, differentiation, hormone receptor signalling, apoptosis, migration and the tumour microenvironment (238).

Structurally all members of the KLF family have a triple zinc finger domain at the carboxyl terminal but the other regions can be highly divergent. Specifically all KLFs contain Cys2/His2 zinc fingers, usually encoded by a unique exon situated at the 3’ end of the gene (239). It is these highly conserved zinc finger and linker domains that give the KLF transcriptional regulatory activity. Several KLFs also share a nuclear localisation signal, allowing transport into the nucleus (240). The divergence of the N-terminus allows for

binding of different co-activators, co-repressors or other factors leading to functional diversity of the family. Individual KLFs can be tumour suppressors or oncogenes, often context dependent on tissue, tumour type or cancer stage (241).

1.4.1 Krüppel-like factors in cancer

The diverse role of KLFs in pathways such as cell proliferation, apoptosis and epithelial-mesenchymal transition suggest a role for this family of proteins in cancer development, growth and metastasis.

A number of KLFs have been implicated in the dysregulation of proliferation, with cell cycle regulators such as the cyclins, CDKs, and CDK inhibitors all common targets for transcriptional regulation. For example, in pancreatic cancer KLF4 decrease tumour cell proliferation by inducing CDK inhibitors and reducing cyclin D1 expression (242). KLF5 can promote cell proliferation in cancer cells by upregulating cyclin A and E2F3, whilst decreasing levels of the CDK inhibitors p27 and p15 promoting progression through the G1/S phase transition (243, 244). KLF6 is ubiquitously expressed in normal tissues controlling cell cycle progression, but expression is lost in many cancers promoting proliferation and tumourigenesis (245). Conversely, KLF8 is highly overexpressed in ovarian, breast and renal cancer, and can promote cyclin D expression and cell progression (246, 247).

KLFs have been recognised to modulate tumour cell migration and metastasis. KLF8 promotes EMT and negatively regulates E-cadherin in breast cancer, promoting invasion and metastasis (247, 248). Methylation of KLF3 inhibits its expression, which normally represses the metastasis inducing miR-182 (249). KLF17 has been documented as a novel

tumour suppressor, with reduced expression mediating activation of the TGF-β pathway and EMT gene transcription, inducing tumour growth and metastasis (250, 251).

KLFs also regulate classic apoptotic and cell survival molecules such as BCL-2 family members (252). KLF4 is upregulated in breast cancer cells by p53 (253) and promotes apoptosis through activation of BAX and downregulation of the pro-apoptotic BCL-2 (254, 255). KLF5, induces TNFα mediated apoptosis (256). A cooperative effect of KLF5 and KLF4 has been suggested (257), with knockdown of both required to suppress the anti-apoptotic MCL1 (258). KLF9 is expressed during drug induced apoptosis and inhibits tumour cell growth through inhibition of AKT activation in prostate cancer (259).

Additionally, increasing evidence suggests KLFs may have a function in ER signalling. For example, estrogen upregulates KLF4 in breast cancer and knockdown of KLF4 inhibits estrogen-stimulated growth of breast cancer cells. KLF6 is able to disrupt ERα signalling and decrease breast cancer proliferation (260). KLF15 inhibits estrogen induced cell proliferation (261). Therefore, KLFs may influence estrogen receptor signalling and modulate ERα target gene transcription and thus have a potential to promote or impair endocrine-responsive cancers.

1.4.2 VAV-interacting Krüppel-like factor

The focus of this PhD is on the role of VAV interacting Krüppel-like factor (VIK-1) in breast cancer. VIK-1 is a newly characterised member of the Krüppel-like factor family (Figure 1.7), which was originally identified in a yeast two-hybrid screen by virtue of its interaction with VAV1.

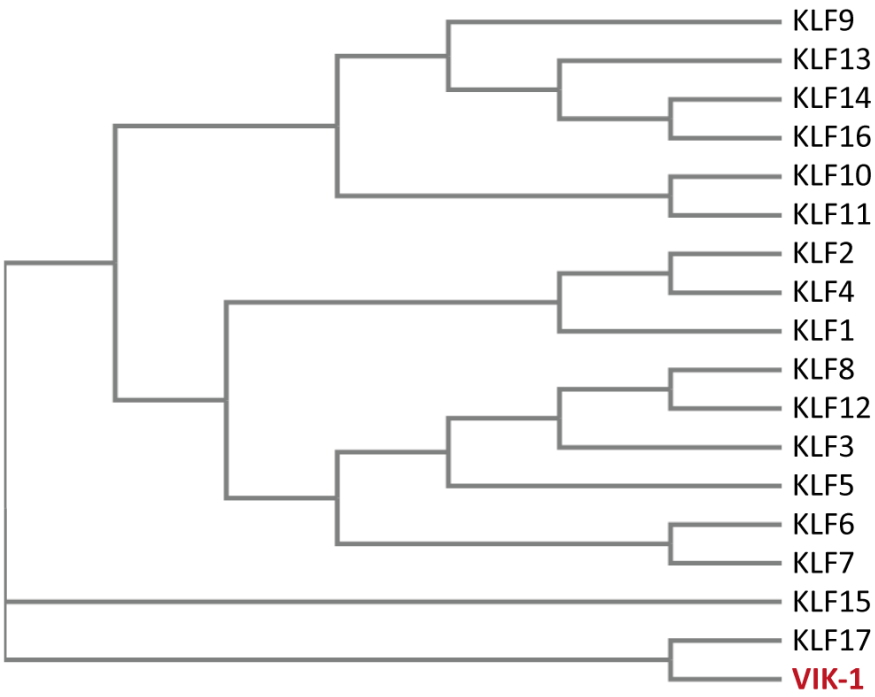

Figure 1.7 Phylogenetic tree of Krüppel-like factors. Molecular phylogenetic analysis based on the protein sequence showing the relationships of known human KLFs including VIK-1. Generated using Clustal Omega (2).

1.4.2.1 VAV1

VAV1 was first identified as a proto-oncogene, whose transforming capacity resulted from production of a truncated protein (262). Its isolation led to identification of wild type VAV1 and subsequent identification of other family members. The VAV proteins are a family of signal transduction molecules. The best known function is that of a Rho-guanine nucleotide exchange factor (GEFs), although increasing evidence indicates the proteins might have other roles. There are currently three known members in mammalian cells VAV1, VAV2, and VAV3, all share a similar structure. In addition to the Dbl (DH) and plekstrin-homology (PH) typical of Rho GEFs, the proteins contain a calponin-homology (CH) domain, an acidic region, a zinc finger domain and two src-homology 3 (SH3) domains flanking a single src-homology 2 (SH2) region (263). These domains support functional activity beyond just GEF.

As GEFs, these proteins act as enzymes to catalyse the release of GDP from the inactive GTPases, a step that favours the subsequent incorporation of GTP and the acquisition by the GTPases of active conformations capable of interacting with effector molecules. VAV proteins differ from other GEFs in that their catalytic activity is modulated by direct tyrosine phosphorylation (264, 265). It is now thought that the GEF function of VAV proteins is highly dependent on the interaction of other adaptor proteins that aid the appropriate phosphorylation of VAV (263).

VAV1 functions as a guanine nucleotide exchange factor for the Rho family of GTPases, and plays an important role in T-cell development and signalling, including calcium flux and cytoskeletal reorganisation (266). VAV1 is normally exclusively expressed in cells of the haematopoietic linage (267), where it is an important mediator of T cell receptor (TCR) signalling and is required for development of T cells in the thymus and for their activation

and proliferation in response to antigen stimulation (268). Despite this normally restricted expression pattern, VAV1 is ectopically expressed in a number of cancers. In a screen of 42 primary neuroblastomas, 76% expressed VAV1 (269). VAV1 was identified in more than 50% of pancreatic ductal adenocarcinomas, where VAV1 positive tumours had a worse prognosis compared to VAV1 negative tumours (270). VAV1 was also over expressed in up to 46% of primary lung cancers (271) and has been correlated with a more aggressive tumour behaviour (272). Expression of VAV1 has also been observed in ovarian and prostate cancers (273). Whilst aberrant expression of VAV1 is clear in a number of cancers, how VAV1 is expressed and the role of ectopic VAV1 in these tissues is uncertain.

Published data on the role of VAV1 in breast cancer is unclear and sometimes contradictory. VAV1 has been reported as overexpressed in 62% of cases (274), whilst another group observed VAV1 expression in all but 5 out of 137 breast tumours (275). In breast cancer cells lines VAV1 was indicated to have pro-apoptotic role dependent on p53 (274). However, another study indicated ER mediated upregulation of VAV1 led to increased cyclin D levels and cell cycle progression, therefore concluded VAV1 might contribute to proliferation of breast cancer cells (276).

1.4.2.2 Vav-interacting Krüppel-like Factor (VIK-1)

VIK-1 is a splice variant of the ZNF655 gene, located on the long arm of chromosome 7 (Figure 1.8), with three splice variants as characterised by Houlard *et al* (277). The best characterised isoform is VIK-1, which was shown to be expressed in a variety of tissues. A larger isoform known as VIK-2, was only detected in peripheral blood lymphocytes and a third smaller isoform known as VIK-3 was weakly detected in all analysed tissues (277). Six zinc finger motifs, organised as three tandem repeats within the c-terminal region are

conserved between both VIK-1 and VIK-2. These classical zinc finger domains, which can bind DNA, RNA and protein, are well conserved between all Krüppel-like factor family members. The slightly larger VIK-2 differs only from VIK-1 by an additional KRAB (Krüppel associated box) B domain. A VAV1 binding region and CDK4-binding region are also conserved between VIK-1 and VIK-2. The smallest isoform, VIK-3 shares only the first 135 base pairs (Exon 1) with the other isoforms, and contains no zinc finger or KRAB B domains. Instead VIK-3 contains a proline-rich domain and a KRAB A domain, not present in VIK-1 or -2, and an additional region with no sequence similarity to any known functional domains (277). KRAB A and KRAB B domains function as transcriptional repressors (278). Proline rich regions are capable of rapid but relatively unspecific binding to substrates and are found in many transcription factors (279).

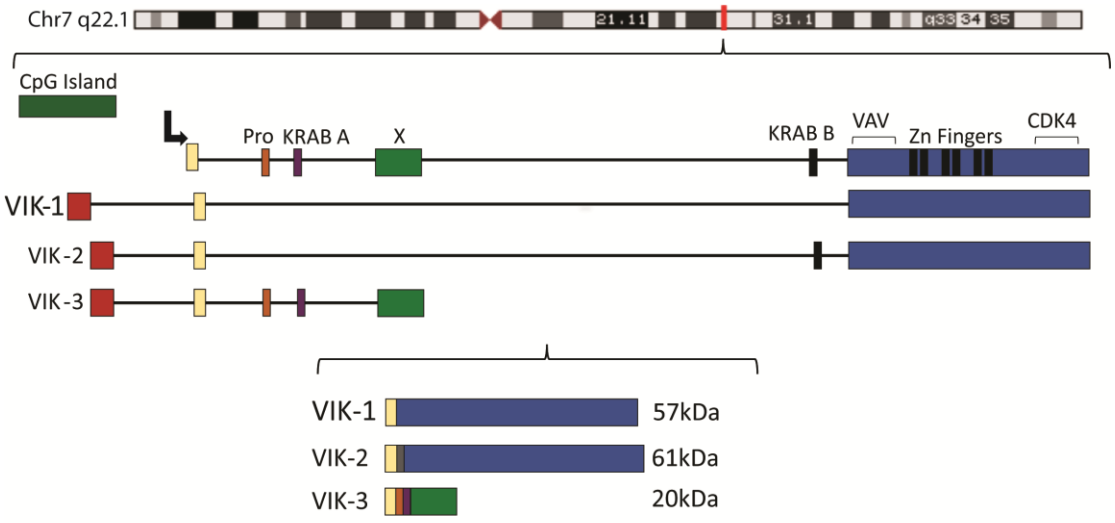

Figure 1.8. Schematic representation of the genomic organisation of the 3 alternately spliced VIK isoforms. There are 3 isoforms VIK-1 (57kDa), VIK-2 (61kDa) and VIK-3 (20kDa). A large CpG island is located upstream of the ATG start site. VIK-1 contains 6 zinc finger domains and a separate VAV1 interacting domain and CDK4 interacting domain. These domains are conserved within the larger isoform VIK-2, which has an extra KRAB B domain. A smaller isoform VIK-3 contains a proline rich domain (Pro), KRAB A domain and an unknown domain (X).

Presently, very little is known about the function of VIK-1. Whilst its structure suggests VIK-1 has the ability to bind DNA, RNA and protein, only its protein interactions have been explored so far in the single published paper regarding VIK-1 (277). In addition to its interaction with the c-terminal SH3 domain of VAV1 (amino acids 787-837), the VIK-1 protein also interacts with CDK4 through another independent domain. Additionally the protein is able to shuttle between the cytoplasm and the nucleus, with a limited expression within the nucleolus, under the control of a functional nuclear export sequence. VIK-1 is variably expressed during the cell cycle, predominantly in the G1 phase. Over-expression of VIK-1 blocks cell cycle progression, an effect reversible by expression of VAV1 as co-expression of both proteins leads to progression through G1 and into S phase (277) (Figure 1.9).

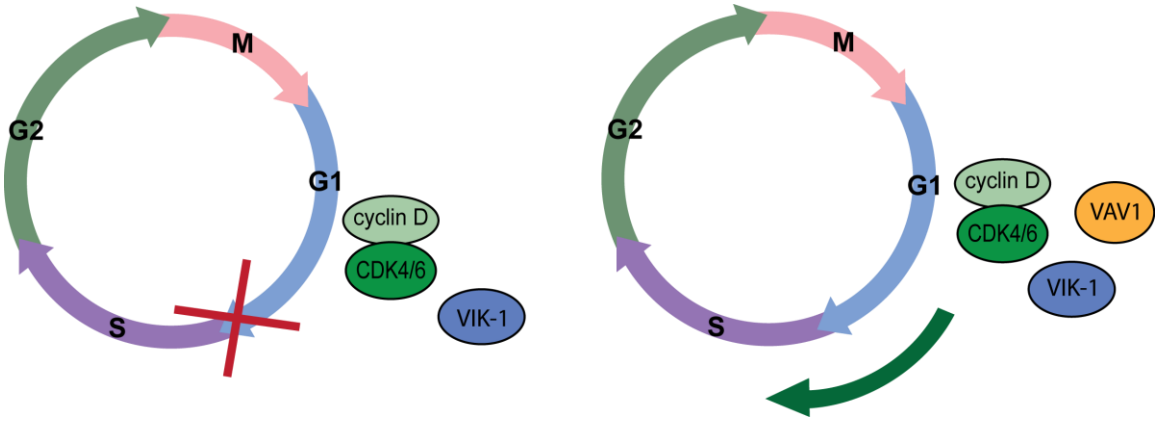

Figure 1.9. Schematic representation of the published role of VIK-1 in cell cycle. VIK-1 is able to interact with both CDK4 and VAV1. When VIK-1 is over-expressed alone, the cell cycle is halted in G1. When VIK-1 is co-expressed with VAV1, cells are able to progress through the G1/S phase checkpoint as normal.

A methylation array identified VIK-1 as a novel target for epigenetic silencing in breast cancer. A genome-wide methylation array was utilised to identify aberrant methylated regions across breast cancer cell lines, to determine potential genes that could be regulated by transcriptional silencing via epigenetic means. Preliminary results from our lab showed that in a cohort of ER positive breast cancer patient samples, VIK-1 methylation was associated with increased risk of recurrence in tamoxifen-treated patients. VIK-1 methylation was additionally associated with poor outcome in patients treated with tamoxifen. There was a strong trend observed towards shorter survival in methylated patients, independently of ER, tumour size or grading (Figure 1.10) (280). This led to the hypothesis that VIK-1 may have a role in estrogen receptor positive breast cancer and VIK-1 methylation could be a marker for poor prognosis in breast cancer. This, combined with the functional role in cell cycle regulation, suggested the role of VIK in breast cancer warranted further investigation.

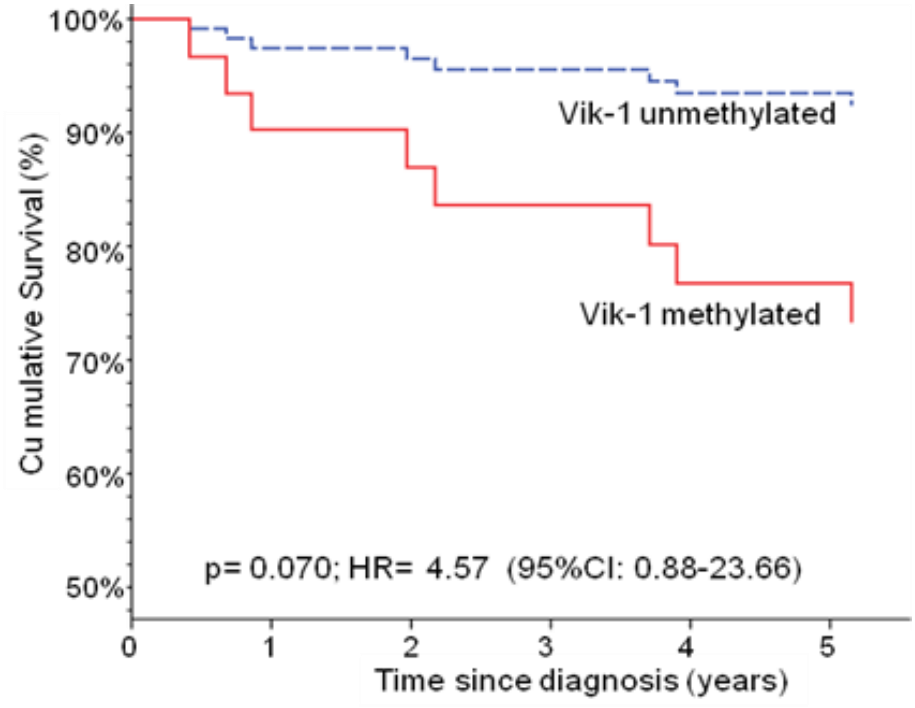

Figure 1.10. Methylation of VIK-1 and patient outcome. Kaplan-Meier curve for overall survival in a panel of 226 patients with stage I-III primary breast cancer treated with adjuvant tamoxifen with respect to VIK-1 methylation status. Figure from Crook et al (unpublished data).

2 Aims and Objectives

Confirm the epigenetic regulation of VIK-1 in breast cancer

Preliminary data identified VIK-1 as a novel potential target for epigenetic silencing in breast cancer cells. The first aim of this PhD was to confirm the whether methylation-dependent transcriptional silencing is a mechanistic basis for VIK-1 down-regulation and to identify the importance of this epigenetic silencing in breast cancer. Further to this, a preliminary patient cohort linked methylation of VIK-1 to patient survival. Therefore, this PhD aimed to further determine VIK-1 expression and methylation in primary breast cancer samples, and confirm the significance of VIK-1 methylation on patient outcome.

Examine the functional role of VIK-1 in estrogen receptor positive breast cancer and potential role in endocrine resistance

Krüppel-like factors have been previously linked to estrogen receptor signalling. The preliminary breast cancer cohort suggested differential outcome in patients receiving endocrine therapy with regards to VIK-1 levels and methylation. Additionally, there was an increased risk of recurrence following tamoxifen treatment. This particularly indicated a role for VIK-1 in estrogen receptor positive breast cancer, and potentially a role in resistance to endocrine therapy. Therefore, the second aim of this PhD was to investigate the potential for VIK as a determinant of sensitivity to endocrine therapy and examine the functional consequences of modulating VIK expression within ER positive breast cancer.

Investigate the role of VIK-1 within the cell cycle with regards to its interaction with VAV1 and CDK4

VIK has been suggested to play a role in cell cycle progression, interacting with CDK4 and VAV1. VIK-1 has been shown to inhibit cell cycle progression through G1 to S phase, an inhibition that might be reversed by presence of VAV1. Therefore, the aim was to investigate, in breast cancer, the role of VIK-1 on cell cycle progression and effect on proteins involved in G1/S phase transition. In addition, to elucidate the interaction of VIK-1 and VAV1. Furthermore, the interaction with CDK4 could suggest VIK-1 as a determinant of sensitivity to CDK4/6 inhibitors. The final aim of this PhD was to investigate any potential relationship between VIK-1 and sensitivity to palbocicilib, a specific CDK4/6 inhibitor.

3. Materials and Methods

3.1 Cell Culture Assays

3.1.1 Cell Culture and reagents

A panel of breast cancer cell lines was selected from a variety of disease states. All cells were grown in a 5% CO_2 humidified atmosphere at 37°C, in cell culture media (base media indicated in Table 3.1). Unless otherwise stated baseline media was supplemented with 2mM L-glutamine and 10% foetal bovine serum (FBS). MLET5 and LCC9 were supplemented with 2nM L-glutamine 10% double stripped serum (DSS). MCF10A media was supplemented with 5% horse serum (Invitrogen), 2mM L-glutamine 20ng/ml, EGF (Sigma), 0.5mg/ml hydrocortisone (Sigma), 100ng/ml cholera toxin (Sigma) and 10μg/ml insulin (Sigma).

All cells were adherent monolayer human cell lines. Cells were passaged through trypsination. Media was removed and cells washed with PBS. 1x trypsin-EDTA was added and cells incubated at 37°C, until cells had visibly detached. Appropriate media supplemented with FCS, which contains trypsin inhibitors, was added to at least 3 times the volume of trypsin, cells were then resuspended and seeded into the new culture vessel.

Cell Line	Media	Tumour origin	Subtype	ER	PR	HER
BT549	RPMI 1640	invasive ductal carcinoma	Triple negative, basal	-	-	-
MDA-MB-231	DMEM	adenocarcinoma	Triple negative, basal	-	-	-
MDA-MB-436	DMEM	adenocarcinoma	Triple negative, basal	-	-	-
Hs578T	DMEM		Triple negative, basal	-	-	-
MDA-MB-468	DMEM	adenocarcinoma	Triple negative, basal	-	-	-
Hcc1937	RPMI 1640	primary ductal carcinoma	Triple negative, basal	-	-	-
MDA-MB-453	DMEM	metastatic luminal	Triple negative	-	-	-
T47D	RPMI 1640	ductal carcinoma	ER positive, luminal A	+	+	-
MCF7	RPMI 1640	adenocarcinoma	ER positive, luminal A	+	+	-
MLET5	DMEM-phenol red	MCF7-derived, ectoposide resistant	ER positive, luminal A	+	+	-
LCC9	DMEM-phenol red	MCF7-derived, fulvestrant resistant	ER positive, luminal A	+	+	-
SUM44	DMEM + 500nM		ER positive, luminal A	+	-	-
ZR751	RPMI 1640	ductal carcinoma	ER positive, luminal A	+	-	-
MDA-MB-361	Leibovitz's L-15	adenocarcinoma	HER2 positive, luminal	+	-	+
SKBR3	McCoys	adenocarcinoma	HER2 positive, basal	-	-	+
JIMT1	DMEM	ductal carcinoma	HER2 positive, basal	-		+
BT474	DMEM	invasive ductal carcinoma	HER2 positive, luminal	-	+	+
Hcc1569	RPMI 1640	primary metastatic	HER2 positive, basal	-	-	+
Hcc1954	RPMI 1640	ductal carcinoma	HER2 positive, basal	-	-	+
MCF10A	DMEM F12	normal breast epithelium		-	-	-

Table 3.1: Panel of breast cancer cell lines. The panel of cell lines covered a wide range of breast cancer subtypes with varying tumour origin. Subtype is determined by positive (+) or negative (-) expression of the estrogen receptor (ER), progesterone receptor (PR) or epidermal growth factor receptor (HER2).

3.1.2 siRNA knockdown

Cells were reverse transfected with gene targeting siRNA (Dharmacon, table 3.2) or a scrambled non-targeting control (Allstars negative control siRNA, Quiagen) and Lipofectomine (Life Technologies). siRNA was added to the well followed by lipofectamine (both prepared in serum free media). Complexes were formed with a lipofectamine:siRNA ratio of either 15:1 with 20nM siRNA (T47D, MCF7, MCF10A) or 6.25:1 with 80nM siRNA (SUM44). Plates were incubated at room temperature for 20 min for complexes to form before cells were seeded. 24 hours after transfection the media was changed. Transfected cells were then used for assays as described below, or washed in PBS and cells collected for RNA and protein isolation.

Table 3.2: siRNA target sequences.

Target Gene	Target Sequence
VIK siRNA 1	CCGACAUGGAACAGGGACU
VIK siRNA 2	CACCAAGGGUCCAGUUUCA
VIK siRNA 3	AGGAAAUACCAGCCCAGGA
VAV1	CGACAAAGCUCUACUCAUC

3.1.3 Vector expression of VIK-1

Cells were seeded to 60% confluency. Complexes of VIK-1 expression vector (PCDNA3.1-VIK-1 or pEGFP-VIK-1) or corresponding empty vector containing no insert with Xtremegene reagent (Roche), at a ratio of 1:2, were incubated for 20 minutes at room temperature before addition to the cells. Cells were either transiently transfected for 72 hours or plasmid expressing cells were selected by growth of drug resistant colonies with G418 (Sigma), either 200µg/ml for MCF7 and MLET5 or 300µg/ml for LCC9. A kill curve was

carried out to determine concentration of G418 and the IC_{50} concentration at day 5 of drug treatment were used.

3.1.4 MTT cytotoxicity assay

3-(4,5-Dimethylthiazol-2-yl)-2,5-Diphenyltetrazolium Bromide (MTT, Alpha Aesar) was dissolved in supplemented media at a stock concentration of 2mg/ml. At the indicated time points, MTT assay was added at a 1:3 dilution, directly to the cell culture well (0.66mg/ml final concentration) and cells incubated for 1.5-3 hours at 37°C. The media was then removed and DMSO added to solubilise the dye (100 µl in a 96 well plate) Optical density (OD) was read at 570nm and 650nm (Perkin-Elmer 1420 Plate reader). The 650nm reading was subtracted from 570nm to account for background.

For IC_{50} assays, cells were seeded or transfected and allowed to adhere for 24 hours then treated with varying concentrations (0.005µM-10µM) of palbociclib (SelleckChem) or DMSO vehicle control as indicated for 6 days. Values were normalised to the vehicle control and IC_{50} determined using GraphPad Prism (GraphPad software). Briefly, drug concentrations were Log_{10} transformed and plotted against the normalised OD value. Non-linear regression for normalised dose-response inhibition was applied to calculate IC_{50} values. Experiments were performed in triplicate and a representative IC_{50} curve is presented as average of technical triplicates ±SD.

3.1.5 Estradiol stimulation

Cells were seeded and after 24 hours cells were washed 3 times with PBS and media replaced with RPMI 1640 without phenol red plus 10% double stripped serum (DSS) for 72 hours before addition of 1nM β-estradiol (E2, Sigma) or equivalent concentration of

ethanol vehicle control. Cells were collected following treatment for RNA or protein analysis.

3.1.6 TGF-β and EGF stimulation

Cells were seeded and allowed to adhere overnight. 10ng/ml TGF-β (Sigma), 40ng/ml EGF (Sigma) or vehicle control was added directly into the cell culture media and incubated at 37°C for the indicated time point.

3.1.7 Hypoxia

For hypoxic treatment cells were exposed to 1% oxygen, 5% CO_2, within a Ruskinn Invivo2 400 hypoxic workstation, for either 24 or 48 hours. The chamber was humidified and maintained at 37°C.

3.2 Generation of palbociclib resistant cell lines

Drug resistant variants of each cell line were derived from the original parental cell line through continuous exposure to pabociclib. Following initial dose-response studies over a range of palbociclib doses (0.1nM-10μM), IC_{50} values were determined. T47D and MCF7 cell lines were cultured in increasing concentrations of pablociclib starting with 200nM, approximately the IC_{50} value. Drug sensitive cells died and the remaining live cells were cultured in this dose until cells were outgrowing the dose. At this point the drug concentration was increased. This was continued over a period of 6 months, gradually increasing the drug concentration to 1μM. Individual clones were selected from each cell line and MTT assays were performed to determine IC_{50} values. Three clones of each cell

line exhibiting drug resistance were continued. Resistant clones were then maintained with 1µM palbociclib in the culture media.

3.3 Quantitative Real Time PCR

3.3.1 RNA extraction and preparation of cDNA

Total RNA was extracted using a phenol based extraction protocol. TriReagent (Sigma) was added to cells and homogenised. 1-bromo-3-chloro-propane (Sigma) was added at 1 in 10 dilution, cells were vortexed then centrifuged for 10min at 12,000rpm 4°C. The aqueous phase top layer was transferred into a new tube and an equal volume of propan-2-ol added. Following vortexing and a 10 minute incubation at room temperature, the sample was centrifuged at 12,000rpm for 5 minutes to pellet the RNA. The supernatant was removed and 75% ethanol added. The sample was centrifuged at 12,000rpm for 5 minutes, the supernatant was removed and air-dried before the pellet was resuspended in RNAse free water. The RNA was quantified using a spectrophotometer (Nanodrop ND-1000). 100ng of RNA was reverse transcribed using Multiscribe Reverse Transcriptase (Applied Biosystems High Capacity Reverse Transcriptase cDNA kit) as per manufacturer's instructions, incubating at: 25°C 25 minutes, 37°C 120 minutes, 85°C 5 minutes (Applied Biosystems 7500 thermal cycler).

3.3.2 TaqMan quantitative PCR

Quantitative real time PCR for total VIK and VAV1 was carried out using individual TaqMan gene expression assays (Life Technologies) and TaqMan Universal PCR Master Mix (Life Technologies) to determine expression of each gene. RPLPO was used as a reference gene

to which VIK-1 and VAV1 expression was relatively calculated. Cycling conditions were as follows: Initially 95°C for 10 min, then 95°C 15 seconds, 60°C 1 minute for 40 cycles using a Stratagene Mx300P QPCR System (Agilent Technologies). C_T values were determined at the intersection of the amplification curve and a threshold line set at 0.1 for all experiments. The average C_T was taken of technical duplicates. For data analysis the comparative C_T method was used (281). C_T values for RPLPO were subtracted from gene of interest values, giving a ΔC_T value. Fold difference was calculated using the formula: $2^{(-\Delta C_T)}$, giving the RNA expression of the gene of interest relative to RPLPO. Standard deviation was calculated for each data set as outlined in the Applied Biosystems guide to performing relative quantitative gene expression.

3.3.3 SYBR Green quantitative PCR

For each VIK isoform SYBR Green assays were utilised (Table 3.2). Primers were designed using Primer3 software (www.primer3.ut.ee). PCR reactions were carried out with a final volume of 10µl, using 500nM of each primer and 2ng of cDNA, and 2x SYBR Green PCR master mix (Life Technologies). Cycling parameters were as above, followed by melt curve acquisition. ΔC_T and fold change were calculated as above. Due to the sequence similarity of VIK-1 and VIK-2 it was not possible to design primers to solely detect VIK-1, so VIK-1 expression was determined by subtraction of VIK-2 expression from total VIK-1+VIK-2 expression. A standard curve of cDNA for each primer pair was performed and efficiency calculated from the slope (efficiency=$-1+10^{(-1/\text{slope})}$) (282)**.** A slope between -3.1 and -3.6, corresponding to an efficiency of 90-110%, is generally considered acceptable. All SYBR Green primers had an efficiency within the acceptable range (Figure 3.1).

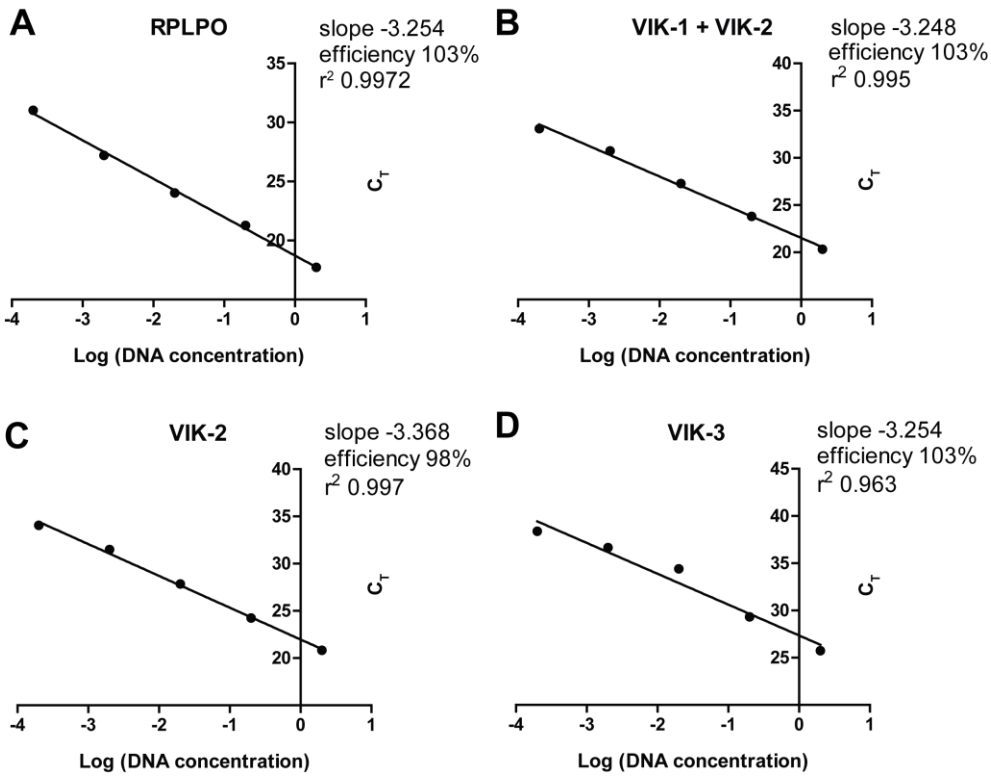

Figure 3.1. Efficiency of SYBR Green primers. A standard curve was performed for each primer pair and primer efficiency was calculated from the slope of the curve where efficiency=$-1+10^{(-1/\text{slope})}$.

Gene	Forward Primer	Reverse Primer	Slope	Primer efficiency
VIK-1 + VIK-2	TGAATGTCATGAACCCGAAA	GGTGGGAGAGATCCATTAAGC	-3.248	103%
VIK-2	ACTGGGGGATTTCCAATTTC	CTGGTCTCTCCATCTGAGCA	-3.368	98%
VIK-3	CAGGAGTTTGTGACATTCG	AGAAGTATGCCCAGTCAG	-3.254	103%
RPLPO	GCGACCTGGAAGTCCAACTA	GGATCTGCTGCATCTGCTTG	-3.254	103%

Table 3.3. SYBR Green qPCR primers. Primer pairs were designed to amplify each isoform of VIK, or the housekeeping gene RPLPO.

3.4 RNA sequencing

RNA was extracted using RNeasy Qiagen kit. The BCI genome centre prepared the RNAseq library (polyA mRNA) sequenced the libraries using paired-end Illumina NextSeq 500 high output Run (150 cycles). TopHat (version 2.0.9) was used to align paired end reads to the human genome (hg19) (283). HTSeq package (version 0.6.1p1) was used to count the overlap of reads with genes using GENCODE version 19 human gene annotation (284). The read count data was filtered to keep genes that achieved at least one read count per million in at least three samples. Reads per kilobase per million mapped reads (RPKM) values were calculated with the conditional quantile normalisation (cqn) counting for gene length and GC content, using the R statistical environment via Bioconductor packages.

3.4.1 Differential expression analysis

LIMMA (linear models for microarray data) was applied to fit a linear model to RPKM values for each gene to determine genes that were differentially expressed between sensitive and resistant groups. Differentially expressed genes were evaluated using LIMMA empirical Bayes statistics module (285). The adjusted p-values (false discovery rate) was estimated by the Benjamini and Hochberg procedure (286). The differentially expressed genes were selected when the adjusted p-value was less than 0.05 and the absolute value of log-fold change was more than 1. Bioinformatic analysis was carried out by the bioinformatics group at BCI.

3.5 Protein Analysis

3.5.1 Cell lysis and quantification

Cells were washed in ice cold PBS and lysed in ice cold RIPA buffer (150 mM sodium chloride, 1.0% NP-40 or Triton X-100, 0.5% sodium deoxycholate, 0.1% sodium dodecyl sulphate, 50 mM Tris, pH 8.0) with protease inhibitor (cOmplete mini Protease Inhibitor, Roche) and phosphatase inhibitors (phosphatase inhibitor cocktail, Sigma) shaking for 20 minutes at 4°C. Lysates were centrifuged 10,000rpm, 4°C for 10 minutes and the supernatant removed into a fresh tube.

Protein was quantified using Pierce BCA protein Assay Kit (Life Technologies). 5µl of bovine serum albumin protein standards ranging from 0.125-2mg/ml were added to a 96 well plate in duplicate and 1µl of sample protein lysates. Reagents A was added to Reagent B at a 1 in 50 dilution and then 200µl was added per well. The plate was incubated at 37°C for 30 minutes and read at 750nm on a plate reader (Perkin Elmer). Protein concentrations were calculated by comparison to the protein standard curve. Lysates were diluted in 2x Laemmli buffer (4% SDS, 20% glycerol, 0.004% bromophenol blue, 0.125M Tris HCl, pH6.8) plus 10% β-mercaptoethanol (Sigma), then denatured at 90°C for 10 minutes.

3.5.2 Western Blot

20-40µg of protein was resolved by SDS-page electrophoresis on a 10% acrylamide gel, run at 150 volts for 1 hour in standard running buffer (Tris Glycine SDS, Severn Biotech) in a Mini Trans Blot system (Bio-Rad). Proteins were transferred onto a PDVF membrane (GE Healthcare) activated in methanol using a wet transfer conditions for 1 hour at 300mA in

transfer buffer (Tris Glycine, Severn Biotech, plus 20% Methanol). Membranes were blocked in 5% non-fat milk in PBS-T (1x TBS with 0.001% Tween) for 1 hour, or 5% BSA-TBS-T (1x PBS with 0.001% Tween) for pRb, shaking at room temperature. Membranes were incubated in primary antibody (Table 3.4) diluted in blocking buffer, shaking overnight at 4°C. After 3 times 10 minute washes in PBS-T, membranes were incubated in secondary antibody at room temperature for 45 minutes. Membranes were washed 3 times again in PBS-T and visualised using ECL Plus (BioRad) using SynGene G:Box system. Densitometry quantification of western blots was performed using the gel analysis tool from ImageJ software. Density of each band was determined and normalised to density of the β-actin loading control from the same lane.

Protein	Dilution	Host Species	Company
β-Actin	1:5000	Rabbit	Cell Signalling #4970
VIK	1:750	Rabbit	Custom made (Eurogentech)
VIK	1:15000	Rabbit	Abnova PAB22301
VIK	1:2000	Rabbit	Aviva ARP39587
CDK4	1:1000	Rabbit	Cell Signalling #12790
Cyclin D	1:500	Rabbit	Santa Cruz sc-753
Rb	1:1000	Mouse	Cell Signalling #9309
pRb s780	1:1000	Rabbit	Cell Signalling #9307
Cyclin E	1:200	Mouse	Santa Cruz sc-56310
CDK1	1:1000	Mouse	Abcam ab18
CDK2	1:500	Mouse	Santa Cruz sc-6248
E2F1	1:200	Mouse	Santa Cruz sc-251
p27	1:100	Mouse	Santa Cruz sc-56338
Full length PARP	1:1000	Rabbit	Cell Signalling #9542
Cleaved PARP	1:1000	Rabbit	Cell Signalling #9661
GFP	1:1000	Mouse	Roche 11814460001
Rabbit	1:2000	Goat	Cell Signalling #7074
Mouse	1:2000	Goat	Cell Signalling #7076

Table 3.4. Table of antibodies used for western blot analysis.

3.5.3 Immunoprecipitation

Cell were first transfected with pEGFP tagged VIK expressing vector, or empty pEGFP vector as described above, for 48 hours. A master mix of 2% BSA/PBS and 2µg of antibody either GFP or Mouse IgG control, was prepared for each reaction. 2µg of antibody was conjugated to 35µl of protein A agarose beads (Millipore) overnight at 4°C with rotation. After 3 washes in ice cold PBS, cells were lysed in RIPA + protease and phosphatase inhibitors. To inhibit any proteasome degradation of VIK protein, 10µM MG132 was added to media for 2 hours prior to cell lysis, and also to the RIPA lysis buffer. Cells were kept on ice and vortexed 3 times, then centrifuged for 14,000rpm for 10 minutes at 4°C. 50µl of the supernatant was saved for input and the remainder used in the IP. Following antibody conjugation, the beads were centrifuged at 3,500rpm for 1 minute. The protein lysate was transferred to the beads and incubated for 4 hours at 4°C with rotation. Beads were washed 3 times with 75:25 RIPA:PBS, then once with PBS. 35ul of 2x Laemmlli sample buffer was added to the beads and sample boiled for 5 minutes at 95°C. Samples were resolved by SDS-page and blotted as described above.

3.5.4 Coomassie Blue staining

Proteins were resolved on an agarose gel as describe above. The gel was rinsed with distilled water then fixed in 50% methanol, 10% acetic acid for 1 hour. The gel was rinsed with distilled water then incubated in staining solution (0.1% coomassie brilliant blue, 50% methanol, 10% acetic acid) for 2 hours with gentle agitation. The gel was destained in destaining solution (40% methanol, 10% acetic acid) for 2 hours with gentle agitation, and replacement of destaining solution several times, until the background of the gel was fully destained. The protein band was cut out from the gel and frozen before mass spectrometry

analysis. Mass spectrometry analysis was carried out by the Barts Cancer Institute mass spectrometry laboratory.

3.5.5 Immunofluorescence

Cells were seeded onto sterile glass coverslips in a 6 well plate and incubated as normal for 3 days. Media was aspirated and wells washed in PBS. Cells were fixed in 4% paraformaldehyde (PFA) for 1 hour at room temperature. After washing in PBS cells were permeabilised in 0.2% triton-X in PBS for 10 minutes at room temperature. Cells were blocked in 1% BSA, 2% FCS in PBS for 30 minutes at room temperature. Cells were incubated with custom Rabbit anti-VIK antibody 1:1000 dilution in blocking buffer, or blocking buffer alone for a secondary only control, overnight at 4°C. After 3 washes, each for 5 minutes, cells were incubated in 1:1000 dilution of secondary antibody (Goat anti Rabbit Alexa Flour 488, Thermo Fisher Scientific), in the dark at room temperature for 45 minutes. Cells were again washed 3 times in PBS, and mounted onto glass microscopy slides using anti-fade fluoromount aqueous mounting medium (Sigma) containing a 1:10000 dilution of DAPI (4',6-diamidino-2-phenylindole). 3D image stacks were acquired on an Olympus DeltaVision microscope (Applied Precision) in 0.2µm steps, using the Olympus X40 oil objective.

3.6 Methylation analysis

3.6.1 DNA extraction from cell lines

Genomic DNA was extracted from cell lines using GenElute blood genomic DNA extraction kit (Sigma). Cells were resuspended in 200µl PBS and added to 10µl of Proteinase K (to digest proteins), then 200µl of resuspension solution added. Cells were lysed by addition of

200µl of Lysis solution C and incubation at 55°C for 10 minutes. 500µl of column preparation solution was added to each column, and centrifuged 12,000rpm for 1 minute, to maximise binding of DNA to the column. To prepare the DNA for binding 200µl absolute ethanol was added to each lysate and thoroughly vortexed, before transfer to the prepared column. Samples were twice washed with Wash Solution and centrifuged for an additional minute to remove any residual ethanol. 200µl of elution solution was added to the column for 5 minutes at room temperature then centrifuged for 1 minute to elute DNA.

DNA was quantified using a spectrophotometer (Nanodrop ND-1000). The ratio of absorbance at 260nm and 280nm was used to assess the purity of the DNA, with a ratio of 1.8 accepted as 'pure' DNA.

3.6.2 DNA extraction from primary breast cancer tissue samples

DNA was extracted from FFPE embedded tissue on uncharged slides. Paraffin was first removed by immersing the slides twice in xylene for 10 seconds, followed by 2 times 10 second washes in ethanol. The slides were air dried to allow ethanol evaporation, and tumour sections were scraped off in lysis buffer with a sterile scalpel and placed into eppendorf tubes. DNA was extracted from FFPE primary breast cancer samples using Allprep DNA/RNA FFPE kit (Qiagen), as per the manufacturer's instructions. Briefly, the tissue was lysed in the presence of proteinase K for 15 minutes at 56°C. Following 3 minutes incubation on ice, samples were centrifuged at 12,000rpm at room temperature. The pellet is further lysed in the presence of proteinase K at 90°C for 2 hours. The genomic DNA was resuspended in buffer AL with ethanol and applied to the mini elute spin column. The DNA was bound to the silica membrane and washed with buffer AW1 and AW2 followed by ethanol to remove contaminants. DNA was eluted in 50µl of buffer TE.

A standard curve of bacteriophage lambda DNA was prepared in TE buffer ranging from 2.5ng/µl to 25pg/µl. In a 96 well plate 1µl of DNA was diluted in 50µl working PicoGreen solution (Life Technologies). The plate was incubated at room temperature for 5 minutes protected from light. The fluorescence was read at 520nm (Perkin Elmer Plate Reader) and DNA concentration calculated from the standard curve.

3.6.3 Bisulphite conversion

DNA was bisulphite converted, where unmethylated cytosine residues are converted to uracil by addition of a bisulphite group. Bisulphate modification was carried out using an EZ DNA methylation kit (ZymoResearch) following manufacturer's instructions, using 500ng DNA extracted from cell lines. The kit is based on the three-step reaction between an unmethylated cytosine and sodium bisulphite (Figure 3.2). Therefore the converted DNA sequence reflects the methylation status. 500ng of DNA was diluted to 45µl in molecular grade water, 5µl of M-dilution buffer was added. Samples were incubated at 37°C for 15 minutes. 100µl of CT conversion reagent was added to each sample, samples were incubated in the dark at 50°C overnight, where unmethylated cytosines were converted to uracils. Samples were incubated on ice for 10 minutes, and then added to 400µl of M-binding buffer preloaded into the Zymo-spin column. Following centrifugation at 12,000rpm for 30 seconds, 100µl of M-wash buffer was added. Columns were again centrifuged, then 200µl of desulphonation buffer added, samples were incubated at room temperature for 15 minutes to desulphonate the DNA. This was followed by 2 washes with M-wash buffer. DNA was eluted in 50µl of M-elution buffer.

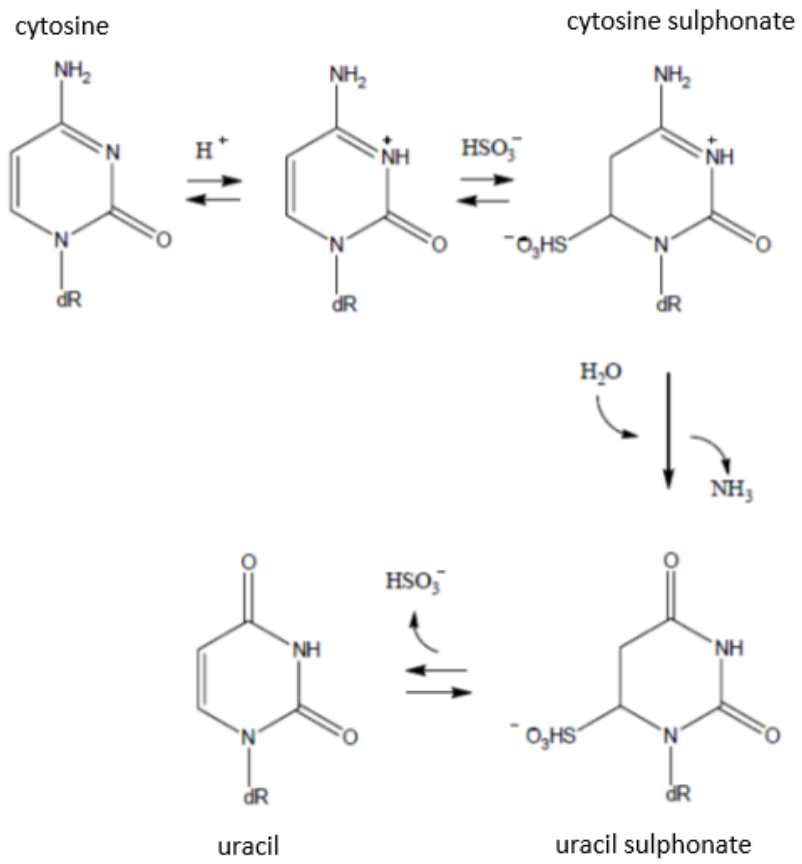

Figure 3.2. Bisulphite conversion of cytosine to uracil. Step 1, unmethylated cytosines are protonated. Bisulphite (HSO_3) treatment transforms the protonated cytosine into cytosine sulphonate. Step 2, overnight incubation produces uracil sulphonate. Step 3, deamination and following desulphonation forms uracil. Only unmethylated cytosines will react with bisulphite, forming uracil. Cytosines methylated at the 5th carbon position will not, thereby remaining cytosine (287).

3.6.4 Pyrosequencing

100ng of bisulphite converted DNA was amplified by PCR using Pyromark PCR kit (Qiagen) using the following conditions: 95°C for 10 min, then 40 cycles of 94°C 30 seconds, 54°C 30 seconds, 72°C 30 seconds followed by 72°C for 10 min. 0.5µM of primers was used in a final reaction volume of 30µl (forward primer GGGTAAGGTTTTTTGAGGA-5'BIOT, reverse primer CCACTTTTAAAATCAAACCCT). The PCR product was then used as the template for pyrosequencing using the PyroMark Q96 Vacuum Prep workstation (Qiagen). The biotinylated PCR product was bound to streptavidin coated sepharose beads, then immobilised, washed, denatured and annealed to the non biotinylated sequencing primer at 80°C for 2 minutes. Commercially available methylated DNA was used as a positive control and placenta DNA used as a negative control. In pyrosequencing the DNA sequence is determined by light emitted upon incorporation of complementary nucleotides. The proportion of methylation at each CpG can be quantified based on the ratio of C to T nucleotides incorporated. Methylation values were calculated as average methylation over 8 CpG sites.

For primary breast cancer samples 100-500 ng of DNA was sent to the Barts Cancer Institute Genome Centre (Queen Mary, University of London) for pyrosequencing using their standard protocols.

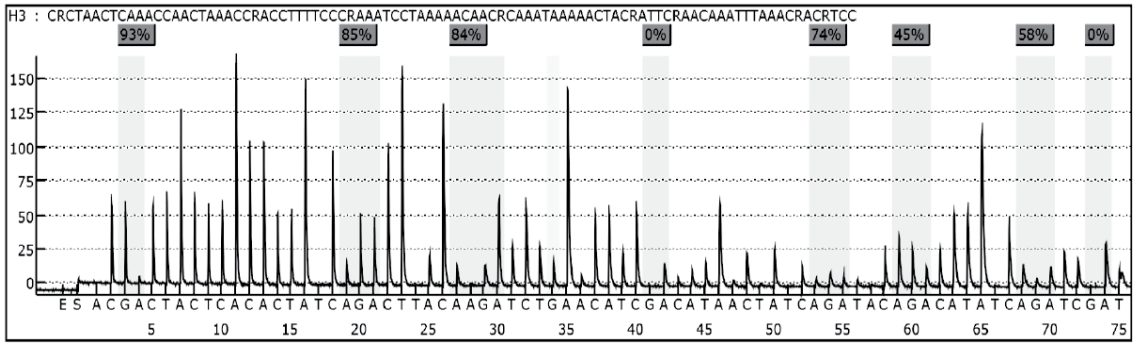

Figure 3.3. Representative pyrogram generated by the Pyro Q-CpG software (Qiagen) showing the methylation levels of 8 CpG dinucleotides. The x-axis shows the nucleotide dispensation and peaks represent emission following nucleotide incorporation. The ratio of C to T is automatically calculated by the software at each CpG site.

3.6.5 Methylation Reversal Assays

Cells were grown until 60% confluent. Media was replaced, and 5µM 5-aza-deoxycytidine (AZA) (Sigma) was added and incubated for 5 days. For the final 16 hours before harvest 0.3nM Trichostatin (TSA) (Sigma) was added to the media. On day 5, cells were washed with PBS, removed from the flask with trypsin, pelleted and stored at -20°C for DNA, RNA or protein extraction.

3.6.6 450K methylation array

Breast cancer cell lines were profiled using the Infinium Human Methylation 450 BeadChip (Illumina). 1µg genomic DNA was extracted from cell lines as described and sent to the Genome Centre, Barts Cancer Institute London, for microarray hybridisation, scanning (Illunmina iScan system) and quality control according to standard operating procedures. The scanned data were first normalised to reduce the differences between the two types of probes within the array. Infinium I probes are designed across the CpG dinucleotide, meaning there are two probes for each, whilst as the Infinium II are designed immediately adjacent to the CpG so there is only one probe. After normalisation methylation status of each CpG site was presented as β-values (the ratio of methylated signal to the total signal).

3.7 Preparation of VIK-1 expressing plasmids

3.7.1 Amplification of pcDNA3.1-VIK vector

A pcDNA3.1 vector containing the full-length coding region of VIK-1 (Figure 3.4) was gifted from Nadine Varin-Blank (Departement d'Hematologie, Institut Cochin, Paris, France). To amplify the plasmid, DNA was transformed into DH5α chemically competent *E.coli* cells (NEB). Cells were thawed on ice and 5ng of DNA added to 50µl of cells. Cells were incubated on ice for 30 minutes followed by heat shock for 45 seconds at 42°C, then placed on ice for 5 minutes. 350µl of S.O.C (super optimal broth with catabolite repression) medium was added and cells incubated at 37°C, shaking at 225rpm for 1 hour. 50µl were plated onto Luria-Bertani (LB) agar plates with 100µg/ml ampicillin. Multiple single colonies were picked from plates and grown overnight in LB broth plus ampicillin. Plasmids were purified from cell cultures using QIAprep Spin Miniprep Kit (Qiagen). DNA was confirmed

by running on 1% agarose gel with gel red (Biotium) alongside a 1kb ladder (NEB) in Tris Borate EDTA (TBE) for 1 hour at 100V. Sequences were confirmed by sequencing (GATC Biotech). Selected colonies were further grown up in 300ml LB broth and purified using the Plasmid Maxiprep Kit (Qiagen).

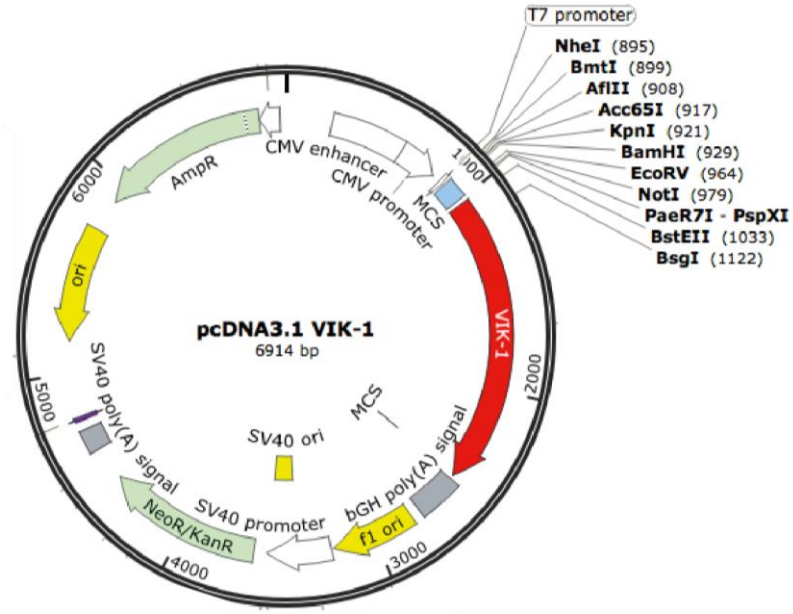

Figure 3.4. Diagrammatic representation of the pcDNA3.1-VIK-1 plasmid. The plasmid contains a cytomegalovirus (CMV) promoter for high level stable expression. The gene of interest, VIK-1, sequence has been cloned into the multiple cloning site (MCS). A neomycin resistance cassette allows for selection using G418 in mammalian cells and ampicillin resistance gene allows selection with ampicillin in bacterial cells.

3.7.2 Cloning into pEGFP vector

VIK-1 gene sequence was amplified from the PCDNA3.1 expression vector and cloned into a pEGFP vector (Figure 3.5). PCR primers were designed with restriction site at the 5' end of the primer:

Forward Primer: ACGAATCTCGAGATGGAGGAAATACCAGC

Reverse primer: ACCAAAGAGAACTCATGAGGTACCACGAAT

Amplification was carried out with Phusion High-Fidelity DNA polymerase (NEB). 5ng of DNA was amplified, with 0.5µM forward primer, 0.5µM reverse primer in a 25µl final reaction volume. Cycling conditions as follows; an initial denaturation step of 98°C for 30 seconds, followed by 25 cycles of: 98°C for 10 seconds, 72°C annealing for 10 seconds, 72°C for 38 seconds (25 seconds/kb for 1.5kb sequence), then a final extension of 72°C for 2 minutes. The PCR product was purified using PCR purification kit (Qiagen). The insert and pEGFP vector were digested with restriction enzymes in Cutsmart buffer (NEB) for 2 hours at 37°C. DNA was run on a 1% agarose gel and DNA extracted from the gel (Qiagen DNA gel extraction kit). 95ng of VIK-1 Insert was ligated into 100ng pEGFP vector (molar ratio 3:1) using instant sticky-end ligase master mix (NEB), an equal volume of DNA and 2x master mix was incubated for 10 minutes at room temperature.

The ligated plasmid was transformed into DH5α chemically competent *E.coli* cells (NEB) as described above. Successful cloning of VIK-1 insert into the pEGFP vector was confirmed by a diagnostic digest with the restriction enzymes and sequencing (GATC).

3.7.3 Site directed mutagenesis for deletion of small DNA sequence

After cloning a small DNA sequence between the end of the GFP sequence and the beginning of the VIK-1 had to be removed for the VIK-1 sequence to be in frame. Site

directed mutagenesis was utilised to delete the small linker DNA sequence. A standard forward primer was designed at the end of the section to be deleted, and a reverse primer from the beginning of the region to be deleted. Following PCR the DNA section is not amplified, and therefore deleted (Forward Primer: GAGGAAATACCAGCCCAG, Reverse Primer: CTTGTACAGCTCGTCCATG).

PCR was carried out using Phusion polymerase as described above. The PCR product is a linear sequence of the DNA including the insertion. This was followed by incubation with a kinase, a ligase and DpnI (KLD) for circularisation of the PCR product. 1µl was incubated with 5µl of 2x KLD reaction buffer, 1µl of 10x KLD enzyme mix, the reaction was incubated for 5 minutes at room temperature then transformed into *E.coli* cells, colonies selected and grown and purified as above. DNA sequence was verified by sequencing (GATC).

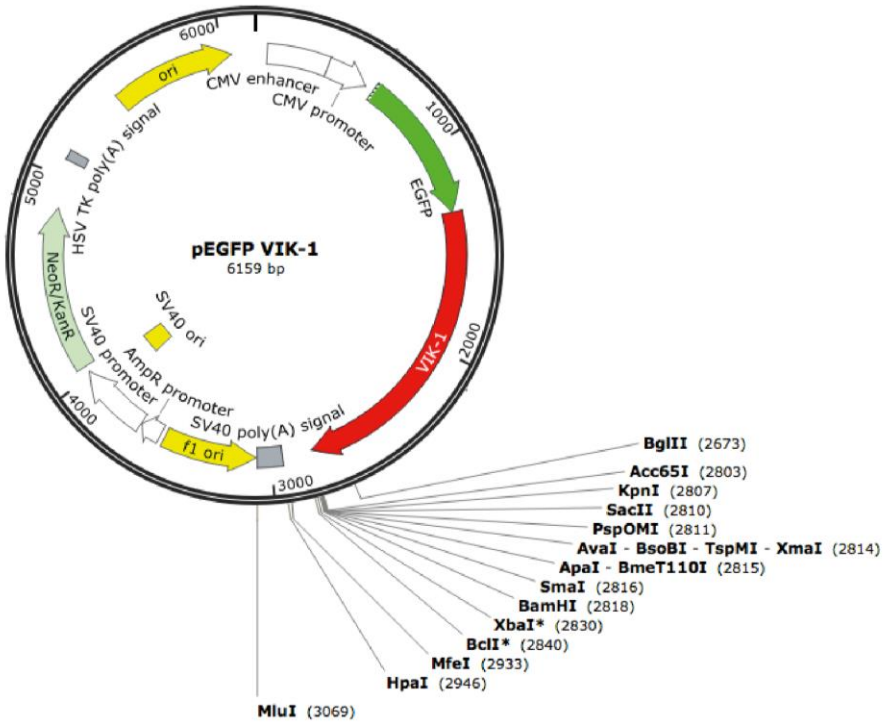

Figure 3.5. Diagrammatic representation of the pEGFP-VIK-1 plasmid. The plasmid contains a cytomegalovirus (CMV) promoter for high level stable expression. The gene of interest, VIK-1, sequence has been cloned into the multiple cloning site. EGFP is located at the N-terminal of VIK-1. A neomycin resistance cassette allows for selection using G418 in mammalian cells and kanamycin selection in bacterial cells.

3.8 Flow Cytometry Analysis

3.8.1 DNA staining for cell cycle profile

Cell cycle analysis was performed by quantification of DNA content using the DNA binding dye DAPI. The stage of the cell cycle can be measured by the relative DNA content of each cell, where cells in G2 have approximately twice the amount of DNA compared to cells in G1. As DNA is synthesised in S phase, these cells have a DNA content ranging in between that of G1 and G2. Samples were collected over indicated time points and fixed in 4% paraformaldehyde (PFA) for 7 minutes at room temperature. Fixed cells were permeabilised with 0.2% Triton X-100 for 3 minutes at room temperature before addition of 1µg/ml DAPI and analysed by flow cytometry (BD Biosciences LSR Fortessa). Samples were recorded using a BD LSR Fortessa flow cytometer and analysed using BD FACS Diva software. Cells were gated based on forward scatter area and height, and side scatter area and width to remove doublets and select a single cell population only. Cells were excited at 350nm and recorded with the 450/50nm emission filter. 10,000 events were acquired for each sample and the percentage of cells in each cell cycle phase was analysed using FlowJo software.

3.8.2 Annexin V staining for apoptosis

Annexin V is a 35-36kDa calcium dependent phospholipid-binding protein that has a high affinity for phosphatidyl serine (PS). In a normal cell PS is located on the cytoplasmic surface of the cell membrane. In apoptotic cells PS is translocated from the inner to the outer leaflet of the plasma membrane, exposing PS to the external cellular environment. Fluorescently labelled annexin V allows detection of apoptotic cells via binding to PS. Co-

staining with DAPI, which is impermeable to live cells, enables distinction between dead cells and apoptotic cells. Annexin V and DAPI negative are alive, DAPI positive only are dead and annexin V positive cells are undergoing apoptosis.

Cells were treated with VIK targeting siRNA, or transfected with VIK expressing plasmid. At indicated time points cells were collected and washed in PBS. 2.5µl of AlexaFluor 647 annexin V conjugate (Thermo Fischer) was added to each sample in 50µl of 1x annexin binding buffer (10mM HEPES, 140mM NaCl, 2.5mM CaCl2, pH 7.4) and incubated for 15 minutes at room temperature. 200µl of 1mg/ml DAPI diluted in 1x annexin binding buffer was added to each sample and cells were analysed by flow cytometry, emission of annexin V was recorded at 670/14nm. The unlabeled control, with negative staining for DAPI and annexin V, was used to draw gates and differentiate positively stained cells from the negatively stained cells.

3.9 Statistical Analysis

3.9.1 Analysis of *in vitro* assays

Data was normalised to control where required and as described. Statistical analysis for all cell line assays was performed using GraphPad Prism software. Where there were only two treatment groups an un-paired one-way Student's T-test was performed. A One-way ANOVA was performed with a Tukey's post-hoc test to compare significance between more than two treatment groups. Two-way ANOVA with Sidak's multicomparison test was performed when there were treatment groups with two independent variables. All graphs show mean of biological triplicates +/- standard deviation unless otherwise stated.

3.9.2 Analysis of primary patient data

SPSS (IBM software) was used to analyse patient samples. A Mann-Whitney test was used for two variables and Kruskal-Wallis one-way ANOVA for more than two variables. Spearman's rank correlation was used to determine correlation between two variables and is reported as correlation coefficient variable (R). Survival was analysed using a Kaplan-Meier curve followed by log-rank and cox-regression analysis.

4. Results: VIK expression and epigenetic regulation in breast cancer

4.1 Methylation in breast cancer cell lines

4.1.1 450K methylation array

A comprehensive genome wide screen was carried out by the Schmid group to identify potential epigenetically silenced genes in breast cancer. Fourteen breast cancer cell lines were screened using the 450K-methylation array (Illumina) to identify aberrantly methylated regions. The array is designed to analyse regulatory regions covering more than 485,000 CpG sites in the human genome. The probes are distributed mainly to cover CpG islands but also include the shore regions (up- and down-stream of each CpG island), gene bodies and 5' and 3' untranslated regions (UTRs). β-values represent methylation levels and range from 0 representing the lowest value to 1 representing the highest.

The methylation array generated a list of candidate genes from which ZNF655 (VIK) was selected for further investigation based on the presence of a CpG island within the 5' regulatory regions and high levels of methylation observed. Additionally VIK was chosen due to the novelty of the gene in the context of breast cancer and potential functional role within the cell cycle, which will be discussed in the following chapters.

VIK is located on chromosome 7 and has a large CpG island of 1098bp containing 90 CpG sites. The CpG island overlaps with the 5' UTR and is upstream of the coding region (Figure 4.1A). Methylation was shown to be only slightly variable across the 13 probes located within the CpG island. Dense methylation was observed in 6 out of 14 cell lines (Figure 4.1B), indicating the gene could undergo transcriptional regulation via epigenetic changes.

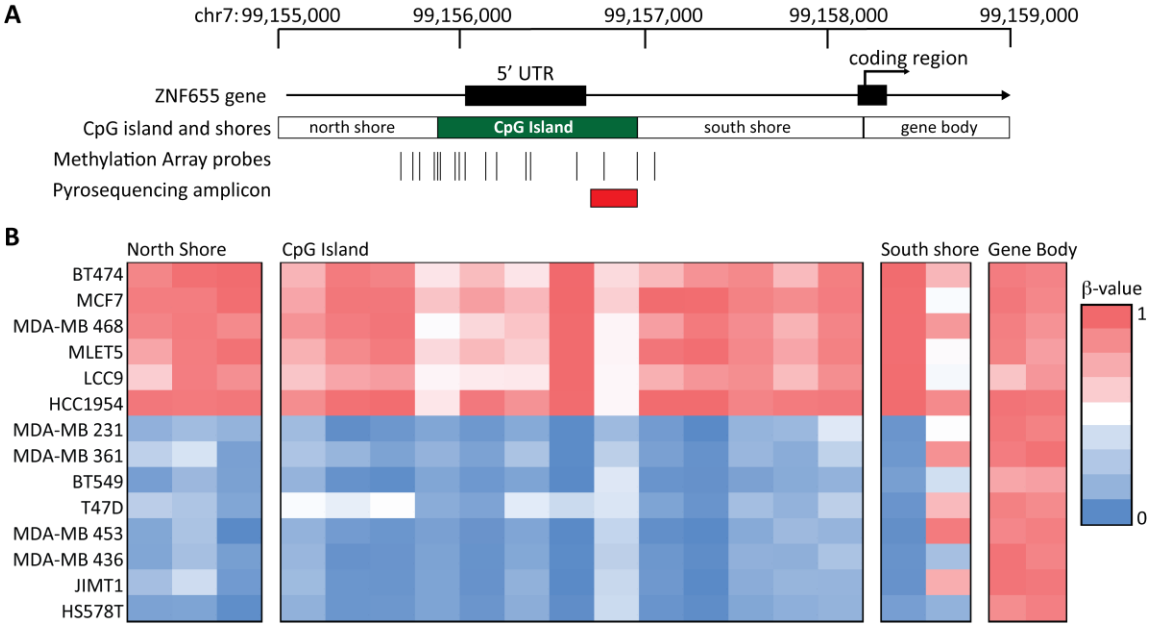

Figure 4.1 Methylation analysis in breast cancer cell lines. A) Schematic representation of the CpG island. The VIK (ZNF655) gene has a CpG island (shown as a green block) within the 5' regulatory region of the gene. Vertical lines below represent methylation array probes targeting a single CpG dinucleotide. Red box displays the location of the region analysed for pyrosequencing. B) Heat map representation of methylation across a panel of cell lines from a 450K methylation array. The heat map is colour coded based on β-values (ratio of methylated signal to total signal). Out of 14 cell lines, 6 exhibited dense methylation across the CpG island.

4.1.2 Pyrosequencing analysis

To validate the results observed using the 450K array, a pyrosequencing assay was designed to investigate the methylation status of the CpG island within the 5' regulatory region of the VIK gene. Based on the methylation array, pyrosequencing primers were designed within a more highly methylated region of the island. Genomic DNA was sodium bisulphite treated which deaminates unmethylated cytosines to uracils. Subsequent PCR amplification leads to incorporation of thymine instead of the original unmethylated cytosine. This gives a DNA sequence dependent on the methylation status. Sequencing of the DNA allows quantification of methylation by ratio of thymines and cytosines. The pyrosequencing assay covered 8 individual CpG sites across the island for all breast cancer cell lines. For the normal breast epithelial cell line, MCF10A, pyrosequencing only reliably covered 6 CpG sites, with the signal strength tailing off over site 7 and 8, therefore only 6 sites were evaluated. Methylation of each individual CpG site was determined and an average percentage across all CpG sites was used to define methylation status of each cell line.

The non-tumour breast epithelial cell line, MCF10A, was unmethylated, whilst methylation varied across the breast cancer cell lines. Pyrosequencing revealed high levels of methylation in 8 out of 19 breast cancer cell lines (Figure 4.2A). The same cell lines were found to be methylated in both the methylation array and pyrosequencing analysis. Linear regression showed close correlation between methylation levels determined by the two methods (r^2=0.9289, $p<0.0001$) (Figure 4.2B). Cell lines were mainly either highly methylated >60% or had low levels of methylation <11%. Only SKBR3 and MLET5 had a more intermediate methylation value of 40% and 39% respectively.

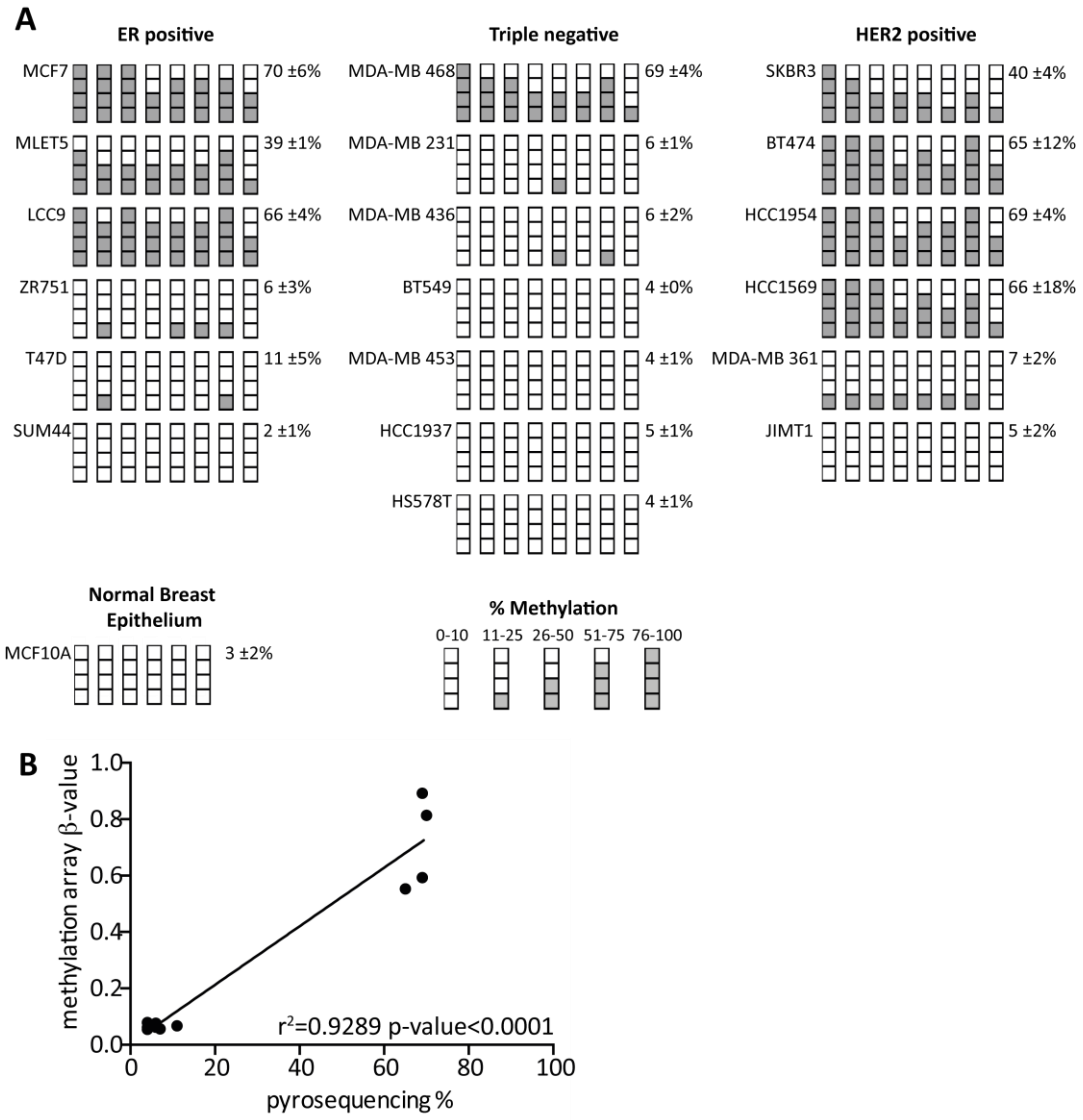

Figure 4.2 Pyrosequencing analysis in breast cancer cell lines. A) Methylation was analysed by pyrosequencing across a panel of cell lines from breast cancer subtypes and normal breast epithelial cells. Each column represents an individual CpG site. Proportion of grey boxes represents % methylation at each site. Percentage methylation of each cell line was calculated by average methylation across all CpG sites. Mean methylation of biological triplicates was calculated to give methylation status for each cell line +/- standard deviation. B) Analysis of correlation by linear regression of methylation determined by the methylation array and pyrosequencing. y-axis shows β-value from the array probe that matched to the region of the CpG island analysed by the pyrosequencing assay. x-axis shows % methylation by pyrosequencing.

4.2 VIK mRNA expression in breast cancer cell lines

To ascertain the implication of methylation on VIK expression, mRNA expression of VIK was analysed across the panel of breast cancer cell lines.

VIK is a splice variant of the Zinc Finger 655 (ZNF655) gene. Three different isoforms have been characterised and confirmed experimentally. VIK-1, VIK-2 and VIK-3, are produced as a result of gene splicing (Figure 4.3) (236). Each isoform has two transcript variants, which differ slightly in the 5'UTR, encoding the same protein. VIK-1 is a 57kDa protein containing 6 zinc finger domains and a separate VAV interacting domain and CDK4 interacting domain. The larger 61kDa protein VIK-2 contains these same domains with the addition of a KRAB B domain. The smaller 20kDa isoform VIK-3 contains a proline rich domain (Pro), KRAB A domain and an unknown domain. There is an additional putative isoform, VIK-4, that has not previously been characterised. VIK-4 is a shorter isoform, 12kDa, which does not have the known functional domains. The total mRNA expression of all VIK isoforms was determined using two separate TaqMan RT-qPCR assays (Figure 4.4A,B). Individual expression of each isoform was determined by SYBR Green assays, using primers designed to amplify each isoform individually (Figure 4.4C). Primer locations are annotated in Figure 4.3. All VIK transcripts are covered over the different RT-qPCR assays. Due to the sequence similarity of VIK-1 and VIK-2 it was not possible to design separate assays, therefore primers were designed to amplify VIK-2 alone and VIK-1 plus VIK-2 combined. Expression of VIK-1 alone was determined by subtracting VIK-2 from VIK-1 + VIK-2. All RT-qPCR assays showed the same mRNA expression pattern. From this point forward, unless otherwise specified, TaqMan assay 1 was used to assess mRNA levels of VIK.

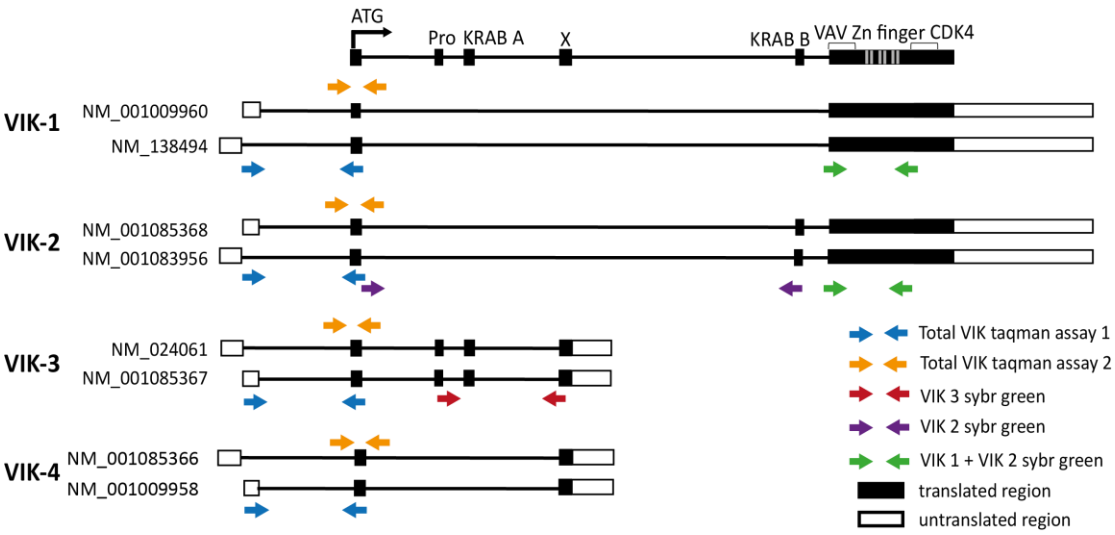

Figure 4.3 Diagrammatic representation of the organisation of the VIK (ZNF655) gene and alternatively spliced isoforms VIK-1, VIK-2, VIK-3, VIK-4. Each isoform has two transcripts encoding the same protein. Location of PCR primers are represented by arrows, over the RT-qPCR assays each isoform and all transcripts are covered.

The cell line panel included the non-tumour breast epithelial line MCF10A and covered a range of breast cancer subtypes: HER2 positive, triple negative and ER positive. Cell lines exhibited either no detectable mRNA expression of any VIK isoform, or variable expression of all three isoforms, with VIK-1 generally being the most highly expressed. There was no correlation between VIK expression, or expression of individual isoforms, and breast cancer subtype. Within the ER positive group were two cell lines derived from MCF7 that do not depend on estrogen for proliferation, the LCC9 and MLET5 cell lines. LCC9 is resistant to the ER antagonist fulvestrant (288). MLET5 is resistant to the cytotoxic drug etoposide and, whilst still ER positive, is able to grow independently of estrogen (289)**.** There was also no difference in VIK expression between the MCF7 cells and the estrogen independent LCC9 or MLET5, all three had undetectable mRNA levels.

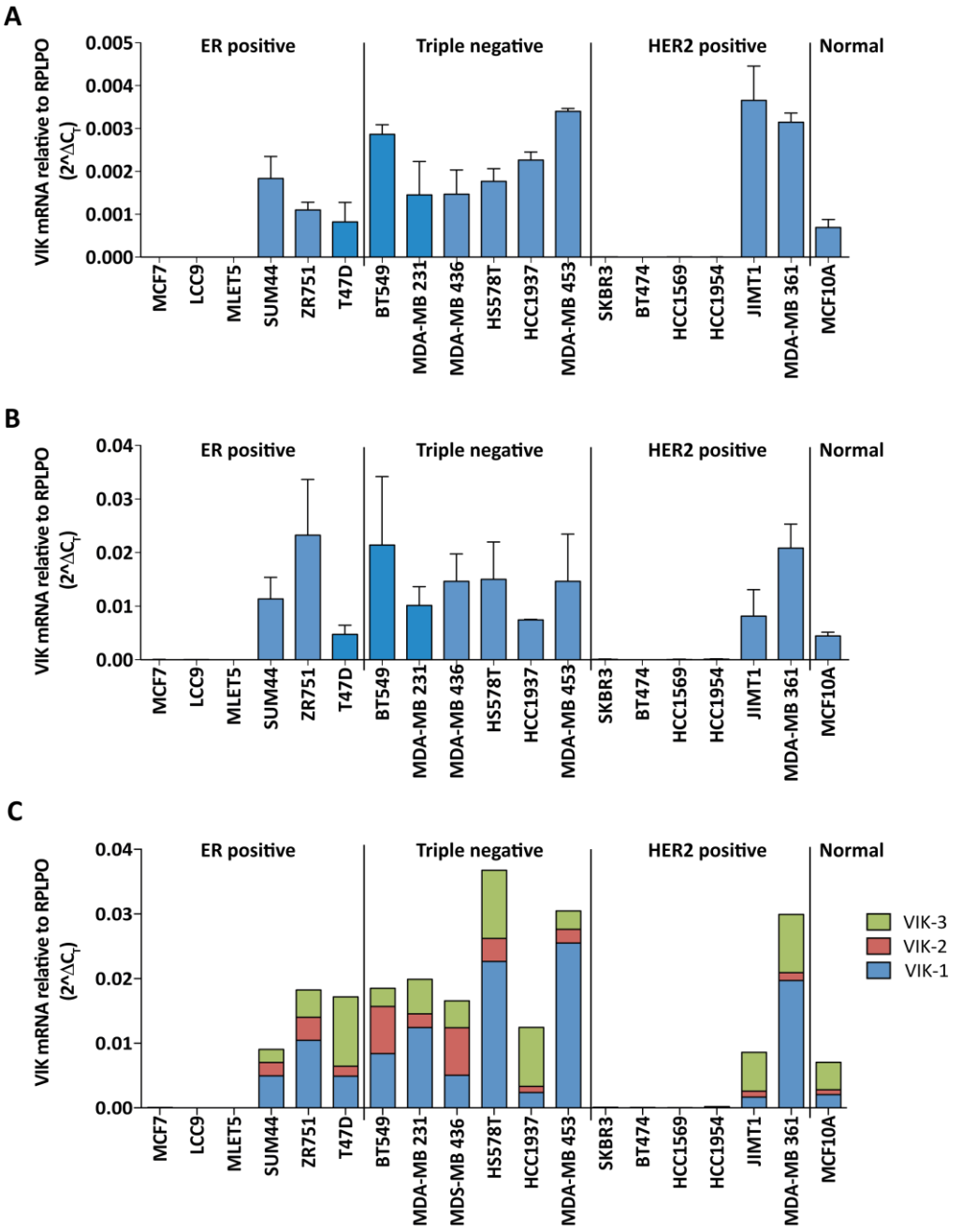

Figure 4.4. Analysis of VIK mRNA expression in breast cancer cell lines. A) Total VIK isoform mRNA expression determined by TaqMan assay 1. B) Total VIK isoform mRNA expression determined by TaqMan assay 2. C) mRNA expression of each separate VIK isoform determined by individual SYBR Green assays. mRNA expression was normalised to the housekeeping gene RPLPO, average of biological triplicates. There was no correlation between VIK expression and breast cancer subtype. Cell lines either expressed variable levels of each isoform, or did not express any of the isoforms.

4.3 Methylation silences VIK transcription

The cell lines with no detectable mRNA levels were the same cells to have been determined as methylated by pyrosequencing analysis. VIK methylation correlated closely with mRNA expression ($R=0.842$, $p<0.0001$, Pearson's correlation coefficient), such that no detectable mRNA was observed in cell lines with methylation above 30% (Figure 4.5A). This suggests VIK is subject to methylation dependent transcriptional silencing.

In order to validate whether methylation is a direct mechanism of transcriptional silencing, epigenetic mechanisms were inhibited in the methylated cell lines MCF7 and SKBR3 and the unmethylated cell line T47D (Figure 4.5B). Cells were treated with 5-aza-2'-deoxycytidine (AZA) and/or Trichostatin A (TSA). AZA is a cytosine homologue, which binds to and inhibits methyl-transferases in proliferating cells leading to global DNA demethylation. TSA is a HDAC inhibitor that reduces chromatin condensation. Upregulation of VIK mRNA expression was seen following AZA treatment in all methylated lines, indicating methylation directly silences VIK transcription. Approximately 100-fold upregulation was seen in the MCF7 and 7-fold in the SKBR3. There was a more limited increase of 2-fold in the already unmethylated T47D. Treatment with TSA had no effect and there was no synergistic effect with combined AZA and TSA treatment. This demonstrates the epigenetic regulation of VIK in our cell lines is restricted to DNA methylation.

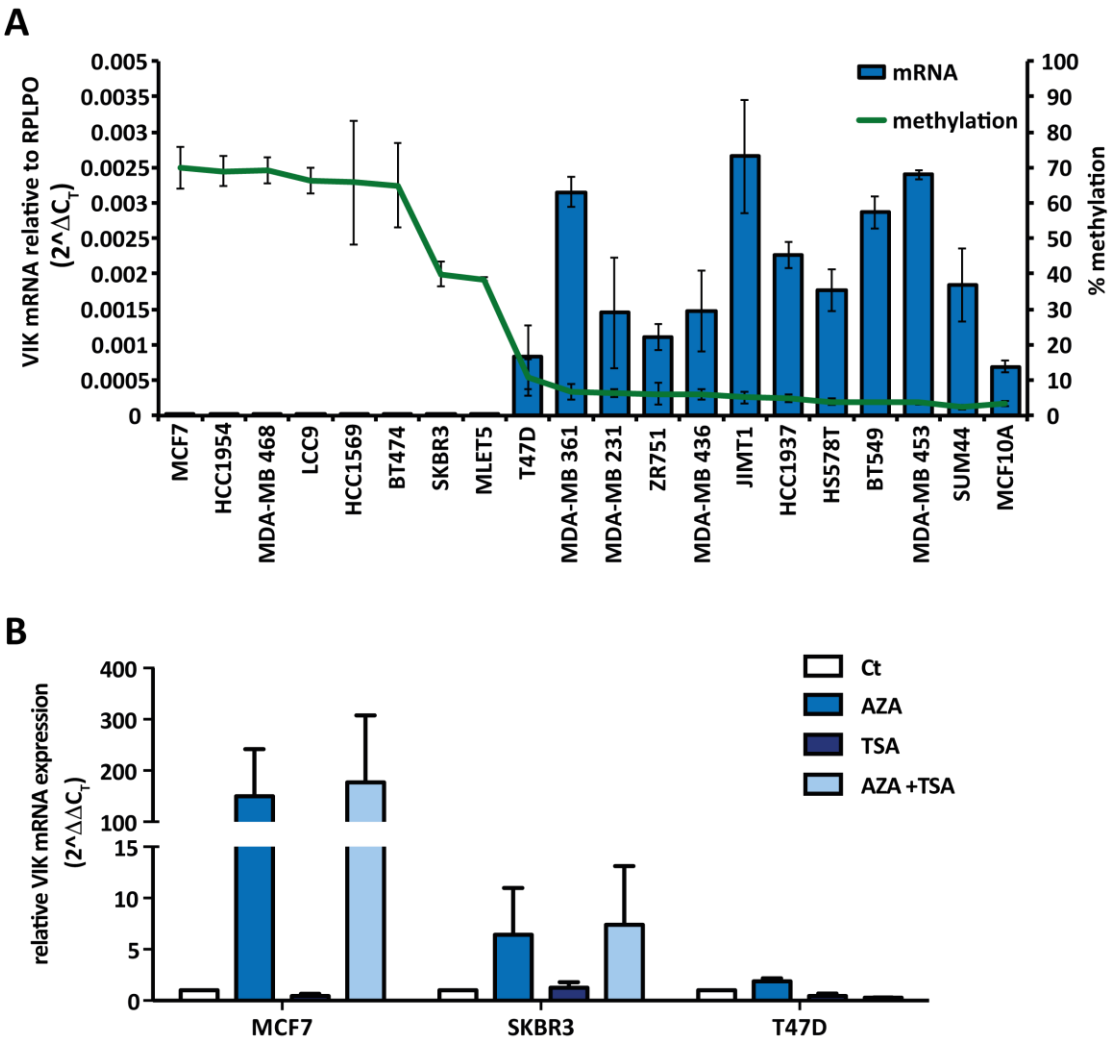

Figure 4.5. Methylation transcriptionally silences VIK. A) Histogram displays mRNA, as measured by RT-qPCR total isoform expression assay 1 (left Y-axis). The green line shows % methylation, determined by pyrosequencing (right Y-axis). Methylation correlates to no detectable mRNA expression. B) Methylation reversal with AZA treatment resulted in upregulation of VIK mRNA, treatment with TSA had no effect. Ct: untreated control AZA: 5-aza-2'-deoxycytidine TSA: Trichostatin A. mRNA expression was normalised to the non-treated control to give a fold change of upregulation. Average of biological triplicates +/- standard deviation is shown.

4.4 VIK expression and methylation in primary breast cancer samples

Having established methylation transcriptionally silences VIK expression in breast cancer cell lines, we next investigated VIK methylation and expression in primary breast cancer samples. An independent breast cancer cohort (Leeds cohort) was analysed as well as publicly available data from the Cancer Genome Atlas (TCGA). The preliminary data in a breast cancer patient cohort linked VIK methylation to poor outcome in patients receiving tamoxifen treatment. In light of the differential outcome with regards to VIK methylation in the preliminary cohort, survival analysis was performed on these two cohorts.

4.4.1 The Cancer Genome Atlas cohort

4.4.1.1 Methylation and expression analysis in TCGA cohort

To explore the expression of VIK and the relationship of VIK and VAV1 in primary tissue, *in silico* analysis was carried out using data from TCGA (290). TCGA is a publically accessible database with high throughput sequencing and array data plus clinical information from a variety of cancer types. Methylation (Illumina Human 450K methylation beadchip), gene expression (Illumina HiSeq 2000 RNA sequencing) and matching clinical data was available for 587 primary breast cancer tissue samples and 83 normal breast tissue samples. Based on the clinical information, tumour samples were divided into breast cancer subtypes: ER+, HER2+ ER+, HER2+ ER- and triple negative. Non-tumour samples were tumour-adjacent tissue, histologically determined as normal. Expression values are normalised data using RNA-seq by expectation maximisation (RSEM) to determine expression levels. Methylation

β-values were taken from the methylation array probe that matched to the same region as the pyrosequencing primers designed to amplify the region of the CpG island for VIK.

Normal samples exhibited no methylation across the CpG island, whilst tumour samples showed variable methylation across the CpG island (Figure 4.6). Tumour samples exhibited significantly higher VIK methylation in comparison to normal tissue. Normal tissue showed no methylation for VIK, with a mean methylation β-value of 0.04, ranging from 0.02 to 0.15. There was approximately a 40% increase in mean methylation β-values in breast cancer tissue compared to normal tissue. This was consistent across all breast cancer subtypes. Tumour tissues displayed a wide range of methylation β-values, from low levels of methylation of 0.02 up to highly methylated 0.83 (Figure 4.7B). All breast cancer subtypes had a subset of the population with higher than normal methylation values (Figure 4.7C).

Within the tumour samples VIK methylation inversely correlated to VIK mRNA expression (Figure 4.7A). Increase in methylation corresponded to a significant decrease in average VIK expression. Tumour samples displayed lower levels of VIK expression in comparison to normal samples (Figure 4.7D). This down-regulation was consistent across all breast cancer subtypes, with all subtypes exhibiting a proportion of samples with lower than normal VIK expression (Figure 4.7E). These results suggest that there is a subset of patients with low levels of VIK expression that are subject to transcriptional silencing due to methylation.

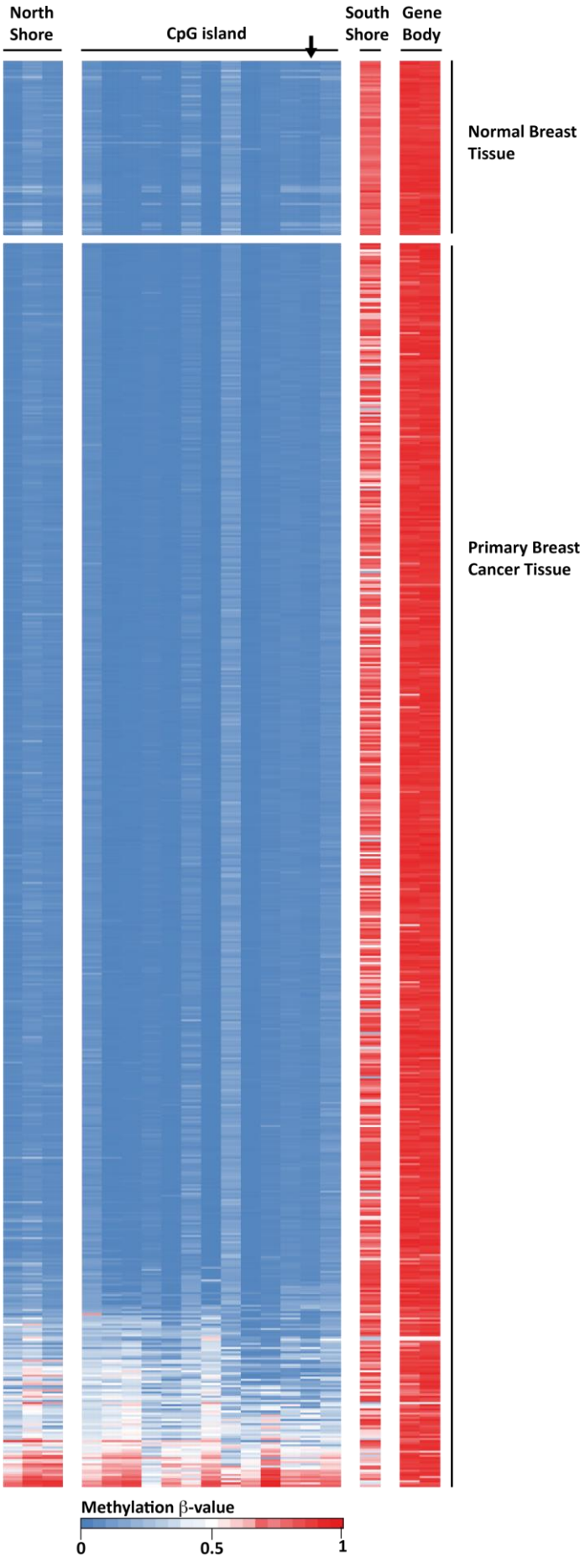

Figure 4.6. Methylation array analysis of TCGA patient cohort. Heat map representation of the distribution of methylation across the promoter region of VIK in 587 patient samples and 83 normal breast tissue samples. Each row represents a single patient. The arrow shows the probe that matches to the same position as the pyrosequencing assay. The heat map is colour coded based on methylation β-value, ranging from 0 (blue) to 1 (red).

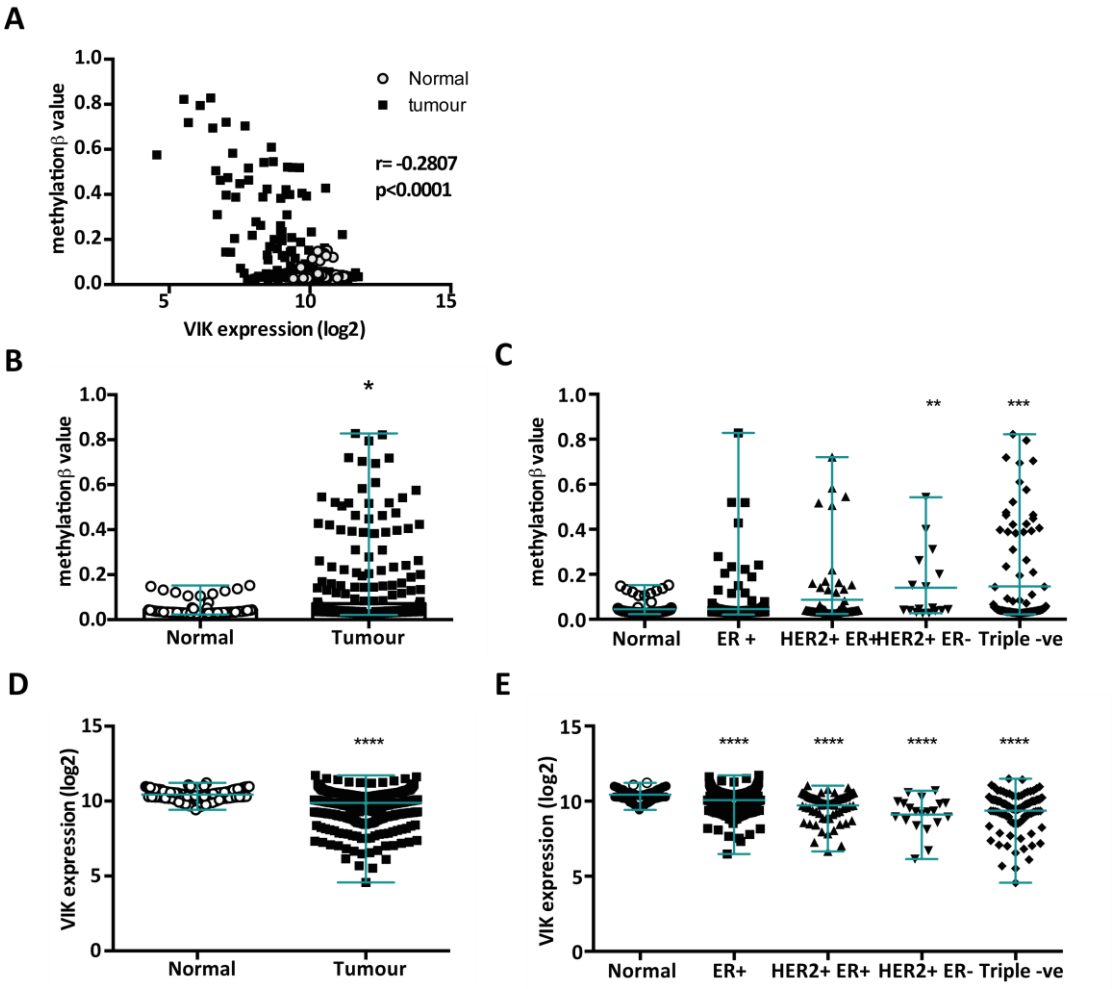

Figure 4.7 Analysis of VIK expression and methylation in primary breast cancer samples from TCGA dataset. A) VIK methylation significantly correlated to VIK expression. Increased methylation corresponded to decreased VIK expression. Methylation is shown as methylation β-value as determined by 450K methylation array, and expression was determined by RNAseq. (P<0.0001 Spearman's correlation test). B) Distribution of methylation in normal and tumour samples. Error bars represent the mean +/- standard deviation. C) Distribution of methylation across breast cancer subtypes compared to normal. D) VIK expression in normal and tumour samples. E) Distribution of VIK expression across each breast cancer subtype compared to normal tissue. *P<0.05, **P<0.01 ***P<0.001 Mann-Whitney test between tumour and normal samples. Kruskal-Wallis test between normal and breast cancer subtypes.

VIK was initially characterised due to its interaction with VAV1 and there is potentially a compensatory mechanism between these two proteins (277)**.** Therefore, VAV1 expression was also evaluated in the breast cancer cohort, to determine if there was a correlation between VIK and VAV1 expression. Conversely to VIK expression, average VAV1 expression was significantly upregulated in tumour samples compared to normal tissue (Figure 4.8A), and this was seen across all subtypes (Figure 4.8B). However, there was no correlation between VIK and VAV1 expression (Figure 4.8C). Additionally, when tumour samples were separated into VIK high or low expressing, determined as the mean expression of normal samples plus or minus 2 standard deviations, there was no difference in VAV1 expression (Figure 4.8D). This indicated no clear relationship between VIK and VAV1 expression in the breast cancer tumour samples.

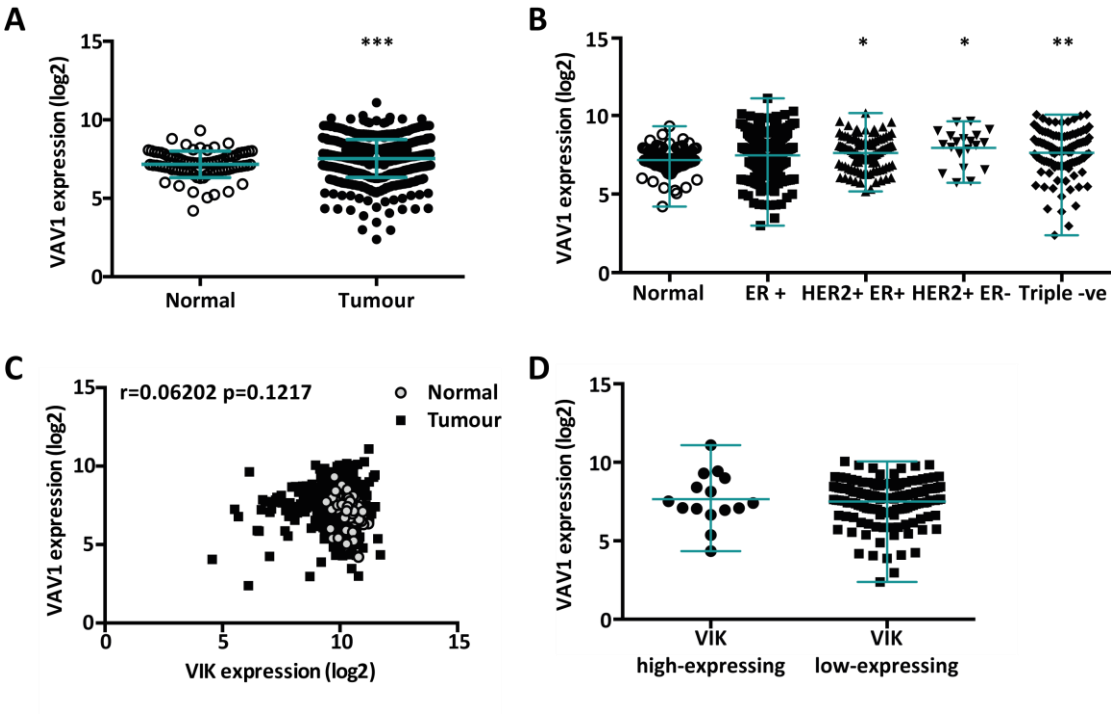

Figure 4.8 Analysis of VAV1 expression in primary breast cancer samples from TCGA dataset. A) Distribution of VAV1 expression in tumour samples compared to normal samples. VAV1 expression was significantly higher in the tumour population compared to normal samples. ***P<0.0001 Mann-Whitney test. B) VAV1 expression was higher in all breast cancer subtypes compared to non-tumour samples. Mean expression was significantly higher in all subtypes compared to normal tissue. Kruskall-Wallis test *P<0.05 **P<0.001 C) There was no correlation between VIK and VAV1 expression in the tumour samples, assessed by Spearman's test. D) Tumour samples were divided into VIK high-expressing and VIK low-expressing. No difference was seen in VAV1 expression between VIK high or low expressing tumour samples.

4.4.1.2 Survival analysis in TCGA cohort

Having demonstrated differential expression and methylation in tumour tissue compared to non-tumour tissue, we investigated the implication of this methylation on patient outcome within this cohort.

Tumour tissues were divided into methylated and unmethylated, based on the single methylation probe that matched to the same region as the pyrosequencing assay. The normal breast samples displayed baseline levels of methylation for VIK. Therefore, mean methylation of the normal tissue plus three standard deviations was used as a cut-off to determine VIK methylated samples. This gave a cut-off β-value of 0.135. Using this cut-off, 9.9% of the tumour population was methylated for VIK. There was no significant difference in the median overall survival time between the methylated and unmethylated groups. Multivariate cox-regression analysis showed that of the characteristics tested only age and tumour subtype significantly correlated to patient overall survival (Figure 4.9A). Neither VIK methylation ($p=0.954$) or VIK expression ($p=0.530$) had a significant effect on survival. Kaplan-Meier curve and log-rank test showed no significant difference in survival time between methylated and unmethylated patients (Figure 4.9B).

A

Tumour Samples- TCGA Breast Cancer Cohort				
	Unmethylated	**Methylated**	**p-value Methylated vs Unmethylated**	**p-value Cox-regression**
Methylation status	529 (90.1%)	58 (9.9%)		0.865
Age at diagnosis (median)	57	56.5	0.812	0.003
Subtype			0.001	0.002
ER+ HER2-	387	15		
HER2+ ER+	10	8		
HER2+ ER-	56	7		
Triple negative	76	28		
Histological Type			0.002	0.113
Ductal Carcinoma	342	51		
Lobular Carcinoma	127	1		
Other	60	6		
Tumour Grade			0.154	0.051
1	95	6		
2	298	34		
3	131	15		
4	5	1		
Median survival (years)	0.97	0.99	0.406	

B

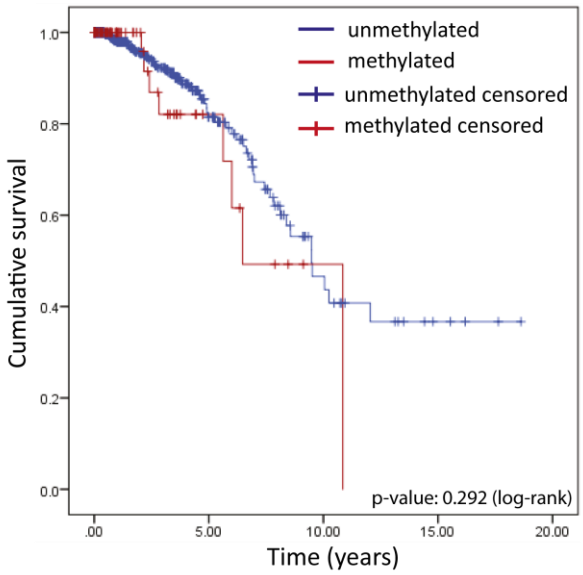

Figure 4.9. Methylation of VIK and patient outcome in TCGA dataset, using a cut-off based on a single probe A) Clinical characteristics of VIK methylated and unmethylated breast cancer patient samples. Patients were divided into methylated and unmethylated based on the methylation probe corresponding to the pyrosequencing assay, giving a cut off β-value of 0.135, with 9.9% of the population characterised as methylated. Columns show number of patients unmethylated or methylated for each characteristic. P-values refer to differences between the methylated and unmethylated groups and survival analysis by multivariate cox-regression. B) Kaplan Meier curve for overall survival with respect to VIK methylation status. The log-rank test was used to analyse significant effect on patient outcome.

However, this analysis only took into account one region of the CpG island. The methylation array showed some variable methylation across the different probes within the CpG island, with some probes exhibiting higher methylation than in other regions (Figure 4.6). Therefore survival analysis was also carried out taking into account average methylation of the whole CpG Island. Average methylation across all CpG island probes for the normal tissue, plus 3 standard deviations was used as a cut-off for methylation. This gave a cut-off methylation β-value of 0.167, above which samples were considered to be methylated. This corresponded to 14% of patients being methylated for VIK. A slightly higher methylated population than described above when only accounting for the single methylation probe. Survival analysis based on this methylated population showed a potential trend towards a poorer outcome in patients methylated for VIK, with the log-rank test approaching significance (p-value 0.074) (Figure 4.10). However, multivariate cox-regression analysis also taking into consideration age, tumour grade and tumour subtype showed VIK methylation had no significant effect on patient outcome (Figure 4.10).

It should be noted that there were few survival events over the entire cohort, only 66 out of a total of 587 patients. This, in combination with the relatively small proportion of patients within the methylated group, makes interpretation of survival data from this cohort inconclusive.

A

Tumour Samples- TCGA Breast Cancer Cohort				
	Unmethylated	**Methylated**	**p-value Methylated vs Unmethylated**	**p-value Cox-regression**
Methylation status	505 (86%)	82 (14%)		0.954
Age at diagnosis (median)	57	57	0.701	0.003
Subtype			0.001	0.002
ER+ HER2-	377	24		
HER2+ ER+	8	11		
HER2+ ER-	52	11		
Triple negative	68	36		
Histological Type			0.001	0.113
Ductal Carcinoma	321	72		
Lobular Carcinoma	126	2		
Other	58	8		
Tumour Grade			0.074	0.051
1	92	9		
2	285	47		
3	124	24		
4	4	2		
Median survival (years)	0.85	1.0	0.742	

B

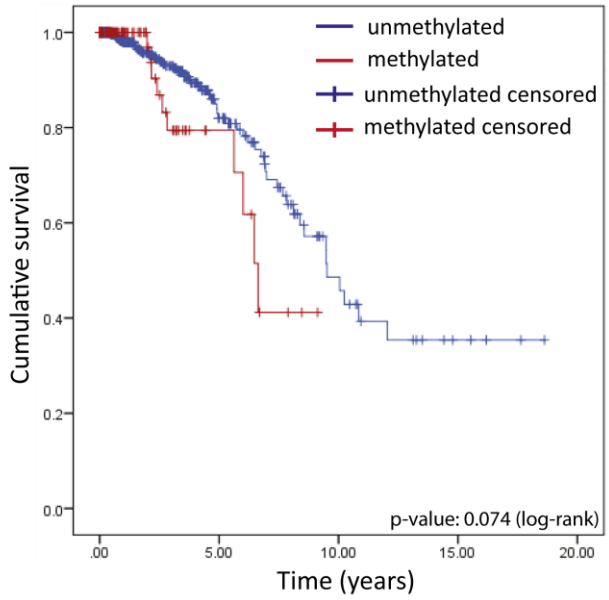

Figure 4.10 Methylation of VIK and patient outcome in TCGA dataset, using a cut-off based on the entire CpG island. A) Clinical characteristics of VIK methylated and unmethylated breast cancer patient samples. Patients were divided into methylated and unmethylated, based on average methylation across the whole CpG island. This gave a cut-off β-value of 0.167, above which samples were considered methylated, corresponding to 14% of the population. Columns show number of patients unmethylated or methylated for each characteristic. P-values refer to differences between the methylated and unmethylated and survival analysis by multivariate cox-regression. B) Kaplan Meier curve for overall survival with respect to VIK methylation status.

4.4.2 Leeds Breast Cancer Cohort

4.4.2.1 Methylation analysis in Leeds breast cancer cohort

A second cohort of 187 formalin-fixed paraffin embedded (FFPE) primary breast cancer tissue samples was analysed for methylation of VIK. Methylation was examined using the same pyrosequencing assay as described for the breast cancer cell lines, giving a % methylation value for 6 individual CpG sites for each patient sample. In this population there was a small distribution of methylation values across the cohort. Although there was one patient was much more highly methylated than the rest of the population, with an average 42% methylation (Figure 4.11A).

There were no normal tissue samples to determine a cut-off for methylated samples, so average methylation of all 6 CpG sites across the population was taken to assess baseline levels of methylation. This determined a cut-off value of 10.6%. There were two CpG sites (CpG site 2 and site 5) that displayed the most variation in methylation. Therefore an average of these two sites was taken plus 2 standard deviations, and all samples with average methylation above 10.6% were determined to be methylated (Figure 4.11B). This corresponded to 13 patients and thus 7% of the population being classified as methylated.

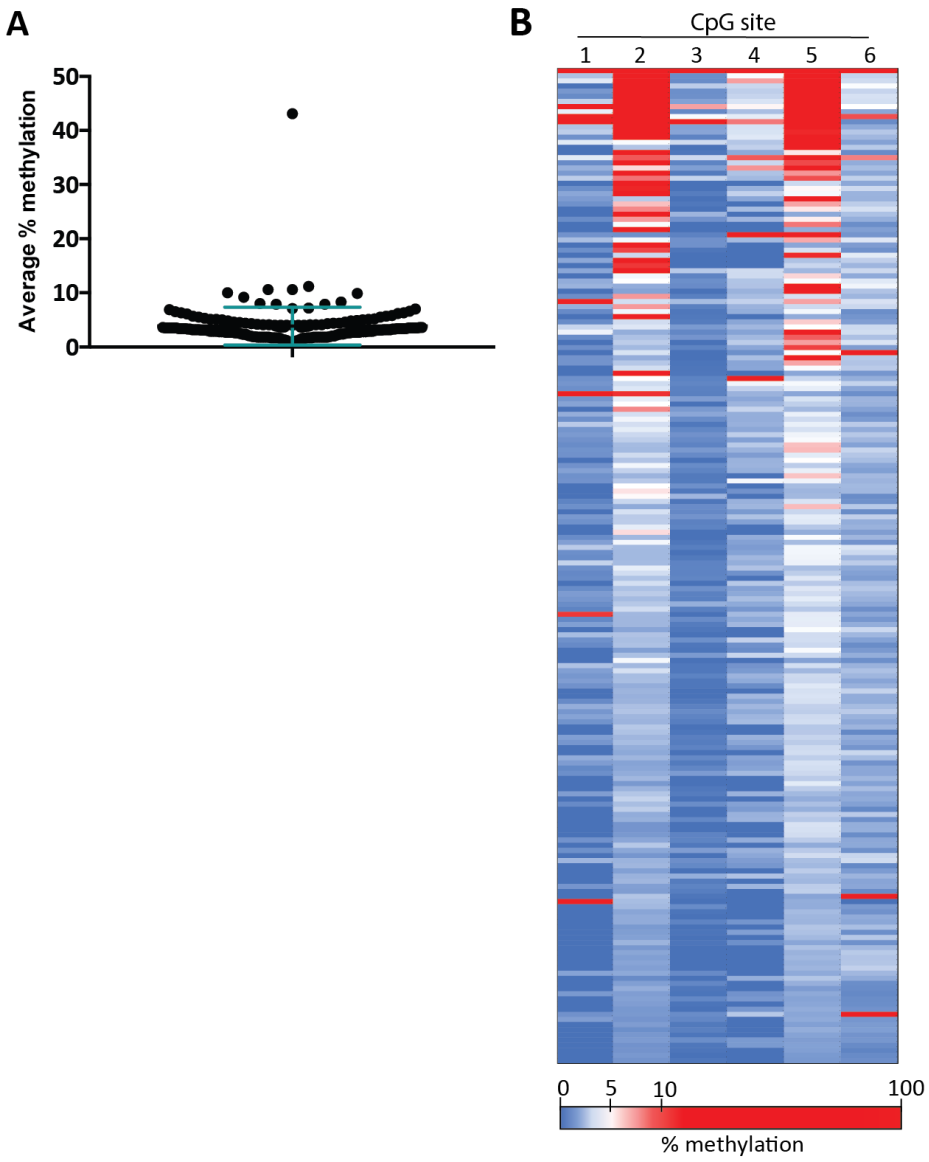

Figure 4.11 Methylation analysis in the Leeds primary breast cancer patient cohort. Methylation was assessed by pyrosequencing. A) Distribution of methylation across the tumour population. B) Heat map representation of methylation across the 6 CpG sites. Based on average methylation plus 2 standard deviations, a cut off of 10.6% was set. All values above this were determined as methylated, corresponding to 7% of the population.

4.4.2.2 Survival analysis in Leeds breast cancer cohort

As described the tumour samples were separated into methylated and unmethylated populations and methylation status analysed for potential as an indicator of overall patient survival. Multivariate cox-regression analysis revealed only age and tumour grade to significantly correlate to survival outcome. Methylation was not found to impact upon patient outcome (Figure 4.12). However, the methylated population size was small and a larger series of patients would be required to properly evaluate the effect of VIK methylation on patient survival.

A

Tumour Samples- Leeds Breast Cancer Cohort				
	Unmethylated	**Methylated**	**p-value Methylated vs Unmethylated**	**p-value Cox-regression**
Methylation status	174 (93%)	13 (7%)		0.628
Age at diagnosis (median)	59	55	0.238	0.0003
Hormone receptor status			0.877	0.132
ER+	118 (63%)	10 (5%)		
ER -	52 (28%)	7 (4%)		
Tumour Grade			0.581	0.038
1	27 90	3 10		
2	56	5		
3	87	9		

B

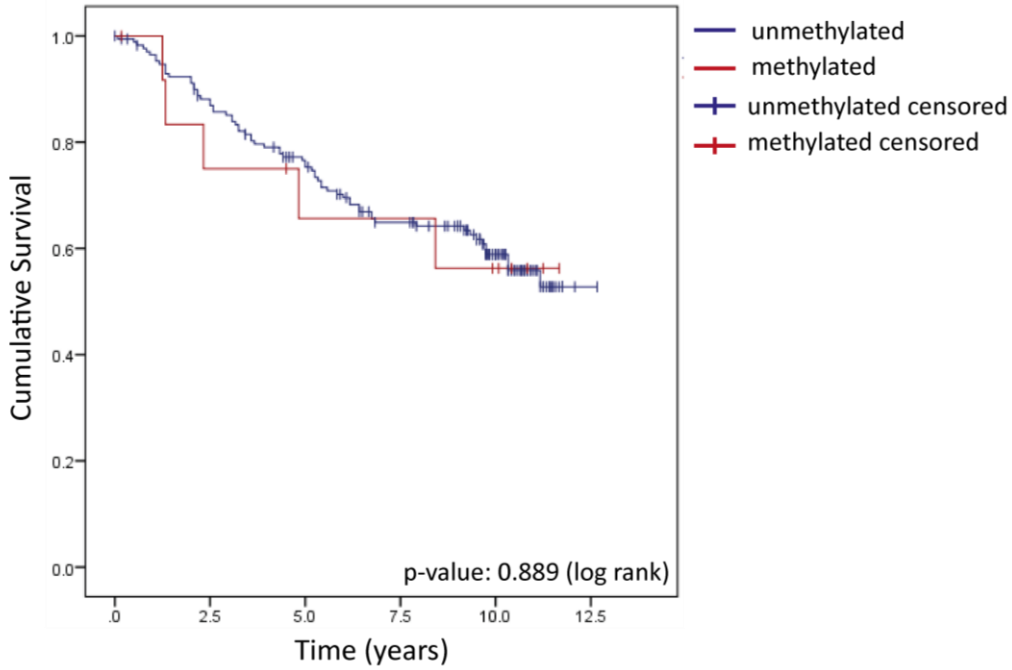

Figure 4.12. Methylation of VIK and patient outcome in the Leeds breast cancer cohort.

A) Clinical characteristics of VIK methylated and unmethylated breast cancer patient samples. Patients were divided into methylated and unmethylated. Columns show number of patients unmethylated or methylated for each characteristic. P-values for each characteristic refer to differences between the methylated and unmethylated groups and survival analysis by multivariate cox-regression. B) Kaplan Meier curve for overall survival with respect to VIK methylation status and survival analysed by the log-rank test.

4.5 VIK protein expression in breast cancer cell lines

So far we have established VIK is subject to methylation dependent transcriptional silencing in both breast cancer cell lines and primary breast cancer samples. To further characterise VIK expression in breast cancer, we analysed protein expression in breast cancer cell lines.

4.5.1 Western blot analysis

Firstly, VIK protein expression was assessed by western blot across the panel of breast cancer cell lines. Detection by western blot with commercial antibodies proved difficult, multiple antibodies were tested, and two commercial antibodies were optimised for western blot analysis, detecting a band at approximately 60kDa. Both antibodies detected a single band but at slightly different sizes. Potentially these antibodies are detecting VIK-1 at 57kDa and VIK-2 at 61kDa. However, protein expression did not correlate to mRNA expression. Methylated cell lines, with no detectable mRNA, still gave a protein band with both antibodies (Figure 4.13B). In order to confirm the accuracy of commercial antibodies for detecting VIK, a custom antibody against VIK was generated (Eurogentech). An epitope was selected to be different from either commercial antibody, within an immunogenic region of the protein and to be within a region that was not highly conserved with other proteins. The custom antibody detected a higher band than anticipated, at approximately 80kDa, which does not correspond to any known isoforms of VIK (Figure 4.13B). Potentially this antibody is detecting a different splice variant of VIK that has not been previously characterised or it is detecting a large post-translational modification to VIK. Again, protein expression using the custom antibody did not correlate to mRNA expression, and all methylated cell lines displayed protein bands. In fact, all three antibodies showed different

expression levels across the cell line panel, and none of the protein levels correlated to any of the mRNA assays.

As methylation status did not correlate to protein expression, we examined if methylation reversal would upregulate protein levels. The methylated MCF7 and SKBR3, and unmethylated T47D cell lines were treated with AZA and/or TSA. Whilst methylation reversal significantly upregulated mRNA expression as shown above (Figure 4.5B), it did not however alter protein expression. Protein levels remained the same following treatment with either AZA or TSA, or the combination (Figure 4.14).

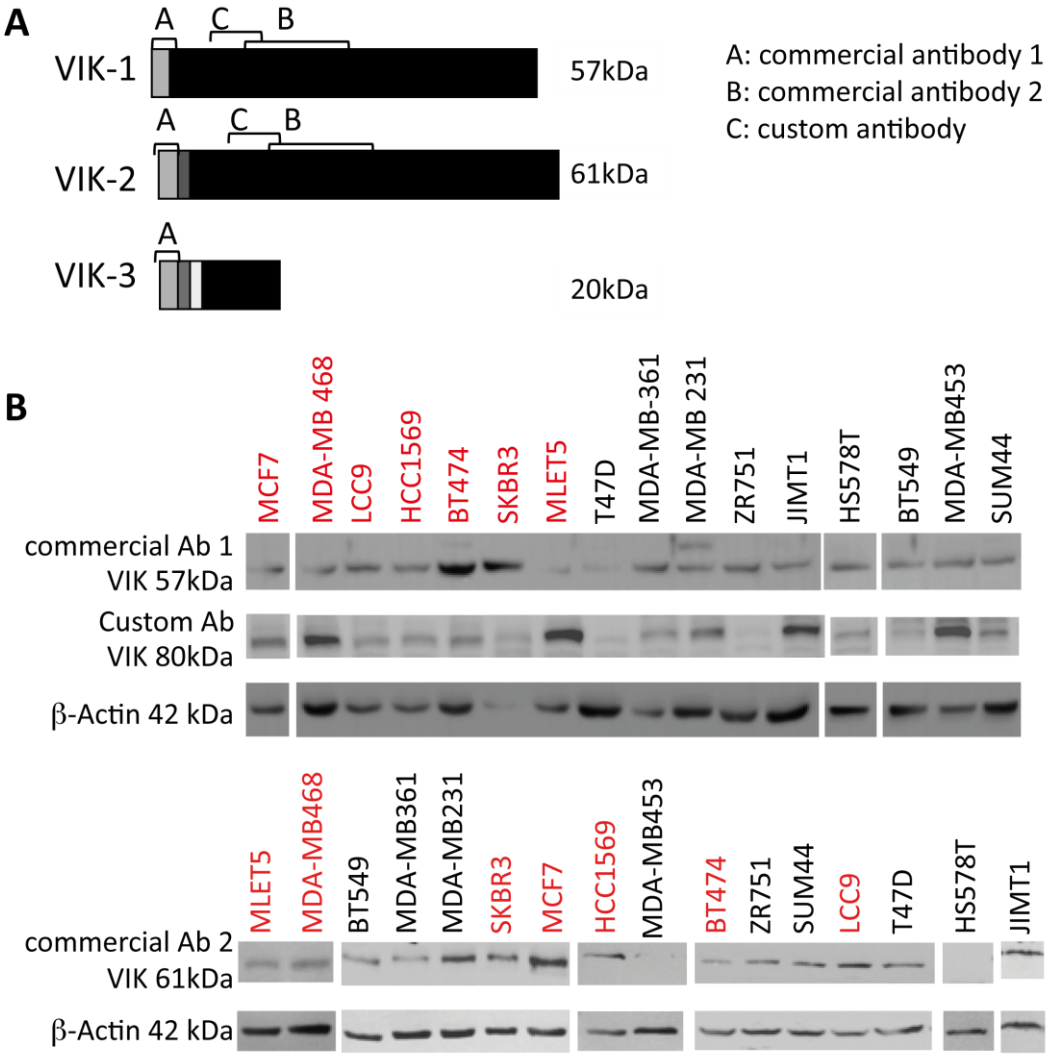

Figure 4.13. VIK protein detection in breast cancer cell lines. A) Diagram of known VIK protein isoforms, and epitopes of each antibody. There are 3 confirmed proteins VIK-1 (57kDa), VIK-2 (61kDa) and VIK-3 (20kDa). B) Representative western blot images, showing protein expression across a panel of breast cancer cell lines using 3 different antibodies against VIK and the corresponding β-actin control. Methylated cell lines are labelled in red, whilst unmethylated cell lines are labelled in black.

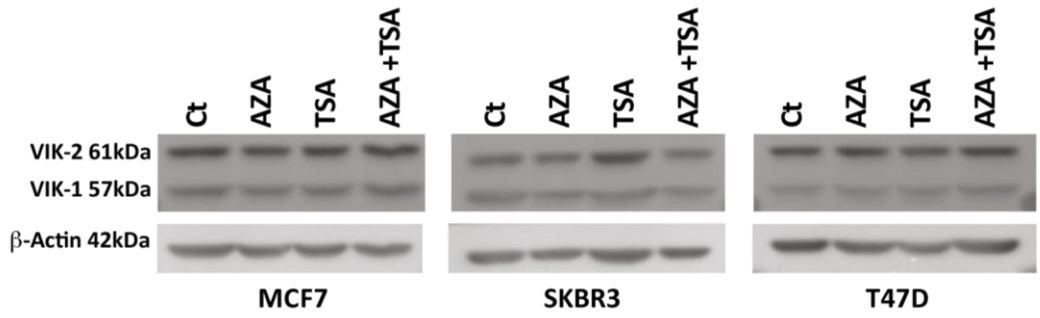

Figure 4.14. Methylation reversal does not upregulate protein. Methylated cell lines, MCF7, SKBR3 and the unmethylated T47D, were treated with a demethylating agent (AZA), a histone deactylatalase inhibitor (TSA), or both. Western blot analysis of protein expression showed no change in protein levels following any treatment.

So far we have been unable to correlate baseline mRNA expression to protein levels, or upregulation of mRNA to protein, leading us to question the accuracy of the detected protein. To further validate if the antibodies are correct, levels of VIK were modulated in cell lines and western blot performed to determine if the protein was also modulated. The unmethylated, VIK expressing cell lines T47D, SUM44 and MCF10A were transfected with VIK siRNA targeting all isoforms. siRNA treatment resulted in depletion of the protein via western blot with all antibodies (Figure 4.15). This would suggest that the antibodies are all correctly detecting VIK.

However, this did not answer the question regarding protein expression in methylated cell lines, therefore we attempted to modulate protein levels in methylated cell lines also (Figure 4.16). siRNA treatment in the methylated MCF7 cells, with no detectable VIK mRNA, did not result in loss of the protein. Upon overexpression of VIK-1 in the MCF7, using a pcDNA3.1 VIK-1 expression plasmid, there was no increase in protein level with any antibody.

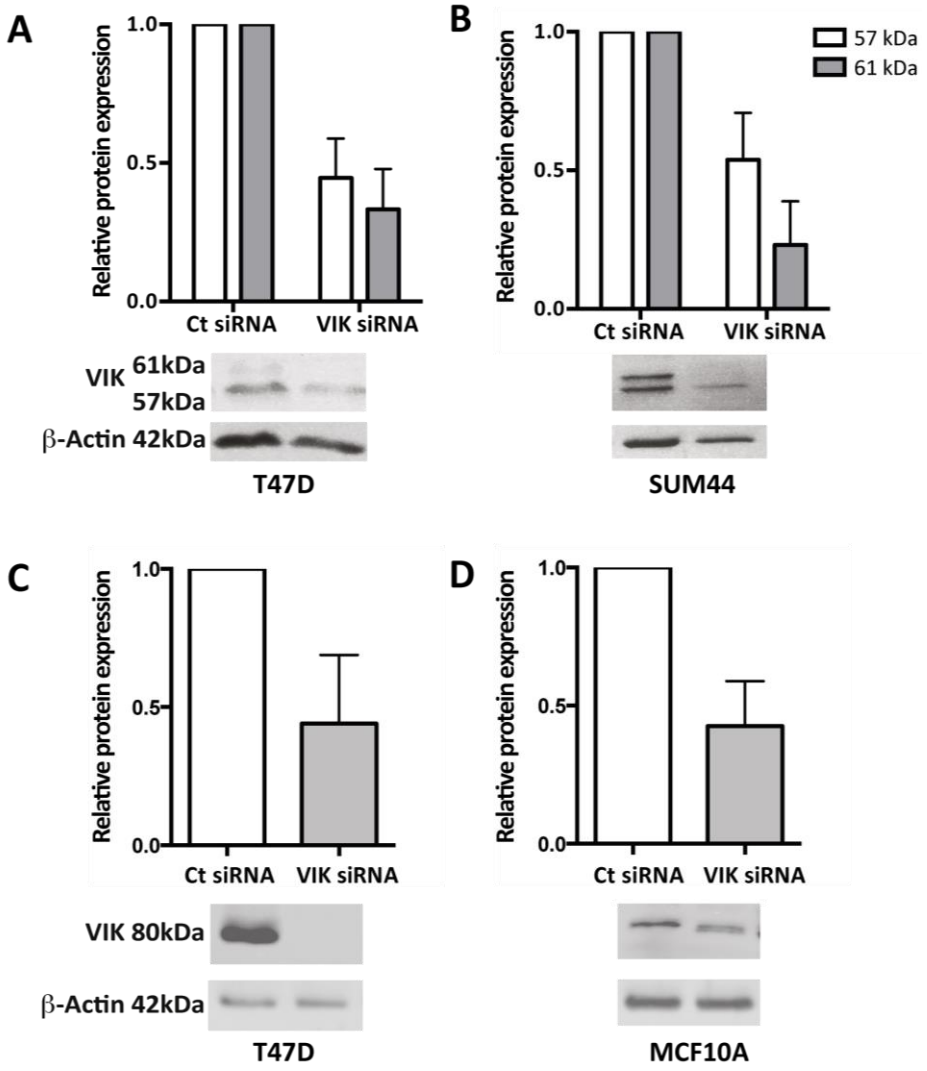

Figure 4.15 Protein detection of VIK following siRNA knockdown in unmethylated cell lines. Protein expression was detected by western blot using the commercial and custom antibodies after modulating VIK levels by siRNA knockdown. A representative western blot is shown alongside quantification of protein levels by densitometry, normalised to the β-actin loading control and shown relative to the non-targeting siRNA control. A) Using the commercial antibodies to detect protein, VIK targeting siRNA knocked-down protein in the unmethylated T47D and B) SUM44 cells. C) The custom antibody also showed decreased protein following siRNA treatment in T47D cells and D) MCF10A cells.

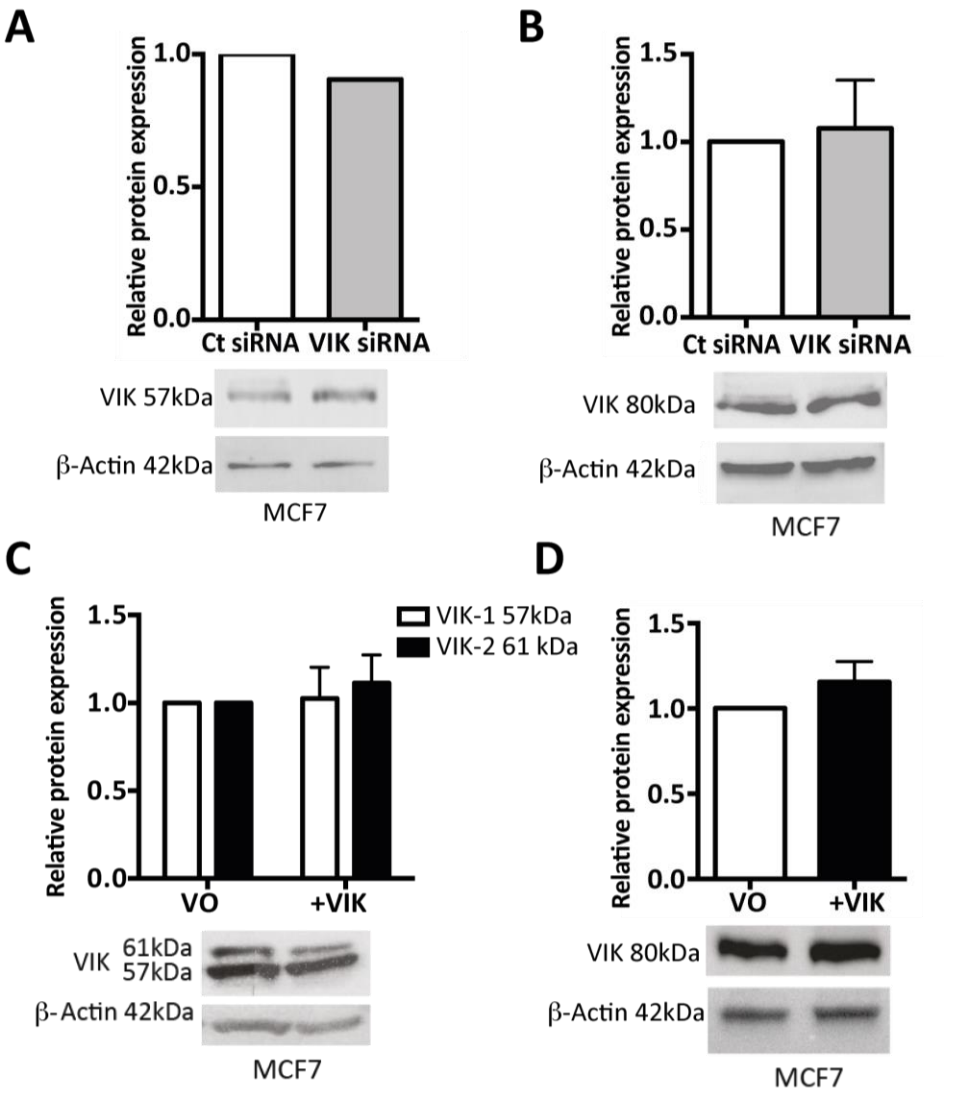

Figure 4.16. Protein expression in methylated MCF7 cells following modulation of VIK expression. A) VIK targeting siRNA did not alter protein expression with either commercial antibody 1 or B) the custom antibody. C) VIK-1 over expression with a pcDNA3.1 expression vector in methylated cell line, MCF7, did not increase the protein band when compared to transfection with pcDNA3.1 vector only (VO). D) The custom antibody also did not show increased protein following transfection with a pcDNA3.1 VIK-1 expressing plasmid. A representative western blot is shown, alongside protein quantification. Protein was quantified relative to β-actin and normalised to the control.

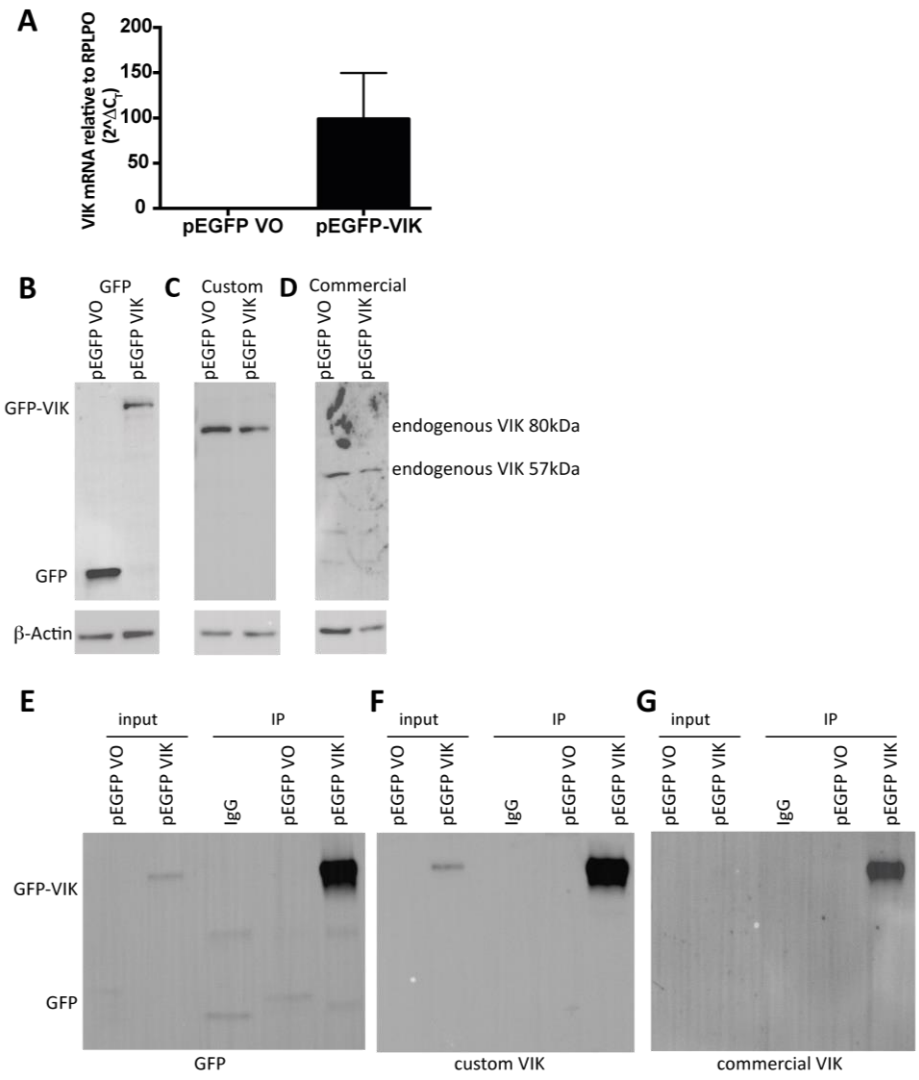

Figure 4.17. Immunopreciptation (IP) of EGFP-tagged VIK. HEK293T cells were transfected with a pEGFP-VIK vector or pEGFP vector only (VO). A) RT-qPCR confirming upregulation of VIK mRNA following transfection. Representative western blot of pEGFP-VIK transfected cells probed with B) GFP antibody C) custom VIK antibody D) commercial VIK antibody. GFP antibody clearly detects the overexpressed EGFP-tagged VIK protein. Immunoprecipitation was performed on transfected cells, using a GFP antibody to pull out the EGFP tagged VIK protein. IP samples were run on a western blot and probed for E) GFP F) custom VIK antibody G) commercial VIK antibody. Both VIK antibodies and the GFP antibody detect the same strong band in cells transfected with pEGFP-VIK.

Thus far, protein expression did not correlate to baseline mRNA levels and increased mRNA expression did not translate to increased protein. This led to concerns for the accuracy of our antibodies. To confirm if the antibodies were actually detecting VIK, immunoprecipitation (IP) was performed followed by mass spectrometry analysis of the protein band. Ideally endogenous IP of VIK from a methylated and unmethylated cell line would have been carried out, to compare the protein in each. However, neither the custom nor commercial antibody was found suitable for immunoprecipitation. Therefore, full length VIK-1 was cloned into a pEGFP vector, and transfected into HEK293T. RT-qPCR confirmed over expression of VIK in cells transfected with pEGFP-VIK compared to pEGFP vector only (Figure 4.4A). The GFP antibody detected a strong band in the pEGFP-VIK transfected cells, that was not present in the vector only transfected cells (Figure 4.17B), although this band was not clearly detected by the commercial or custom antibody (Figure 4.17 C,D). Following IP, the GFP antibody and both VIK antibodies detected the same single band at the same size, approximately 100kDa, in pEGFP-VIK transfected cells. This indicates both the custom and commercial antibody do detect VIK (Figure 4.17 E-G). The IP product was resolved on an acrylamide gel to separate out the proteins and the gel was stained with coomassie blue. The gel was cut around the band corresponding to pEGFP-VIK and mass spectrometry carried out to determine identity of the protein.

ID	Protein Name	Protein Score	Mass, kDa
PARP1	Poly [ADP-ribose] polymerase 1	915.62	116
GRP78	78 kDa glucose-regulated protein	912.24	78
XRCC5	X-ray repair cross-complementing protein	708.86	83
ZN655 (VIK)	**Zinc finger protein 655**	**694.33**	**61, 57, 20**
NUCL	Nucleolin	683.30	77
DDX21	Nucleolar RNA helicase	636.18	87, 79
HS90B	Heat shock protein HSP 90-beta	618.11	90
HS71B	Heat shock 70 kDa protein 1B	543.71	70
SSRP1	FACT complex subunit SSRP1	503.17	90
HS90A	Heat shock protein HSP 90-alpha	493.44	90
ILF3	Interleukin enhancer-binding factor	463.67	95, 76, 82, 75, 76
EF2	Elongation factor 2	381.33	95
HS71L	Heat shock 70 kDa protein 1-like	371.11	70
HSP7C	Heat shock cognate 71 kDa protein	363.03	71

Figure 4.18. Top results from mass spectrometry. Following IP for EGFP-VIK, the IP sample was separated on an acrylamide gel, stained with coomassie blue and the band corresponding to EGFP-VIK analysed by mass spectrometry. ZNF655 (VIK) was among the top protein scores. Protein score is the parameter characterising the reliability of protein identification.

Mass spectrometry produced a list of proteins with a corresponding protein score. This is the measure characterising the reliability of protein identification. Out of 419 proteins in total, 75 proteins had a high score above 100. Of the top scoring proteins, VIK (ZNF655) was 4th highest with a score of 694.33 (Figure 4.18). The presence of VIK indicates the antibodies could be correctly detecting VIK. However, it is possible that our antibodies detect another protein from the list. Although, comparison of the antibody epitopes and the protein sequences demonstrated no region for the antibodies to bind to any of the proteins from the list other than VIK. Therefore it is likely the other proteins are unspecific. Many of the proteins listed were heat shock proteins, which function as chaperone proteins. Additionally, a number of the highly scoring proteins are all involved in the DNA damage response (PARP, XRCC5, SSRP1, DDX21, NUCL).

4.5.2 Immunofluorescence

To further understand the protein expression of VIK, it may be important to consider localisation of the protein, and therefore, immunofluorescence was performed to confirm where the protein we detected was localised. The only paper regarding VIK has shown immunofluorescence of VIK with primarily nuclear staining (277). Neither commercial antibody was found to be suitable for immunofluorescence, however the custom antibody was optimised. The methylated MCF7 and unmethylated T47D were stained using the anti-VIK antibody and DAPI for nuclear staining (Figure 4.19). In the methylated and unmethylated cell lines, VIK was observed in both the nucleus and the cytoplasm. However, contradictory to expectation, VIK was predominantly in the cytoplasm, in both the methylated and unmethylated cell lines.

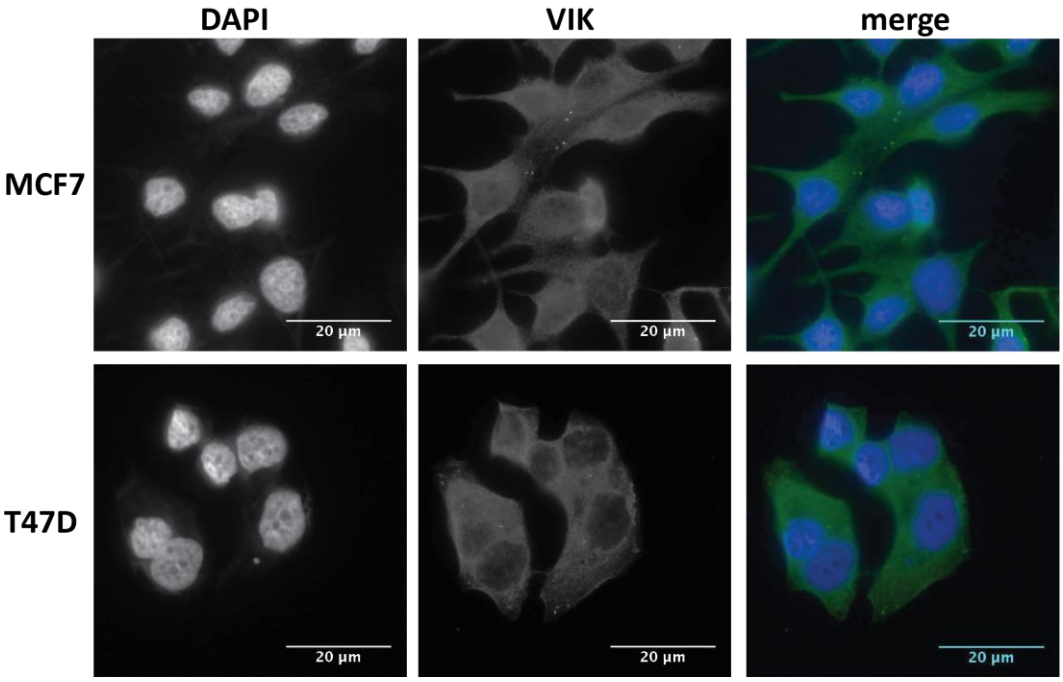

Figure 4.19. Immunofluorescence reveals sub-cellular localisation of VIK. Cells were stained for VIK (green) and nuclear staining with DAPI (blue). VIK was observed in both the nucleus and the cytoplasm, but was predominantly cytoplasmic. Scale bar= 20µm.

4.6 Inducible expression of VIK

As we were unable to show how VIK protein expression correlated with mRNA levels or methylation status, it is possible that whilst methylation does not affect baseline levels of VIK protein, methylation might inhibit inducible expression of the protein. To investigate this, the methylated cell line MCF7 and unmethylated cell line, T47D, were treated with conditions that might induce VIK expression.

4.6.1 Growth factor stimulation

We hypothesised that methylation of VIK might inhibit inducible expression of VIK, by inhibiting binding of transcription factors in the gene promoter region. To identify any putative transcription factor binding domains, an *in silico* analysis of the 5'UTR region, which is overlapped by the CpG island, was performed using MatInspector software (291). This analysis compared the input DNA sequence with known nucleotide binding motifs of transcription factors or co-activators. An algorithm assigns each putative binding site match with a score between 0 and 1, which indicates the similarity between the input DNA sequence and the database of known binding motifs. A score of 1 reflects a perfect match of the sequence to the identified binding motif. Any score above 0.8 indicates the transcription factor could bind to the DNA sequence, although there may be some nucleotide deviations between the known database sequence and the input DNA sequence. This analysis produced a list of 315 matches, of which 242 had 'good' scores above 0.8 and 150 scored above 0.9. There were 8 matches with a perfect score of 1.0. These included FOXP1 (Forkhead box protein P1), TAIP3 (TGF-β induced apoptosis protein 3) and signal transducer and activator of transcription 1 (STAT1). These are all activated by growth factor stimulation. FOXP1 and TAIP3 by transforming growth factor β (TGF-β) and

STAT1 by epidermal growth factor (EGF), therefore we needed to confirm if either of these growth factors would induce VIK expression.

EGF treatment did not alter VIK mRNA expression in MCF7 cells, but did show a potential upregulation of mRNA in T47D cells following 8 hours EGF treatment (Figure 4.20A), however there was no change in protein levels in either cell line (Figure 4.20B). In both cell lines, treatment with TGF-β had no effect on mRNA (Figure 4.20C) or protein via western blot with the custom antibody (Figure 4.20D).

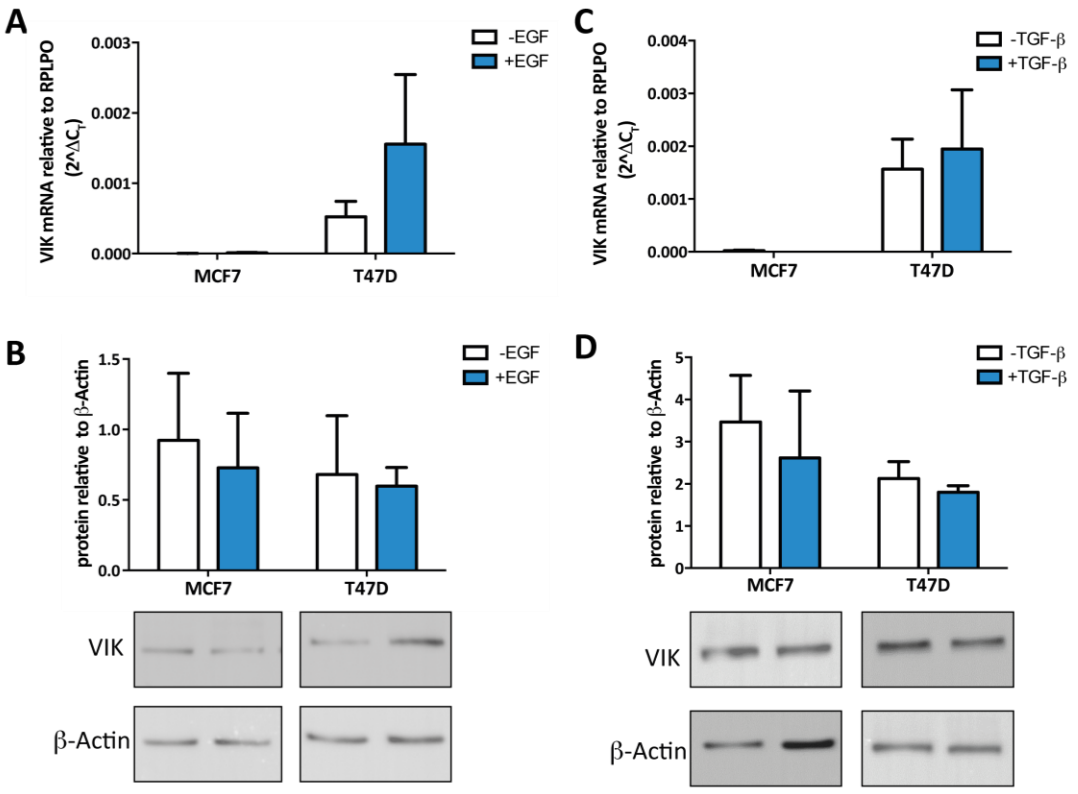

Figure 4.20. TGF-β or EGF treatment does not induce VIK expression. Methylated MCF7 and unmethylated T47D were treated with either 40ng/ml EGF or 10ng/ml TGF-β or a vehicle control, for 8 hours. A) RT-qPCR analysis after EGF treatment. There was no change in MCF7 cells, but some upregulation in T47D cells. B) Quantification of protein levels showed no change in either cell line upon EGF treatment. Underneath is a representative western blot, samples are in the same order as the histogram above. C) RT-qPCR analysis revealed there was no change in mRNA levels following TGF-β treatment. D) Quantification of protein expression following TGF-β treatment showed no change in protein levels, alongside a representative western blot image. Graphs show average of duplicate experiments +/- SD.

4.6.2 Hypoxic stress response

To determine if VIK expression might be induced with the context of a generalised stress response, cells were placed under hypoxic stress via incubation at 1% oxygen (Figure 4.21). Hypoxic conditions had no effect on mRNA levels in the methylated MCF7 cells, mRNA expression remained undetectable. However, following protein detection with the custom antibody, the MCF7 did show a nearly 2-fold increase in protein levels at 24 hours, but less so at 48 hours. In the unmethylated T47D, 24 hours in hypoxia induced a modest mRNA induction, and significantly higher mRNA was observed at 48 hours. The T47D demonstrated a significantly larger increase in protein expression, than the MCF7, with a 5-fold increase in protein at 24 hours and 3-fold higher at 48 hours.

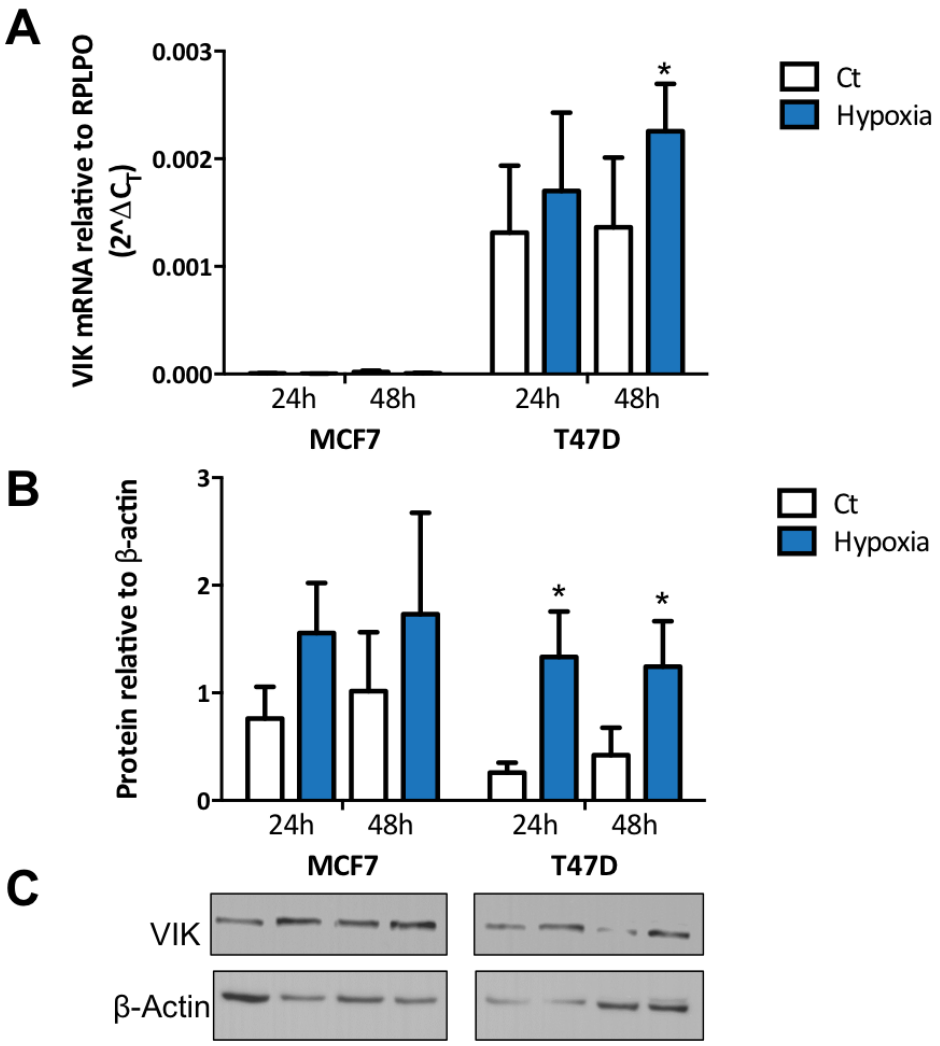

Figure 4.21 Hypoxic conditions induce VIK expression. The methylated MCF7 cell line and unmethylated T47D were cultured in 1% oxygen (Hypoxia) or normal 20% oxygen (Ct). A) RT-qPCR analysis shows small induction of mRNA at 24 and further induction at 48 hours in T47D cells in hypoxic conditions. mRNA levels in MCF7 cells remained undetectable. B) Quantification of western blot analysis of VIK protein levels. Protein levels were normalised to β-actin loading control. C) Representative western blot image. Samples are in the order of the histogram above. Graphs display mean of triplicates +/- standard deviation.

4.7 Summary

Across a panel of breast cancer cell lines VIK expression was variable. The normal cell line MCF10A, was VIK expressing and unmethylated. Methylation closely correlated to VIK mRNA expression, with VIK mRNA undetectable in all methylated cell lines. Additionally, reversal of methylation upregulated mRNA expression. Together, this demonstrates a mechanism for methylation dependent transcriptional silencing of VIK, although we were unable to correlate protein expression with methylation or mRNA.

Analysis of methylation in patient cohorts indicated approximately 7-14% of breast cancer patients to be methylated for VIK. Compared to normal samples, primary tumour samples exhibited higher levels of VIK methylation and decreased expression of VIK. Methylation significantly correlated to VIK expression, indicating DNA methylation transcriptionally silences VIK expression in a subset of breast cancer tumours.

5 Results: VIK in cell death and sensitivity to endocrine treatment

5.1 Modulating levels of VIK induces cell death

Having established that promoter methylation results in transcriptional silencing of VIK mRNA, investigation began into the functional consequences of this silencing in breast cancer. Firstly, we began by overexpression of VIK in methylated cell lines and knocking down VIK isoforms in unmethylated cell lines.

5.1.1 Overexpression of VIK induces cell death

To investigate the effect of ectopic VIK expression in methylated cell lines, cells were transfected with either a pcDNA3.1 vector only (VO) or full length VIK-1 expression vector, followed by antibiotic selection over 7 days for successfully transfected cells. However, ectopic expression of VIK-1 resulted in cell death. Whilst vector only cells grew normally after stable transfection and selection, cells over-expressing VIK-1 were unable to survive (Figure 5.1). This was true for both methylated cell lines (MCF7, BT474) and also the unmethylated cell line T47D, demonstrating cells will not tolerate overexpression of VIK-1 regardless of endogenous expression levels.

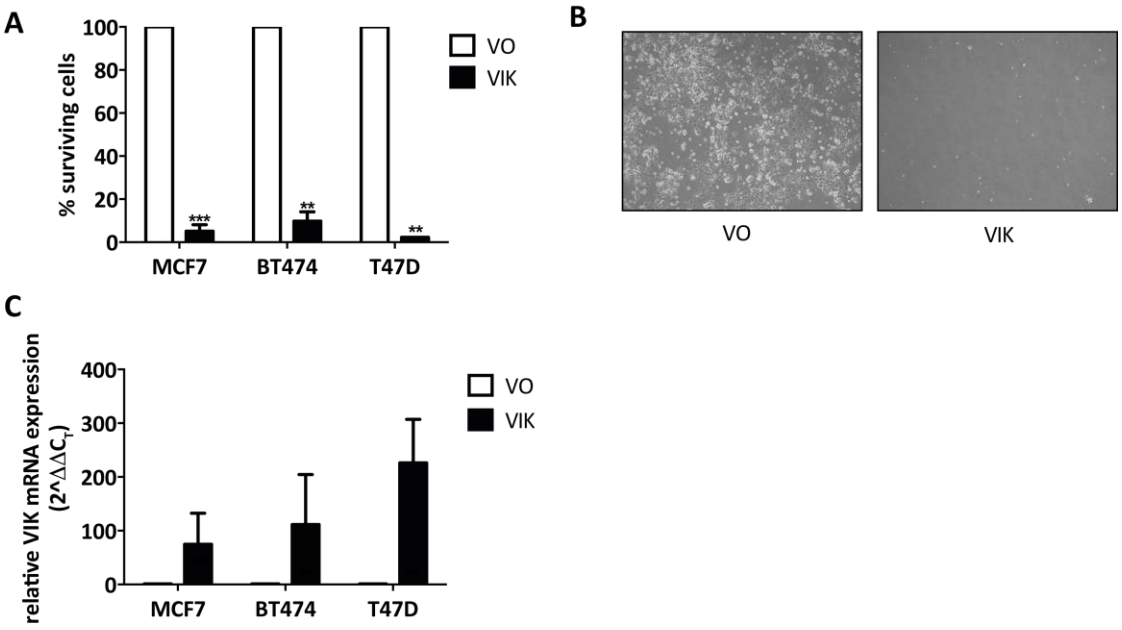

Figure 5.1 Over-expression of VIK-1 causes cell death. A) Cells were transfected with an empty pcDNA3.1 vector (VO) or pcDNA3.1 vector containing full length VIK-1. After selection with G418 treatment for 7 days, number of live cell was determined by MTT assay. B) Representative image following transfection with vector only (VO) or pcDNA3.1-VIK for 7 days in T47D cells. C) RT-qPCR confirms upregulation of VIK mRNA following 3 days transfection with the expression vector.

5.1.2 Knockdown of VIK induces cell death via apoptosis

To determine the functional role of loss of VIK expression, VIK was knocked down in unmethylated, VIK mRNA expressing cell lines. As there are multiple transcripts and isoforms of VIK, the siRNA was required to knockdown all isoforms. Of all siRNA's tested, only three were able to reduce the mRNA levels of VIK. When tested across all RT-qPCR assays only siRNA 2 and siRNA 3 showed mRNA knockdown of all isoforms (Figure 5.2A). siRNA 2 gave at least 80% knockdown across all assays compared to the non-targeting siRNA control. Analysis of surviving cells following knockdown by MTT assay displayed significant cell death after treatment with both siRNA 2 and siRNA 3. However, siRNA 3 displayed significantly more cell death than siRNA 2 leaving only 16% of cells alive at day 5 (Figure 5.2B). Therefore, all following knockdown experiments were conducted using siRNA 2, so there would be sufficient cells alive for analysis.

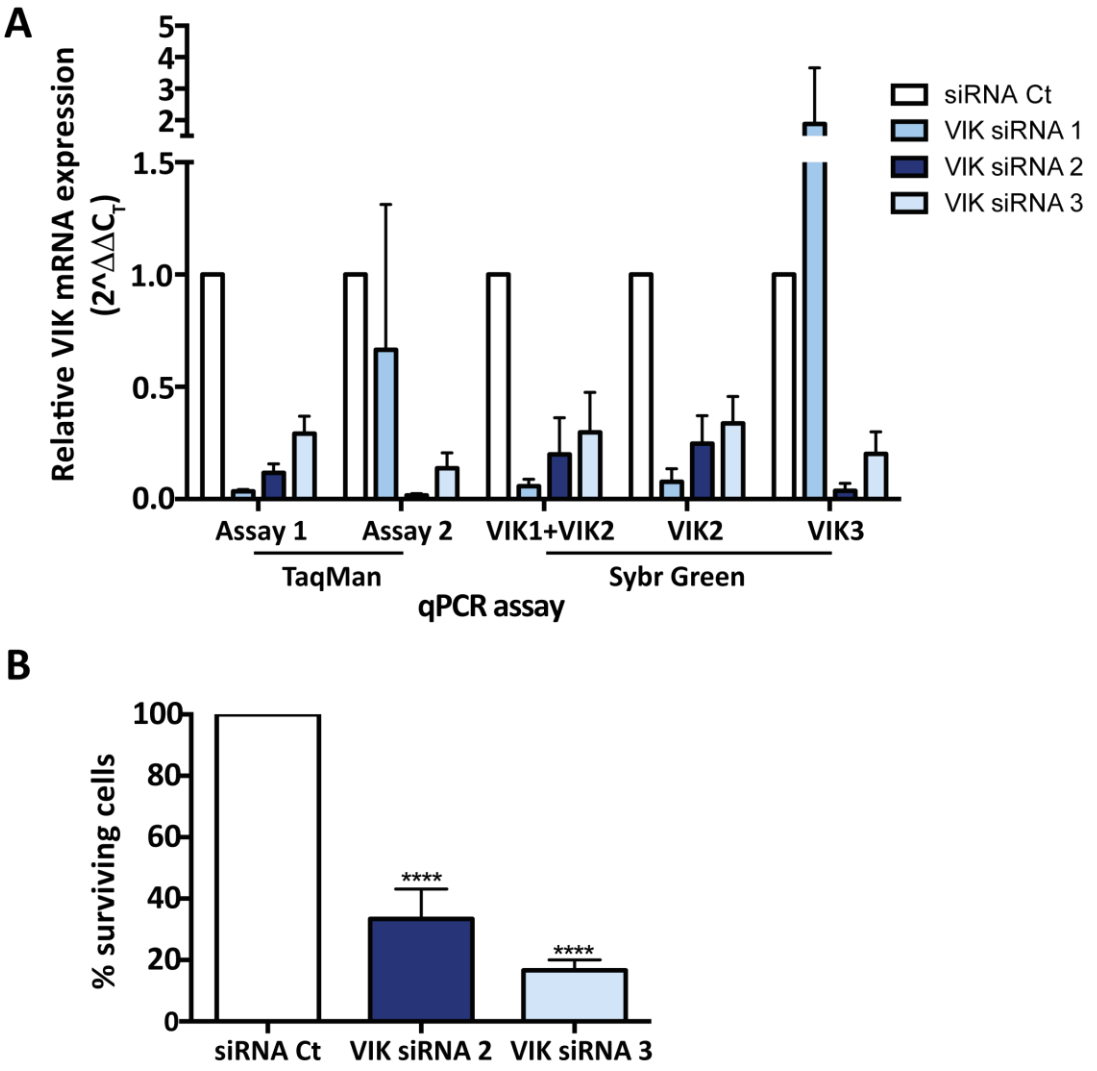

Figure 5.2 Optimisation of VIK siRNA knockdown in T47D cells. A) VIK mRNA expression following 72 hours treatment with VIK siRNA. Three VIK targeting siRNAs were tested across all RT-qPCR assays. mRNA was analysed relative to the housekeeping gene RPLPO and each siRNA normalised to the non-targeting siRNA control. B) Proportion of cells surviving after day 5 of VIK knockdown relative to the non-targeting siRNA. Surviving cells were assessed by MTT assay. ****P<0.0001 1-way ANOVA.

As there was significant cell death at 5 days post transfection, the proportion of surviving cells was followed over time after siRNA treatment in unmethylated cell lines. Reduction of VIK mRNA resulted in gradual cell death, as measured by MTT assay, over time (Figure 5.3). Cells were treated with siRNA for up to 7 days, mRNA analysis showed successful knockdown of VIK compared to the non-targeting control siRNA. In the T47D, 20% of cells died after 3 days of knockdown increasing by day 5 to 60%. The SUM44 showed 10% cell death at day 3 increasing to 40% at day 4. Additionally siRNA knockdown caused cell death in the normal breast cell line MCF10A. The normal breast cell line was in fact more sensitive to VIK knockdown. Only half of the cells survived after 2 days of siRNA treatment, dropping to 10% on day 4, and the cells began to recover as the VIK mRNA expression increased again on day 7. These results indicate that the death inducing effects of VIK modulation is not tumour specific.

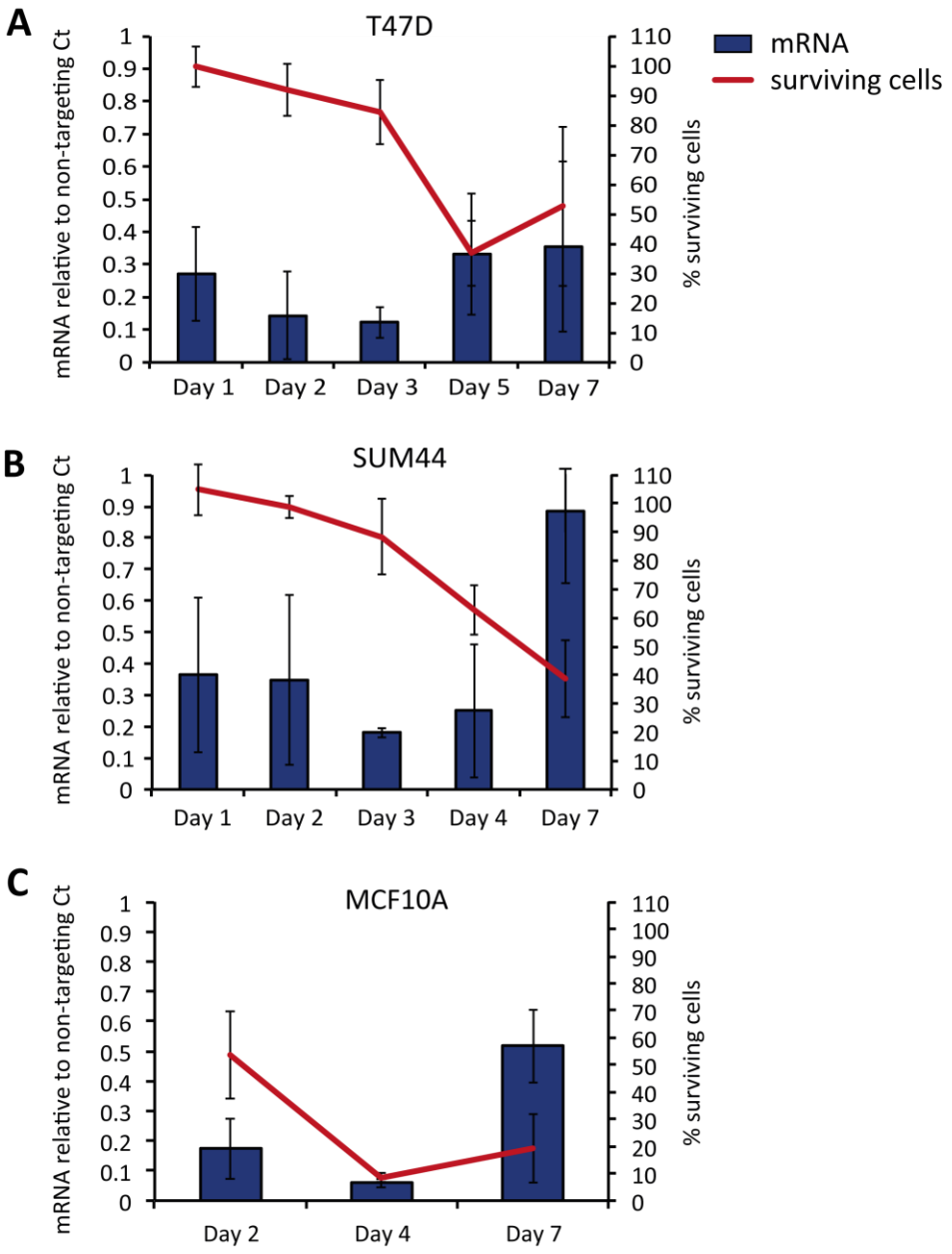

Figure 5.3 VIK knockdown is lethal to breast cancer cells. Cancer cell lines A) T47D B) SUM44 and the normal breast cell line C) MCF10A were transfected with VIK targeting siRNA or a non-targeting control. Over time, the proportion of surviving cells was measured by MTT assay. The histogram displays VIK mRNA levels normalised to the non-targeting control (left Y-axis). The red line shows % of surviving cells with VIK knockdown normalised to the non-targeting control (right Y-axis).

Having established cells do not survive with reduced levels of VIK expression, we sought to determine the mechanism by which cells were dying. Therefore apoptosis was investigated. Apoptosis is a tightly controlled process of cell death, co-ordinated by a complex event of signalling cascades involving caspase activation, cleavage of intracellular proteins, exocytosis of cellular contents leading to eventual shrinkage of cells and phagocytosis. A key event in the earlier stages of apoptosis is translocation of phosphatidylserine (PS) to the extracellular membrane, aiding phagocytosis (292). Externalisation of PS can be measured using annexin V. Another marker of cell death is uptake of DAPI, which is excluded by live cells. This allows distinction between alive, dead, and apoptotic cells. Annexin V and DAPI negative are alive, DAPI positive only are dead and annexin V positive cells are undergoing apoptosis. All cell lines showed some apoptosis and cell death following transfection with the non-targeting siRNA alone, especially the MCF10A and SUM44 cells which were particularly sensitive to siRNA transfection. In T47D cells there was a significant increase in annexin V staining, with VIK knockdown doubling the proportion of apoptotic cells (Figure 5.4A). SUM44 cells also showed a trend for increased annexin V staining with an increase from 17% apoptotic cells with control siRNA to 29% with VIK knockdown (Figure 5.4B). In concordance with the MTT cell survival analysis, the non-tumour cell line, MCF10A, showed a higher proportion of cells in apoptosis. Knockdown of VIK significantly increased annexin V staining, with 76% of cells in apoptosis (Figure 5.4C).

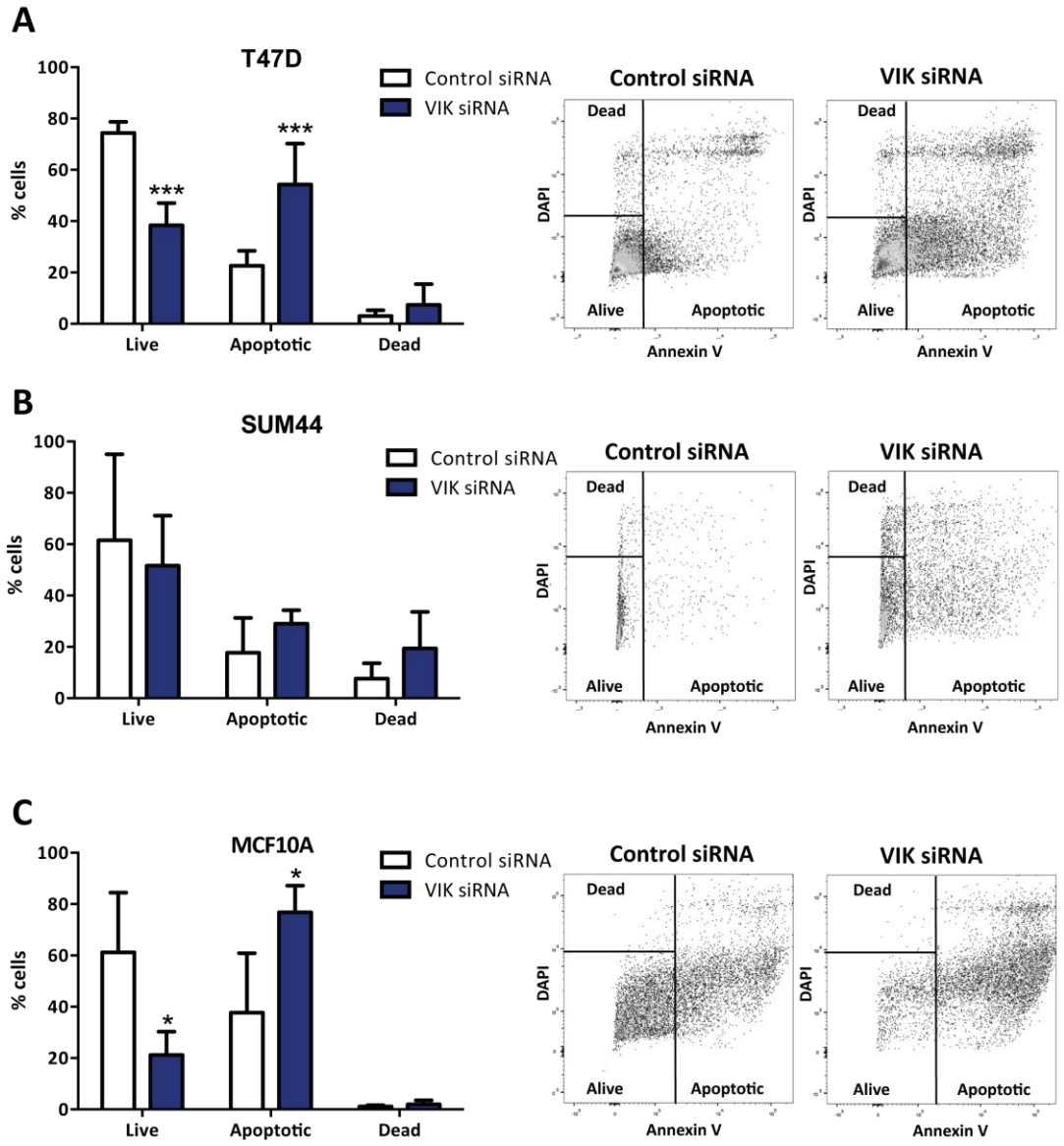

Figure 5.4 Knockdown of VIK induced apoptosis. The VIK expressing tumour cell lines A) T47D and B) SUM44 or the normal cell line C) MCF10A were transfected with siRNA targeting VIK or a scrambled non-targeting control. After 5 days knockdown cells were stained for DAPI or annexin V. Cells negative for DAPI and annexin V were considered alive, cells positive for DAPI but negative for annexin V cells were dead, whilst cells positive for annexin V were undergoing apoptosis. Proportion of cells in each state is shown in the histogram, alongside an example flow cytometry plot. *P<0.05 ***P<0.001 2-way ANOVA.

To confirm apoptosis with a second marker, cleavage of poly(ADP-ribose) polymerase (PARP) was assessed. Full length-PARP is an 116kDa protein involved in DNA repair. During apoptosis the protein is cleaved into an 89kDa fragment by activated caspases (293). Both the tumour cell lines, T47D and SUM44, and the non-tumour line MCF10A, showed significantly increased levels of cleaved PARP after VIK knockdown when compared to the non-targeting siRNA (Figure 5.5). The increased cleavage of PARP, in combination with increased annexin V staining, shows VIK knockdown induces apoptosis.

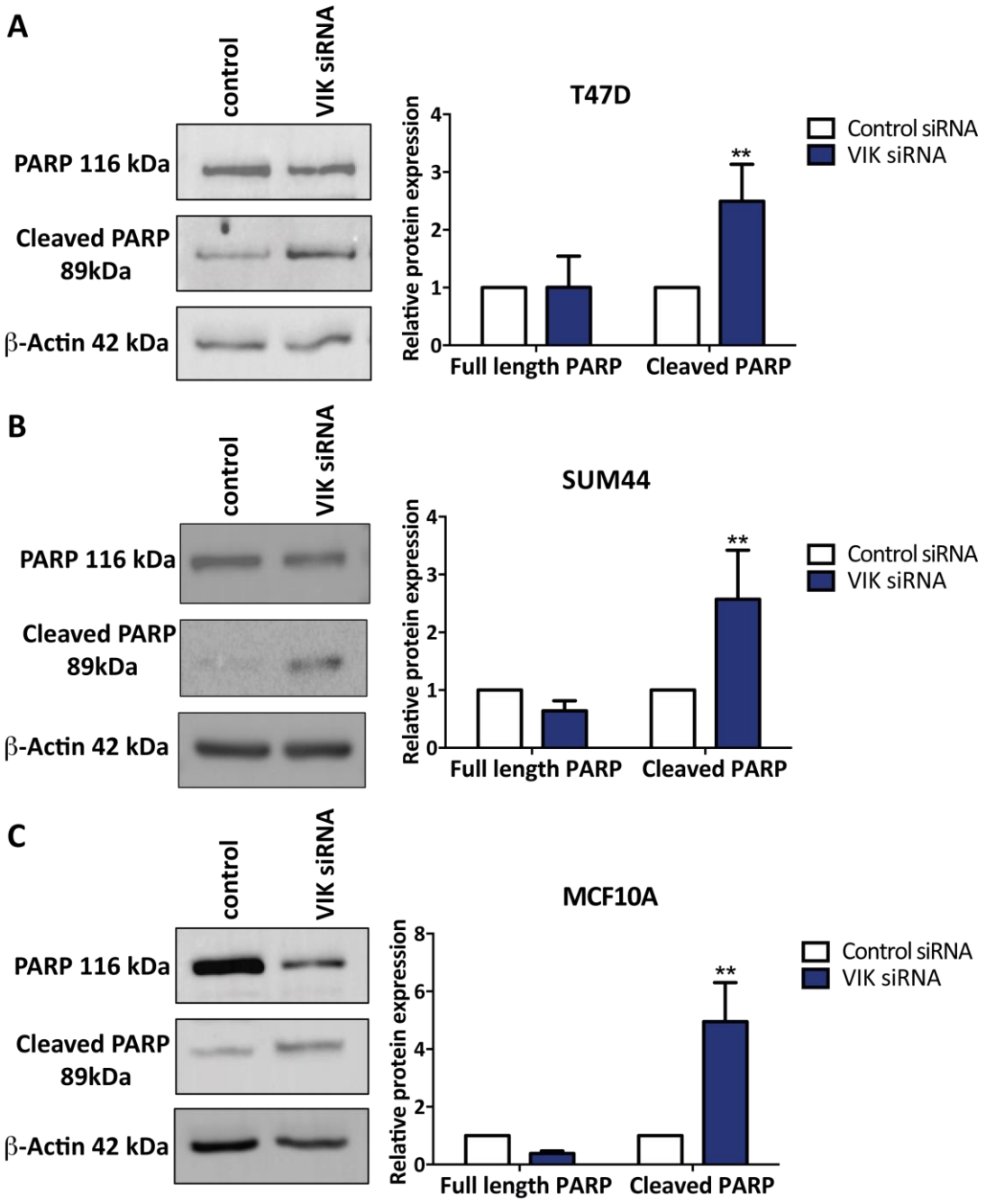

Figure 5.5. VIK knockdown increased cleavage of PARP. Western blot analysis of PARP and cleaved PARP in A) T47D B) SUM44 and C) MCF10A cells. An example western blot and quantification of triplicate blots is shown. Western blots were quantified by densitometry, relative to the β-actin loading control and normalised to the non-targeting control siRNA.

5.2 The effect of VIK on sensitivity to endocrine treatment.

The preliminary patient cohort linked VIK methylation to poor outcome in patients following treatment with tamoxifen. Additionally VIK was associated with lower ER expression and an increased risk of recurrence in tamoxifen-treated patients. This suggested a role for VIK in endocrine resistance; therefore we wanted to investigate the effect of VIK on sensitivity to endocrine therapy *in vitro*.

5.2.1 VIK expression is not induced by estrogen

To determine if VIK might have a role in ER+ breast cancer via an involvement with estrogen signalling, we hypothesised that VIK expression might be induced by estrogen. Therefore, MCF7 (VIK methylated) and T47D (VIK unmethylated) were treated with estradiol (E2) for 1 hour and 8 hours.

No significant increase in VIK mRNA was seen following estradiol treatment in either the methylated or unmethylated cell line. Induction of MYC, a well-characterised downstream target of estradiol, confirmed cell response to estradiol treatment. In MCF7, estradiol induced greater than 2-fold increase in MYC mRNA at 1 hour, sustained until 8 hours. T47D cells exhibited an initial 4-fold upregulation following 1 hour, and 1.7-fold increase at 8 hours. However, no significant increase in VIK mRNA was seen following estradiol treatment in either the MCF7 or T47D cell line. VIK mRNA remained undetectable in the methylated MCF7 cell line, and there was no change in expression levels in the unmethylated T47D.

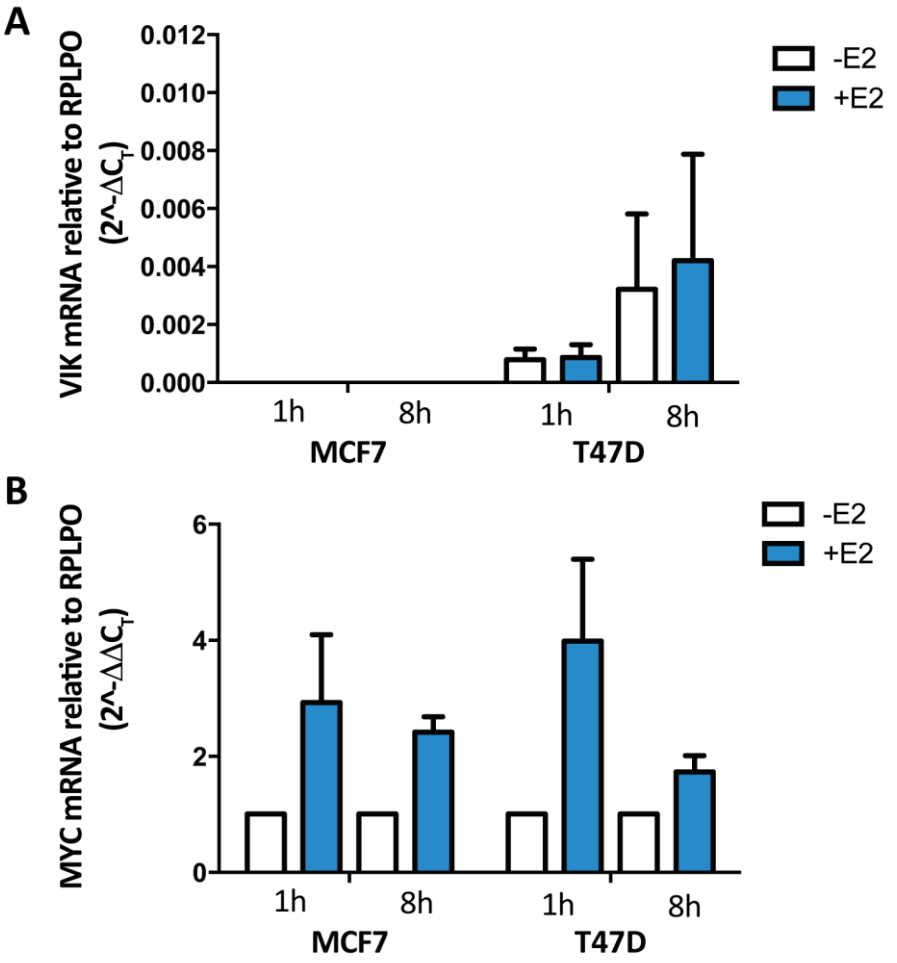

Figure 5.6. VIK expression is not induced by estradiol. A) The VIK methylated cell line MCF7 and unmethylated cell line T47D were stimulated with estradiol for 1 hour and 8 hours. There was no change in mRNA following treatment. mRNA expression is normalised to the RPLPO housekeeping gene. B) Expression levels of MYC mRNA following estradiol treatment, estradiol induces upregulation of MYC expression. mRNA levels are normalised to the non-treated control. Graphs show mean of triplicates +/- standard deviation.

5.2.2 VIK expression is not a determinant of sensitivity to tamoxifen

To investigate any role of VIK in sensitivity to endocrine therapy *in vitro*, VIK was knocked down in the ER+ VIK expressing cell lines, T47D and SUM44. Following siRNA knockdown, IC_{50} (the drug concentration required to kill 50% of cells) determination was performed to evaluate sensitivity to tamoxifen. Given that VIK methylation was associated with increased risk of recurrence in patients following tamoxifen treatment, it might be expected that knockdown of VIK would increase resistance to tamoxifen in sensitive cell lines. However, VIK knockdown did not affect sensitivity to tamoxifen. No difference was seen in IC_{50} values after transfection with the VIK targeting siRNA when compared to a non-targeting siRNA control in either T47D or SUM44 cells (Figure 5.7).

As previously mentioned there was no correlation between VIK expression and expression of ER in breast cancer lines (Figure 4.4). Additionally, there was no change in VIK expression levels between the MCF7 cells and the LCC9, the endocrine resistant cell line, or MLET5, the estrogen independent cell line, both derived from the MCF7. All three cell lines were methylated and showed no detectable VIK mRNA levels. These results suggest that VIK is not involved in resistance to tamoxifen.

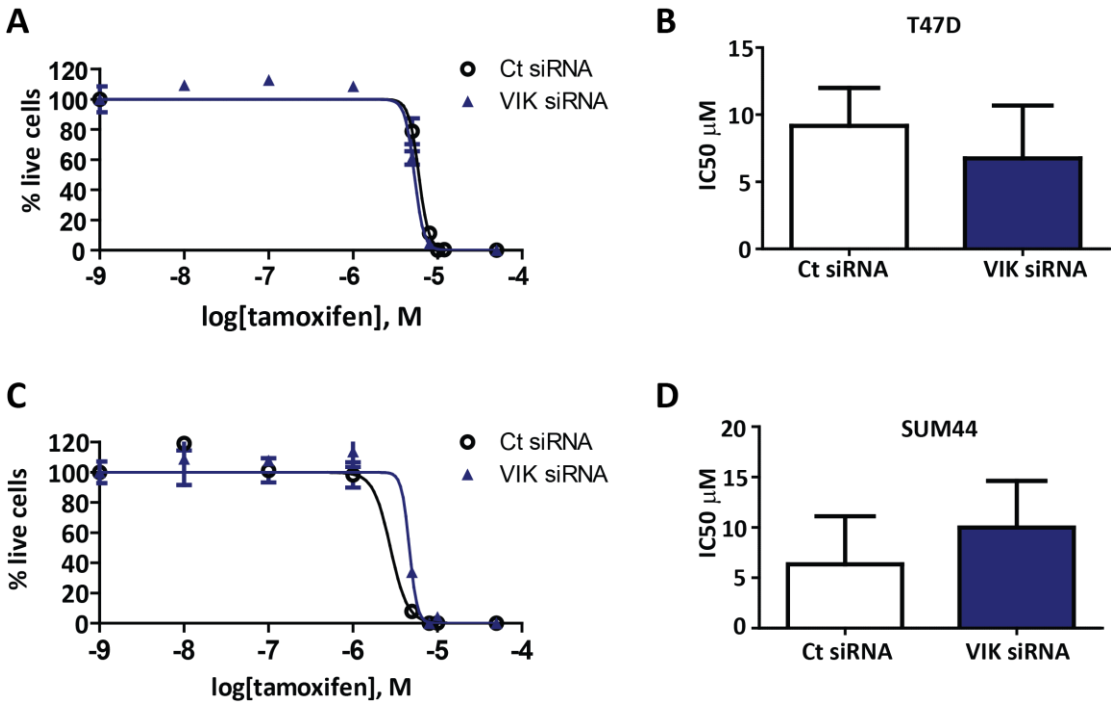

Figure 5.7 VIK and tamoxifen sensitivity. Following transfection with either a non-targeting control siRNA or VIK-targeting siRNA, cells were treated with a range of tamoxifen doses for three days to determine IC_{50} value. A) Representative survival curve for T47D cells and B) average IC_{50} values. C) Representative survival curve for SUM44 cells and D) average IC_{50} values.

5.3 VAV1 compensates for loss of VIK

VIK-1 was first identified via its interaction with VAV1, where VIK-1 and VAV1 were suggested to have a coordinated role within cell cycle regulation (277). To investigate this relationship further, VAV1 expression across the breast cancer cell line panel was determined by RT-qPCR (Figure 5.8A). The non-tumour MCF10A breast cell line did not express VAV1 mRNA. There was variable expression of VAV1 across the panel of breast cancer lines, with no correlation to any particular subtype. VAV1 expression levels did not correspond to VIK methylation status.

Following VIK siRNA knockdown in the unmethylated cell lines, an increase in VAV1 mRNA was observed (Figure 5.8B). In the T47D cells, which express VAV1 endogenously, almost 2-fold increase of VAV1 was observed after 3 days VIK siRNA treatment, this was sustained until day 7. In the SUM44, a cell line that ordinarily expresses very low levels of VAV1, a 2-fold increase was seen also at day 3, after which VAV1 levels returned to normal (Figure 5.8C). Additionally, VAV1 knockdown in T47D cells resulted in an increase in VIK mRNA at 48 hours, and then VIK mRNA was again downregulated to nearly normal levels (Figure 5.8D). However, VAV1 knockdown did not affect VIK expression in the methylated cell line, MCF7. mRNA levels of VIK remained undetectable following siRNA knockdown of VAV1 (Figure 5.8E). These results support a compensatory mechanism between VIK and VAV1 expression.

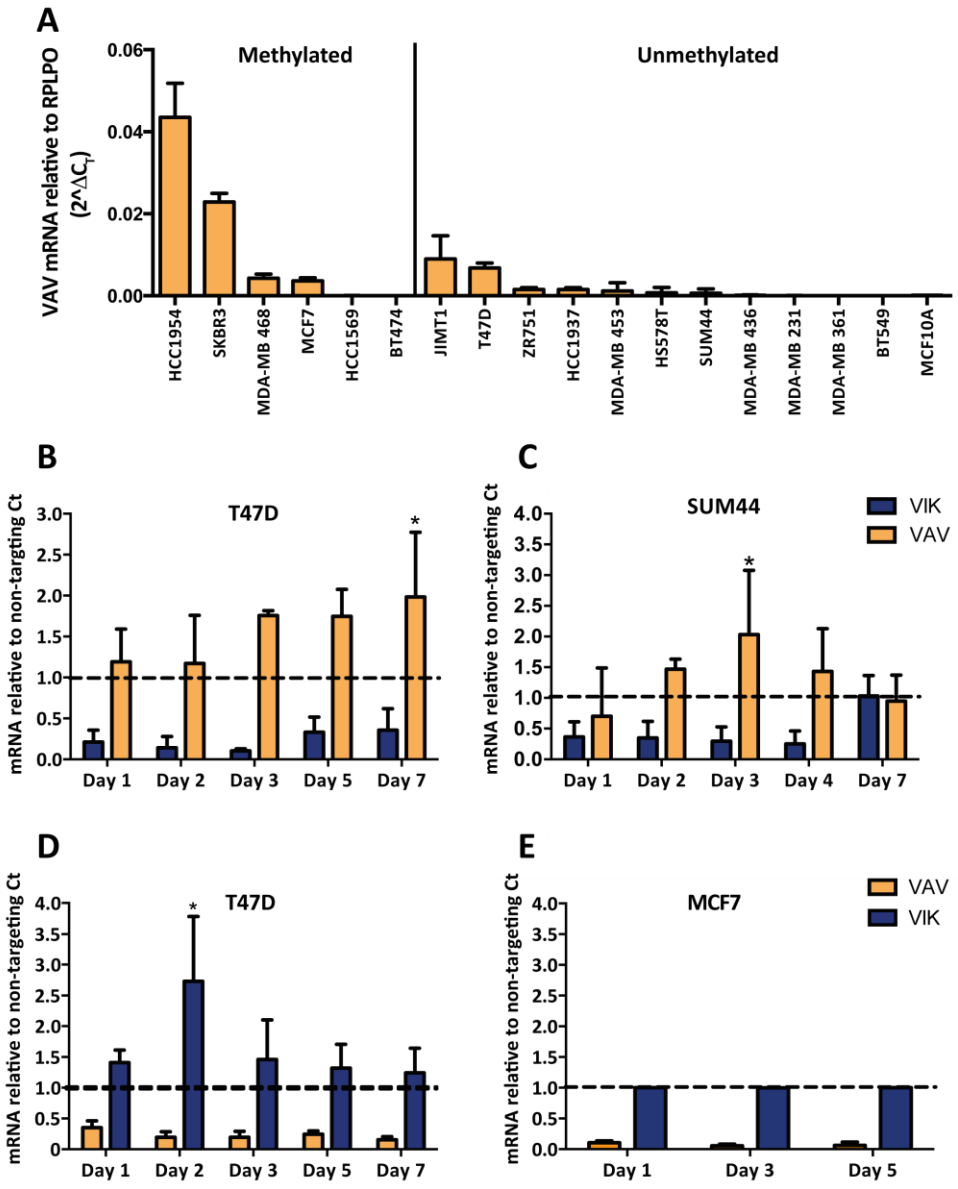

Figure 5.8. A) VAV1 mRNA expression across a panel of breast cancer cell lines, determined by RT-qPCR. The cell lines are divided into VIK methylated and VIK unmethylated. VAV1 expression did not correspond to VIK methylation. B) VAV1 mRNA levels (orange bars) following VIK siRNA knockdown (blue bars) over time in T47D cells and C) SUM44 cells. D) VIK mRNA levels (blue bars) after VAV1 siRNA knockdown (orange bars) in the unmethylated T47D cells and E) methylated MCF7 cells. Graphs show mRNA normalized to the non-targeting siRNA control at each indicated time point.

5.4 Summary

Methylated and unmethylated breast cancer cell lines were unable to survive over-expression of VIK. Additionally, knockdown of VIK caused cell death via apoptosis, as demonstrated by increased extracellular PS and cleavage of PARP. This effect was not cancer-specific, but also occurred in normal breast cells. This suggests an optimum VIK expression level that is important for cell survival.

Although a preliminary patient cohort indicated a role for VIK in endocrine resistance, *in vitro* analysis suggests VIK expression does not affect sensitivity to tamoxifen. In unmethylated cell lines VAV1 was upregulated in response to VIK knockdown, and VIK was upregulated following VAV1 knockdown, indicating a potential compensatory mechanism.

6. Results: The involvement of VIK in cell cycle regulation and CDK4/6 inhibitors

The previous publication regarding VIK function gave evidence for a role of VIK in cell cycle progression. Houlard *et al* (277) demonstrated VIK overexpression to inhibit the progression through the G1/S checkpoint in the leukaemia cell line K562, potentially due to an interaction with CDK4. There is no published data on the role of VIK within the cell cycle in breast cancer, thus we wanted to determine how VIK might modulate cell cycle progression in breast cancer. It was of particular interest that VIK has been shown to interact with CDK4. Selective CDK4/6 inhibitors are promising to be an effective novel therapy in ER positive breast cancer. Therefore we sought to determine if VIK expression has an effect on sensitivity to CDK4/6 inhibition.

6.1 VIK-1 and the cell cycle

6.1.1 VIK knockdown modulates cell cycle progression

Cell cycle progression was determined following VIK siRNA knockdown in the VIK unmethylated, expressing breast cancer cell line, T47D. Flow cytometry was utilised to analyse cell cycle progression using DAPI staining for DNA content. Following 48 hours siRNA knockdown, there was very little difference in cell cycle progression in VIK siRNA knockdown cells compared to the non-targeting scrambled control (Figure 6.1A). At 72 hours post transfection, significantly more cells were observed in G1 phase with an increase of 13% of cells in G1 phase in VIK knockdown cells (Figure 6.1B). This halt in G1 was sustained at 96 hours post siRNA transfection, where again 13% more cells were seen in G1 phase in the VIK knockdown cells (Figure 6.1C). The increased number of cells in G1 was accompanied by reduced proportion of cells in G2. These results indicate that, although the whole population of cells were not halted in G1 and some cells were still able to cycle normally, knockdown of VIK alters progression from G1 to S phase.

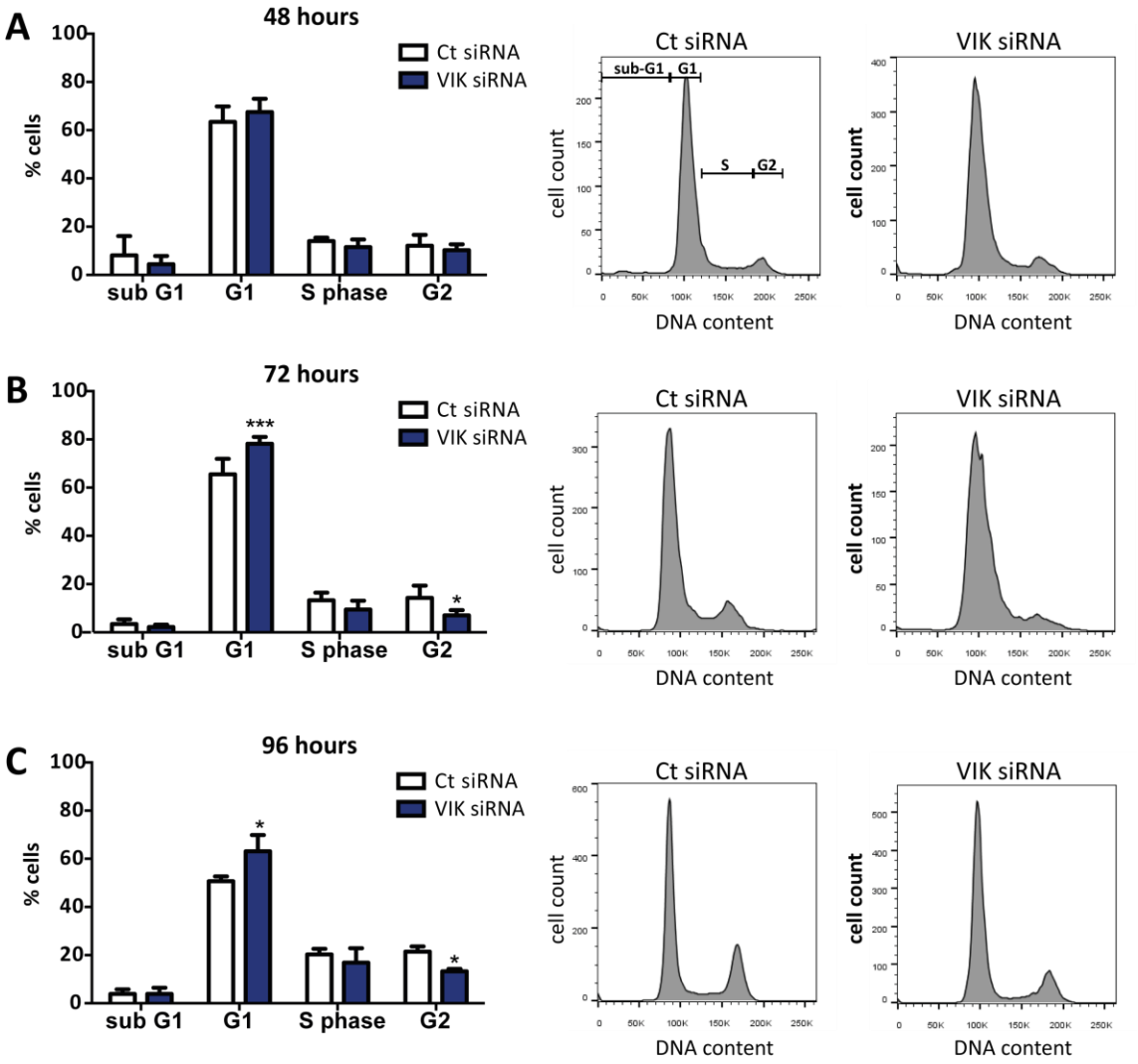

Figure 6.1 VIK siRNA knockdown alters cell cycle progression. VIK expressing T47D cells were transfected with a non-targeting scrambled siRNA or VIK targeting siRNA, cell cycle profile was assessed by flow cytometry analysis. A) VIK knockdown had no effect on cell cycle progression after 48 hours. B) 72 hours and C) 96 hours post transfection, significantly more cells were observed in G1 phase in VIK knockdown cells compared to scrambled siRNA. A representative cell cycle profile is shown of triplicate experiments. 2-way ANOVA *P<0.05 ***P<0.001.

6.1.2 VIK knockdown alters expression of G1/S phase checkpoint regulators

To further confirm the effect of VIK on cell cycle progression in breast cancer cells, the expression of essential proteins involved in progression from G1 to S phase was investigated following VIK knockdown (Figure 6.2). VIK was knocked down via siRNA in the unmethylated breast cancer cell line T47D and the normal breast epithelial cell line MCF10A. siRNA knockdown of VIK led to changes in the level of multiple proteins that regulate the cell cycle in both T47D and MCF10A.

In the T47D cancer cells CDK4 levels were not considerably altered, but there was a small downregulation in cyclin D. The downstream target of CDK4/cyclin D is the phosphorylation of Rb at serine 780. Knockdown of VIK led to a decrease in phosphorylated Rb at this site. Although there was also a decrease in total Rb, there was a larger reduction in Rb phosphorylation than in the total protein. Additionally the level of CDK1 was significantly decreased, along with CDK2, whilst the CDK2 binding partner, cyclin E, was significantly upregulated by 3-fold. E2F1, the key transcription factor in G1/S phase progression was also downregulated. There was a 3-fold increase of the cell cycle inhibitor p27.

VIK knockdown also altered cell cycle protein expression in the normal MCF10A cells. CDK4 was more significantly downregulated and there was a small decrease in cyclin D. Total Rb was decreased but there was a significantly larger reduction in phosphorylation of Rb. CDK1, CDK2 and E2F1 were all significantly decreased, whilst p27 increased. Unlike in the T47D cells, cyclin E remained unchanged in the MCF10A.

These results suggest that VIK regulates expression of multiple cell cycle proteins. The changes in levels of the cell cycle proteins following VIK knockdown, are consistent with the observed cell cycle profile. Knockdown of VIK decreased expression of the key proteins

involved in progression from G1 to S phase, therefore corroborating the increased proportion of cells in observed in G1. As this was seen in both cancer and normal breast cell lines, this effect is not cancer specific. However, there might be different regulatory mechanisms in the normal compared to the tumour cell lines, as the upregulation of cyclin E was only observed in the tumour cells. This cyclin E upregulation might confer a survival advantage to tumour cells over normal cells, especially taking into account that the MCF10A were more sensitive to cell death following VIK knockdown.

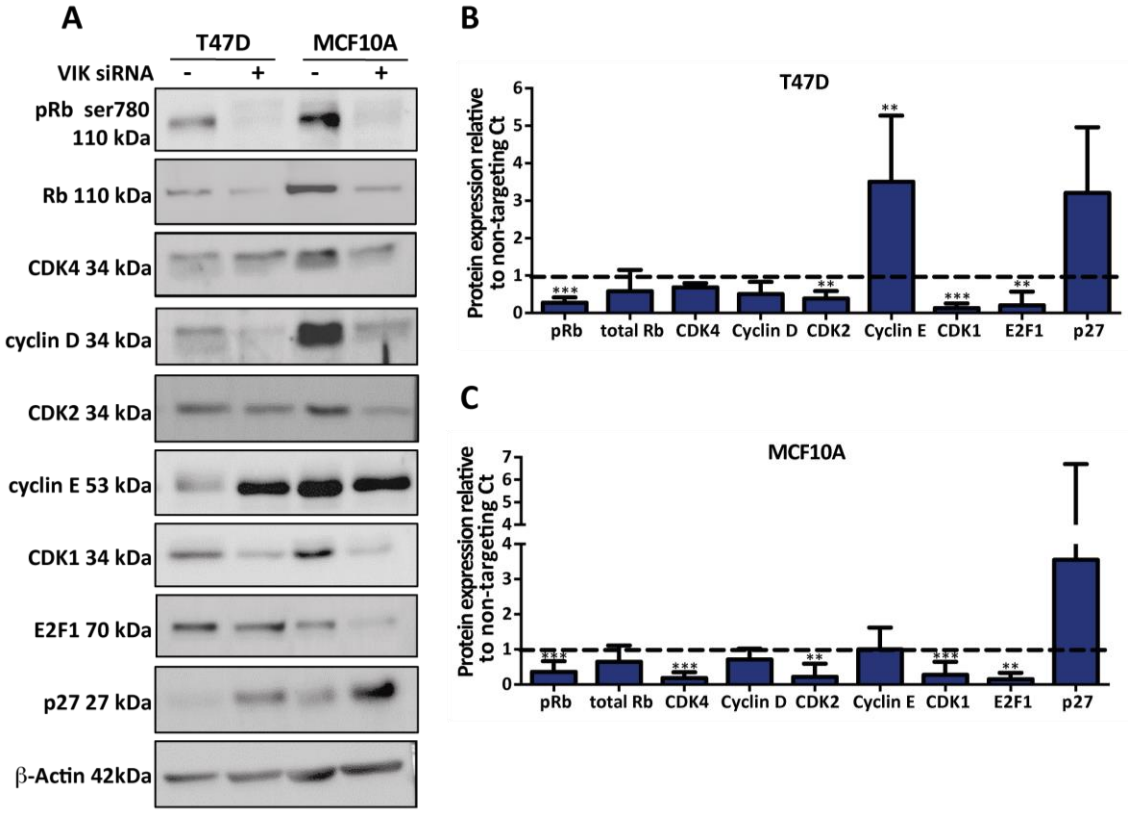

Figure 6.2 VIK knockdown alters expression of proteins involved in cell cycle regulation. Following 72 hours of VIK siRNA knockdown in breast cancer cells T47D and normal breast epithelial cells MCF10A, protein expression of cell cycle regulators was determined by western blot. A) Example western blot of triplicate experiments. Protein expression was quantified relative to β-actin, and expression levels normalised to the non-targeting siRNA control in B) T47D breast cancer cells and C) MCF10A normal breast epithelial cells.

6.2 Loss of VIK is associated with resistance to CDK4/6 inhibitors

6.2.1 VIK knockdown decreases sensitivity to the CDK4/6 inhibitor, palbociclib

The CDK4/6 inhibitor palbociclib (Pfizer) is a novel therapy for the treatment of ER+HER2- breast cancer. As we have shown that knockdown of VIK expression in breast cancer cells modulated G1/S phase transition, and altered expression of cell cycle regulators, we investigated the effect of VIK on sensitivity to palbociclib in breast cancer cell lines. IC_{50} values were determined in a panel of breast cancer cell lines with variable VIK expression and methylation (Figure 6.3A). Cell lines with an IC_{50} value above 1μM were defined as resistant as previously described by Finn *et al* (1). There was no association between methylation of VIK and sensitivity to palbociclib. There were varying IC_{50} values across the cell line panel, methylated and unmethylated cell lines exhibited both sensitivity and resistance to palbociclib. For example, the two resistant cell lines in the panel, MDA-MB 468 and Jimt1, were VIK methylated and unmethylated respectively. This suggests that baseline VIK methylation status is not an indicator of palbociclib sensitivity.

In the VIK expressing cell lines T47D and SUM44, the IC_{50} for palbociclib was determined upon VIK siRNA knockdown. Both T47D and SUM44 cells became more resistant to palbociclib after siRNA knockdown of VIK (Figure 6.3B). Upon knockdown of VIK there was a 7.6-fold increase in IC_{50} from 44nM to 334nM in T47D cells (Figure 6.3C). Whilst VIK knockdown in SUM44 cells lines caused and IC_{50} shift towards resistance from 200nM to 1.3μM, an increase of 6.7-fold (Figure 6.3E). In the VIK methylated cell line MCF7, IC_{50} values were determined after transient transfection with vector only (VO) or a VIK expressing vector. However, no difference was seen in IC_{50} values (Figure 6.3G). These

results suggest that VIK plays a role in palbociclib resistance in unmethylated, VIK expressing, cell lines only.

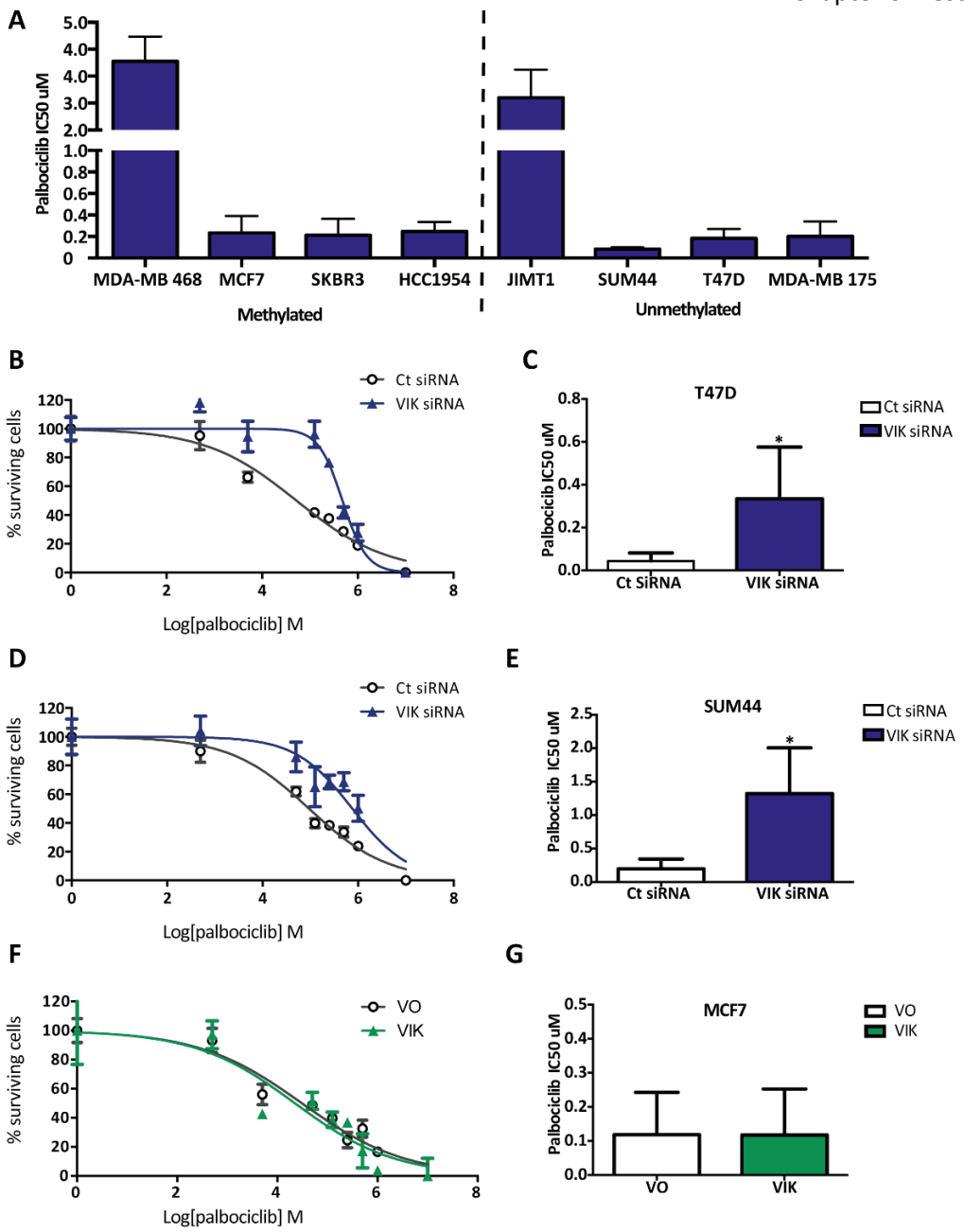

Figure 6.3. VIK and palbociclib sensitivity A) IC_{50} values across a panel of breast cancer cell lines. Cells were treated with increasing doses of palbociclib. After 6 days of drug treatment the concentration required to kill 50% of cells (IC_{50} value) was determined. B) IC_{50} shift following VIK siRNA knockdown in T47D cells. C) Average IC_{50} value in T47D cells following siRNA treatment D) IC_{50} shift towards resistance in SUM44 cells following VIK knockdown. E) Average IC_{50} values in SUM44 following siRNA treatment. F) IC_{50} curve for palbociclib following transfection with either vector only (VO) or VIK expressing vector on MCF7 cells and G) average IC_{50} values. A representative IC_{50} curve is shown of biological triplicates, % cell survival is normalised to DMSO vehicle control. *P<0.05 Students T-test.

6.2.2 VIK expression is lost in Palbociclib resistant cell lines

Whilst clinical trials show many patients respond to treatment with palbociclib (235, 236), increasing clinical use is likely to lead to development of drug resistance. Understanding mechanisms of this resistance will be key to improving treatment. To investigate these mechanisms *in vitro*, palbociclib resistant cell lines were generated. The ER positive cell lines T47D and MCF7 were selected, as they were sensitive to palbociclib treatment and corresponded to VIK unmethylated and methylated respectively. Long-term culture with concentrations of palbociclib starting at 200nM and increasing to 1µM generated cell lines with acquired resistance to the drug. Three distinct resistant clones were selected for each cell line. MCF7 resistant clones M4, M5 and M8 and T47D resistant clones T5, T7, and T9. Resistant clones showed an IC_{50} shift from sensitive to resistant of approximately 220nM to at least 2µM for MCF7 and 200nM to 5µM for T47D, respectively (Figure 6.4).

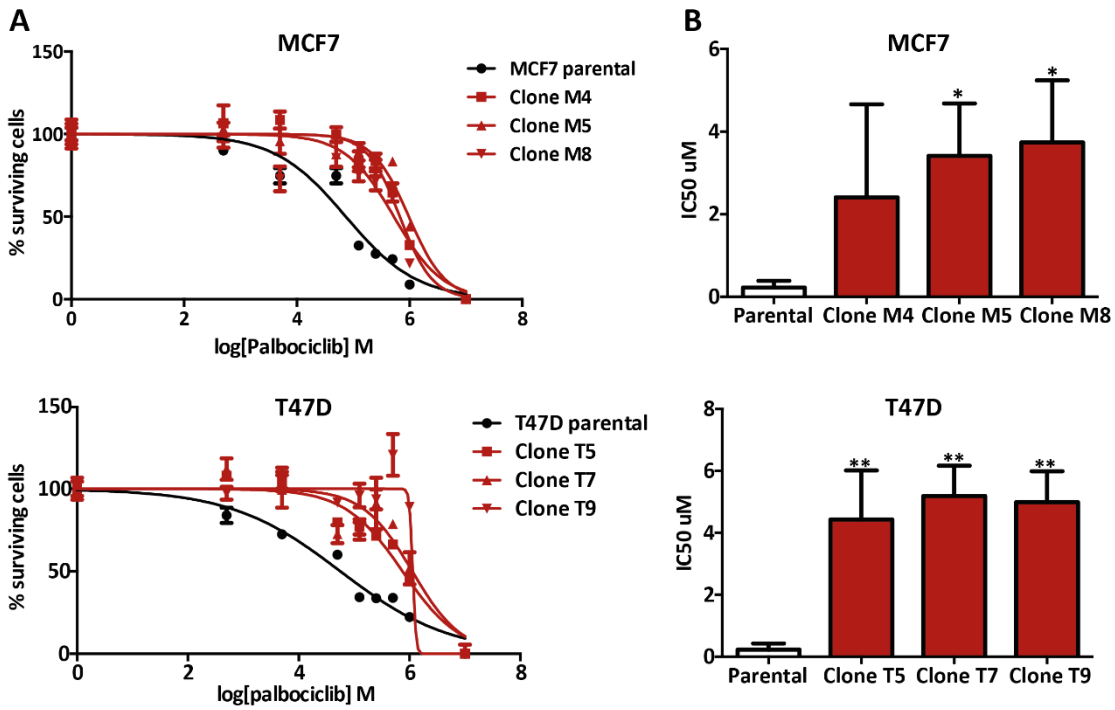

Figure 6.4. Generation of palbociclib resistant cell lines. MCF7 and T47D cells were cultured in increasing concentrations of palbociclib and resistant cells clonally selected. Three resistant clones for each cell line were chosen M8, M4 and M5 for MCF7 and T5, T7, T9 for T47D. A) A representative IC_{50} curve for sensitive and resistant clones after 6 days of drug treatment, all resistant clones for both MCF7 and T47D show a shift in IC_{50} towards resistance. B) Average IC_{50} value for each cell line. All clones have higher IC_{50} values than their corresponding sensitive parental cell line. Average +/- standard deviation is shown. *P<0.05 **P<0.01, 1-way ANOVA Tukey's multiple comparison test.

Having established resistant cell lines, RNAseq was carried out to determine changes in gene expression following acquired resistance to palbociclib. The resistant cells derived from the methylated MCF7, showed little difference in VIK expression compared to sensitive. The T47D resistant clones, which are normally unmethylated and VIK expressing, showed down-regulation of VIK expression (Figure 6.5A). However, this was not statistically significant with adjusted p-values estimated by Benjamini-Hochberg procedure all >0.05.

To validate the RNA sequencing results, RT-qPCR was performed (Figure 6.5B). In the MCF7 resistant clones, there was no change in VIK expression and VIK mRNA remained undetectable. T47D cells with acquired palbociclib resistance showed significant reduction in VIK expression. In all three resistant clones VIK mRNA expression was reduced to barely detectable levels. This suggests loss of VIK is involved in development of resistance to palbociclib.

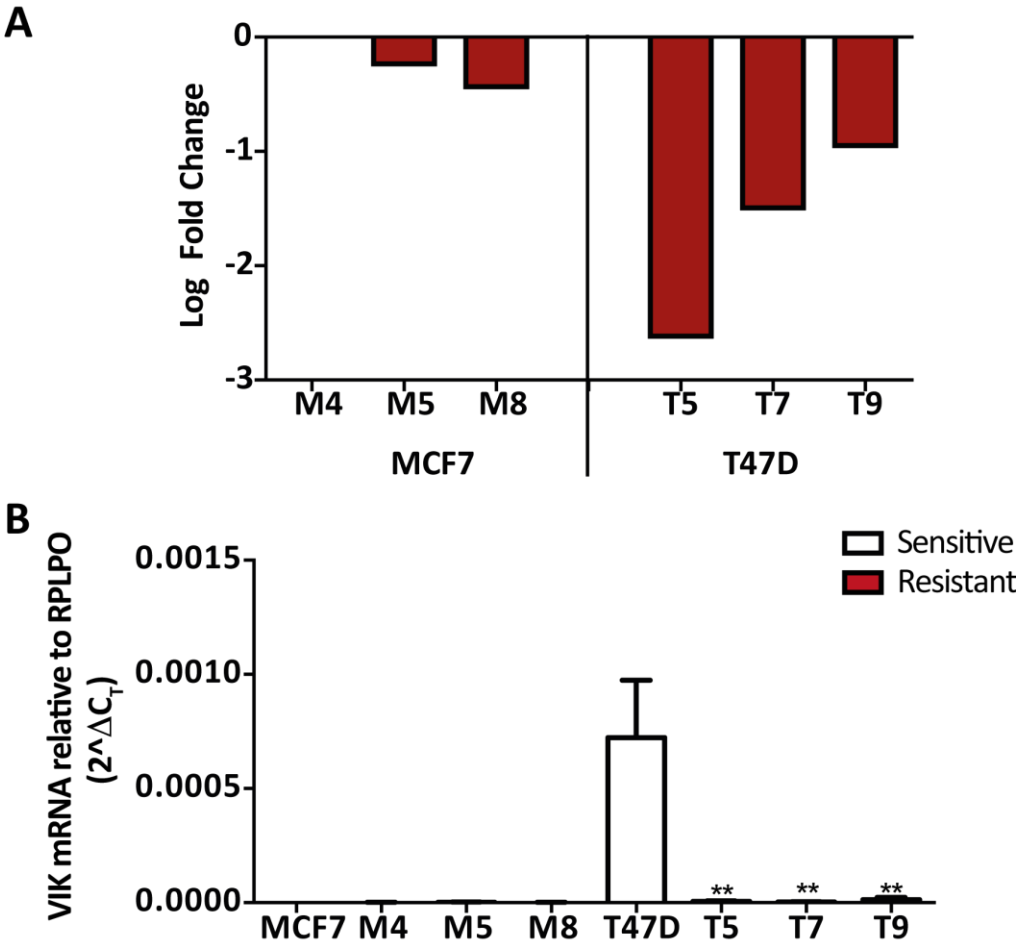

Figure 6.5. VIK mRNA expression in palbociclib resistant cell lines. A) Fold change of VIK expression as determined by RNA sequencing in MCF7 palbociclib resistant clones (M4, M5, M8) and T47D resistant clones (T5, T7, T9). Expression values are log fold change relative to the sensitive control cells, where <0 indicates a downregulation in expression. B) Validation of RNAseq by RT-qPCR VIK. mRNA was undetectable in both sensitive and resistant MCF7 lines. VIK was significantly decreased in all T47D resistant clones. ** P>0.01 1-way ANOVA Tukey's post-hoc comparison test.

6.3 Summary

VIK was identified as a novel regulator of the cell cycle in breast cancer. Knockdown of VIK altered the expression of multiple proteins regulating the cell cycle, in particular the G1/S phase transition, inducing cells to arrest in G1. This effect on cell cycle proteins was not tumour specific, but was also observed in normal breast epithelial cells. Although there were some differences in the tumour cells compared to the normal cells, indicating potential different regulatory mechanisms.

Loss of VIK was associated with resistance to the CDK4/6 inhibitor, palbociclib. siRNA knockdown in VIK expressing cells led to an increase in IC_{50} values. Additionally VIK mRNA expression was lost in cell lines with acquired resistance to palbociclib. In combination these results show loss of VIK in endogenously expressing breast cancer cells does have a role in development of acquired palbociclib resistance.

7. Discussion

7.1 Overview

VIK was initially identified as of interest in breast cancer following a methylation array detecting aberrant methylation across the CpG island in breast cancer cell lines. Preliminary analysis of primary breast cancer patient samples associated VIK methylation with decreased survival in estrogen receptor positive breast cancer. Functionally, VIK is not well characterised, except it is a member of the Krüppel-like transcription factor family, and the protein interacts with VAV1 and CDK4 to block cell cycle progression (277).

In this thesis I have demonstrated VIK to be epigenetically regulated on a transcriptional level, although this may not translate to protein expression. Analysis of patient samples revealed methylation in approximately 8-14% of breast cancer samples, however this could not be correlated to patient outcome. *In vitro* analysis established expression of VIK to be important to cell survival in both normal and cancer cell lines. Decreased VIK expression induced apoptosis via cell cycle arrest in G1. This suggests a role for VIK in regulating cell cycle progression through the G1/S phase checkpoint. This role could be of particular importance in the context of CDK4/6 inhibition, where I have demonstrated loss of VIK expression to might be involved in development of acquired resistance to CDK4/6 inhibitors.

7.2 Methylation transcriptionally silences VIK

The methylation array identified the CpG island within the 5' regulatory region of the gene to be highly methylated within breast cancer cell lines. Methylation dependent transcriptional silencing was further confirmed upon methylation analysis via pyrosequencing. Transcription of VIK is clearly epigenetically regulated, there is a direct

correlation between methylation and mRNA expression. In cell lines with methylation above 30%, no detectable mRNA was observed across any of the RT-qPCR assays utilised. Additionally, demethylation treatment released the transcriptional repression in methylated cell lines and upregulated mRNA levels. This epigenetic regulation is supported by the TCGA data in primary patient samples, with higher VIK methylation correlating to decreased mRNA expression in the tumour samples.

However, in our cell line panel, protein levels, as determined by western blot, did not correlate with mRNA levels. Using three antibodies (2 commercially available and a single custom), all showed similar trend. In unmethylated cell lines, mRNA and protein were both expressed as expected. However, in the methylated cell lines, protein was expressed despite the lack of mRNA expression. We were unable to correlate or confirm our results as there is only one published paper regarding VIK protein expression, where a custom antibody was used, and there is no published data on VIK protein expression in breast cancer cells.

siRNA treatment knocked down both mRNA and protein in the unmethylated cell line, this could suggest the antibodies are detecting the correct protein in unmethylated cell lines. However, it should be considered that the most likely explanation is that the antibodies tested are incorrect or are not fit for the purpose of detecting VIK expression by western blot and the protein bands we observe are unspecific. Each antibody detected a different size, with the custom antibody detecting 80kDa, not corresponding to any known transcript of VIK. Additionally, each antibody did show different protein levels across the same cell line panel. Ectopically expressed VIK by means of the pcDNA3.1-VIK vector did not alter detectable protein levels, despite increase in mRNA. Although the inability to detect

transfected over-expressed VIK could instead be due to some misfolding or rapid degradation of the protein, not allowing for antibody detection. However, even upon methylation reversal, upregulation of mRNA did not correspond to increased protein levels. In fact, the only instance where detection of increased mRNA levels was accompanied with an increase in protein was with the unmethylated cell line in hypoxic conditions. However, in the context of a stress response in hypoxia, proteins are often stabilised rather than an increase in protein synthesis, so the increase in protein levels could be due to stabilisation of the protein, rather than an induced expression. Additionally, upon, immunofluorescence analysis the antibody detected a primarily cytoplasmic protein, when the only published data on VIK-1 protein expression showed VIK to be predominantly nuclear (277). Localisation of the protein does not disprove the protein expression, as VIK has been shown to shuttle between the nucleus and the cytoplasm due to a nuclear import and export sequence (277). However, rather than just looking at baseline protein, immunofluorescence following siRNA treatment to determine depletion of the protein would provide more information of the specificity of the antibody.

As the antibody data was unclear, we sought to confirm if the antibodies were correctly detecting VIK by means of an IP assay. Unfortunately we were unable to perform an endogenous IP with our antibodies. This would have been ideal, as the endogenous protein in methylated and unmethylated cell lines could be compared. Instead, an IP was performed on overexpressed pEGFP-VIK. When the IP sample was probed back for GFP and VIK, the same band was seen. Mass spectrometry for this band revealed presence of VIK, providing evidence for the antibodies detecting the protein correctly. However, over a hundred other proteins were also detected, most likely these are unspecific proteins. The high number of other proteins could potentially indicate VIK has a number of protein

binding partners. This would be expected based on the structure of VIK, which has 6 tandem zinc fingers. Zinc finger domains are known to have activity for protein-protein interactions (294). A number of the proteins identified after mass spectrometry were heat shock proteins, which could act as chaperone proteins for VIK. For example Heat Shock protein 90 was a top hit and is known to act as a molecular chaperone for stability of proteins involved in cell growth and proliferation in cancer.

However, if there is the protein is present in methylated cell lines, this raises the question; if methylation means repressed transcription and no detectable levels of mRNA, how can protein be present in methylated cell lines? In this case an alternative hypothesis is that all cell lines have a basal expression of protein, potentially inactive, with a long half-life, that is easily detectable by western blot, whilst mRNA is readily degraded and below the detectable qPCR levels. Other proteins involved in cell cycle regulation exhibit a similar expression pattern to this, with a constant baseline protein expression followed by transient peaks in synthesis. For example, cyclin D shows cell cycle-dependent oscillation in expression and is upregulated in G1 for orderly progression into S phase (295).

It is often reported that protein levels do not correlate strongly to mRNA levels, with changes on the gene expression level frequently not reflected at the protein level (296). Short mRNA stability and long half-life of proteins is cited as a big factor, in addition to a low rate of mRNA transcription compared to protein translation in mammalian cells (297). Cooper and Shedden suggest this can be particularly complicated with regards to the cell cycle, concluding that changes in mRNA levels have only a minimal effect on protein variation during the cell cycle (298). The 3'UTR plays an important role in determining the translational efficiency and stability of mRNA, primarily due to the addition of a poly A tail

and microRNA (miRNA) binding sites (299). Transcripts encoding proliferative genes and proto-oncogenes tend to have longer 3'UTRs, and a longer 3'UTR can indicate increased number of miRNA binding sites (300), which could lead to increased mRNA degradation. All VIK transcripts do have a particularly long 3'UTR of approximately 2869 bases, which could be indicative of targeted degradation of the mRNA. It is increasingly understood that epigenetic changes do not act in isolation, but DNA methylation regulates miRNA expression (301) and methylation can be regulated by miRNAs (302, 303). Therefore genes may be subject to multiple regulatory controls such as both DNA methylation and miRNA degradation. Although correlation between gene methylation and miRNA targeting has not been largely explored, it has been suggested that genes with promoters containing high CpG content are more often targeted by miRNAs (304). There are examples of genes such as suppressor of cytokine signalling (SOCS3), which functions as a tumour suppressor in breast cancer and is subject to both methylation and miRNA mediated epigenetic regulation (305, 306).

In the case of a rapidly degraded mRNA and basal protein expression in all cells, the baseline protein would likely have a long half-life or slow turnover and there could potentially be a difference in protein stability between methylated and unmethylated cells. Furthermore, it could be the case that control of production of VIK protein is tightly regulated, it would then be likely that the baseline protein and induced protein have a difference in stability i.e. the baseline levels of VIK are stable, however the upregulated levels of VIK are unstable. If protein expression is induced unnecessarily, the protein is quickly degraded when cells produce more than is required. It would be of interest to determine half-life of the protein by treatment with cycloheximide to inhibit biosynthesis and measuring the length of time required for the protein to be depleted. VIK could have

multiple binding partners, which could increase stability of the protein. Additionally, the baseline protein could be inactive and require a post translational modification for activation, such as phosphorylation, glycosylation or ubiquitination. Potential evidence for this is seen by the different sizes detected by different antibodies.

If it is the case that all cell lines exhibit a stable baseline protein then methylation of the promoter region might inhibit inducible upregulation of the gene, by actively inhibiting binding of required transcription factors within the gene promoter region. We see some evidence of this on the mRNA level, via knockdown of VAV1 leading to an increase in VIK mRNA expression in the VIK unmethylated cell line, whilst there is no induction of VIK mRNA in the methylated cell line. Additionally in hypoxia, we observed induced upregulation of mRNA levels in the unmethylated cell line but not the methylated cell line.

There is no published data regarding regulation of VIK transcription by transcription factors. Although as mentioned in results chapter 2, analysis of the DNA sequence of the CpG island within the regulatory domain of the VIK gene showed putative binding sites for over 150 transcription factors including the FOX family and STAT family. We experimentally tested induction by TGF-β and EGF, however no real effect was seen on induction of VIK expression with the conditions tested. Based on the large number of putative transcription binding sites, to further analyse the control of VIK by transcriptional regulators experimentally, a more systematic approach would be required. For example, mutations of the promoter region could be produced and transcription of the gene measured by use of a luciferase reporter assay. This could determine precisely which region of the promoter region transcription is dependent upon and what transcription factor might bind to that particular region.

7.3 Methylation of the VIK promoter region is prevalent in breast tumour tissue

Having established methylation within breast cancer cell lines, and based on a preliminary patient cohort where methylation was associated with shorter overall patient survival, we wanted to confirm if VIK could be a prognostic biomarker in breast cancer. We confirmed within primary breast cancer patient samples that there are a proportion of patients where VIK expression is subject to methylation dependent transcriptional silencing. VIK methylation was observed to be higher in tumour samples, with non-tumour samples showing no methylation for VIK. Moreover, higher methylation significantly correlated to decreased mRNA expression. Two patient cohorts were analysed; one experimental (Leeds cohort) and one *in silico* (TCGA cohort). Methylation of the two cohorts was determined via two different methods. The Leeds cohort was analysed using pyrosequencing, covering 6 individual CpG sites over a small portion of the CpG island, 259 nucleotides out of a large CpG island of 1059 nucleotides in total. For the TCGA cohort methylation array data was available, covering 13 CpG sites across the whole CpG island region. As shown in chapter 1, the methylation array and pryosequencing had a strong correlation between methylation values in our cell line samples. When analysing the region of the CpG island covered by the pyrosequencing primers, methylation of VIK was of similar prevalence in both cohorts, 7% and 9% in the Leeds and TCGA cohorts respectively. This was slightly lower than the preliminary cohort, where 15% of patients were methylated. Methylation in the preliminary cohort was determined by means of methylation specific PCR (MSP), compared to pyrosequencing for the Leeds cohort and methylation array for TCGA dataset. The MSP primers used to assess methylation within the preliminary cohort covered CpG sites

upstream of the pyrosequencing assay. The region of the CpG island analysed might be of more importance, especially considering the methylation array from TCGA dataset showed more variation across the CpG island within the patient tumour samples than was observed in our own methylation array in the breast cancer cell lines. When methylation across the whole CpG island was taken into account the number of methylated samples was increased to 14%, a similar proportion to the preliminary cohort. Considering this, the different determination of methylation and region of the CpG island analysed for the preliminary cohort could account for the discrepancy between the proportion of methylated populations within the Leeds cohort.

The preliminary patient cohort showed a trend for poorer survival in patients with methylated VIK. However, within the two patient cohorts examined we were unable to confirm this observed trend. There was no significant difference in overall survival times in the methylated or unmethylated populations in either cohort. This difference could be due to the fact the preliminary cohort consisted of only estrogen receptor positive breast cancer patients, whereas both the cohorts examined within this thesis were of mixed hormone status. Due to the small proportion of methylated samples, we were unable to examine the estrogen receptor positive population only within our cohorts to directly compare to the preliminary cohort. Furthermore, within the TCGA dataset, there were too few survival events across the cohort to properly assess the impact of VIK methylation on patient outcome. Whilst the Leeds cohort was not large enough considering the small number of patients within the methylated group. Due to these reasons, the survival data from these cohorts is inconclusive. Further analysis with larger patient sample size would be required to further elucidate the effect of methylation on patient outcome and use of VIK methylation as an indicator of patient prognosis. Although we were unable to confirm

methylation of VIK as a prognostic marker, our patient cohorts suggest there is a small population of breast cancer patients in which VIK is transcriptionally repressed by methylation.

7.4 VIK is not a determinant of sensitivity to endocrine therapy

The preliminary patient cohort associated methylation of VIK with lower ER expression, and increased risk of recurrence in tamoxifen treated patients. This, in addition to the decreased overall survival in tamoxifen treated patients, indicated a role for VIK in resistance to endocrine therapy. Although, we were unable to replicate the differential outcome with regards to VIK methylation in our patient cohorts, we did investigate the potential role for VIK in endocrine resistance *in vitro*. There is precedence for KLFs interacting with estrogen signalling. Other KLFs have been shown to bind to the DNA binding region of ERα, thereby modulating the binding of ERα to endocrine response elements (ERE) within target genes (307, 308) and there is evidence for KLF induction via estrogen signalling (309, 310). However, estrogen stimulation in breast cancer cell lines did not induce VIK expression. This is supported by published ER binding studies. Multiple approaches have been applied to determine ER target genes including genome wide arrays and high throughput chromatin immunoprecipitation sequencing data (ChIP-Seq), from which supplementary material including gene expression arrays and ER binding site data is accessible. Within the available data, there is no evidence for VIK being differentially expressed upon estrogen induction or for ER directly interacting within gene regulatory sequences for VIK in breast cancer cells (310-312). In addition to this, VIK did not correlate to ER expression within the cell line panel; VIK was not differentially methylated in ER+ breast cancer in comparison to other subtypes. Furthermore, knockdown of VIK did not

alter sensitivity to tamoxifen, this indicates no direct link between VIK and endocrine resistance with regards to tamoxifen treatment. As we were unable to confirm our initial hypothesis of an involvement of VIK in endocrine resistance, we instead focused on identifying other functional roles for VIK in breast cancer.

7.5 VIK expression is important for cell survival

We sought to further determine the functional role for VIK in breast cancer using siRNA knockdown of VIK in cell lines that were unmethylated and VIK expressing. Our first observation was that reduction in VIK levels caused cell death. Ideally more than one siRNA would have been used to confirm the effects seen were not due to off target effects, however VIK was not easy to knockdown, and when knockdown was successful there were significant levels of cell death. Unfortunately the levels of cell death with the second siRNA made it unsuitable for use in other assays as there were too few surviving cells remaining at the end point. The ideal situation would have been use of an inducible knockdown system, such as use of a Tet Repressor and lentiviral shRNA transduction, which would provide a more stable knockdown system.

It is clear from our data that modulation of VIK levels cannot be tolerated by cells, both over expression and knockdown caused cell death. This implies that cells have an optimal VIK expression level, and cells cannot survive disruption of this. Although it should be noted that transfection with the VIK expression plasmid led to over-expression of VIK beyond physiological mRNA levels in endogenously expressing VIK cell lines. Therefore the cell death could be due to extra stress on the cells due to such high levels of VIK mRNA.

Loss of VIK expression via siRNA induced significant levels of cell death. While this was true for both normal and tumour breast cell lines, the non-tumour cells appeared more sensitive to cell death following VIK knockdown. Further analysis revealed loss of VIK induced cells to enter apoptosis; this would suggest that VIK expression normally protects cells from apoptotic cell death. Consequently, VIK expression is important to cell survival.

7.6 VAV1 and VIK reciprocal expression upon knockdown

Aside from cell death, our second observation following VIK knockdown was an upregulation of VAV1. The function of VIK to date is not well characterised, however it is known that VIK has a direct interaction with VAV1. Previous evidence shows over-expression of VIK halts the cell cycle in G1, whilst co-expression with VAV1 reverses this inhibitory effect to drive cell cycle progression forward (313).

Although there was no direct correlation between VIK and VAV1 expression across a panel of breast cancer cell lines, knockdown of VIK in unmethylated cell lines did lead to a compensatory increase in VAV1, and knockdown of VAV1 led to an upregulation of VIK. This supports the hypothesis of a dual role for these two proteins, and a potential feedback between the two. However, the upregulation of VAV1 occurred at day 3 following VIK knockdown and cells still continued to die past day 5, which suggests the upregulation of VAV1 does not provide a survival advantage for the cells.

Additionally, the reciprocal expression of VIK and VAV1 was not further supported in patient tissue samples. VIK was downregulated in breast cancer samples in comparison to normal breast tissue and conversely VAV1 was upregulated. However, this was not true in those patients who were specifically VIK under-expressing. In the patient cohorts analysed

there was no direct correlation between VIK expression and VAV1 expression, and there was no difference between VAV1 expression in VIK -high or -low expressing samples. There is no published data on VIK expression in tumour samples, but the VAV1 expression is in concordance with other work. It is known that VAV1 expression is normally haematopoietic-restricted, and aberrant expression has been demonstrated in a number of human cancers, including breast (277), brain (274) and pancreatic (266). Our cell line data in combination with the patient samples could indicate that VIK and VAV1 only transiently compensate for each other. When one is lost the other is upregulated initially to compensate. However, there is no long-term compensation for each other and the dynamics of VIK and VAV1 expression may not be so important in primary breast cancer, potentially the observed initial compensatory upregulation is functionally redundant.

7.7 VIK is involved in cell cycle progression

In addition to its interaction with VAV1, VIK-1 has been shown to interact with CDK4 and overexpression was shown to halt the cell cycle in G1 (270). Therefore, the initial hypothesis was that the interaction of VIK and CDK4 would inhibit CDK4 activity. Consequently, knockdown of VIK should result in release of this inhibition leading to increased Rb phosphorylation, and progression from G1 to S phase. However, this effect was not observed, in fact the reverse was true and VIK knock down induced arrest in G1, indicating the interaction between CDK4 and VIK is not inhibitory. The published study used a leukaemia cell line, and there is no published data on the role of VIK in breast cell lines, so potentially the role of VIK in cell cycle regulation is tissue dependent. This would not be unexpected, as other Krüppel-like factors have diverse context dependent functions. KLF5 is associated with shorter disease free survival in breast cancer (277) but

improved outcome in lung cancer (314). KLF4, in particular, depending on the cellular context, can function as a tumour suppressor e.g. in colon (315), gastric (254) and pancreatic cancers (316), or an oncogene, e.g. in squamous epithelial dysplasia (317) or breast cancer (318-320).

In breast cells, VIK knockdown resulted in altered expression of a number of proteins involved in the G1/S phase transition and halted cells in G1 (Figure 6.2). This demonstrates VIK expression is required for normal cell cycle progression. The changes in cell cycle proteins were observed in the normal breast cell line as well as the breast cancer cell line, showing a more universal role for VIK within the cell cycle rather than a cancer specific role. Some changes in proteins were similar in both the tumour and normal cell line i.e. downregulation of pRb, CDK1, CDK2, E2F1 and upregulation of p27. Yet there were some differences, increase in cyclin E in occurred in tumour cells only and CDK4 was only significantly decreased in normal cells. This indicates there are different mechanisms occurring in the normal and tumour cells.

Phosphorylation of Rb at serine 780 was markedly reduced in both the normal and tumour cell line. This site is phosphorylated by CDK4/cyclin D complexes. Cyclin D was only downregulated to a small degree in both cell lines. In the normal cell line there was a marked reduction in CDK4, which could explain the reduced pRb. In the tumour line there was only minimal change in CDK4, and the small reduction in cyclin D is unlikely to be sufficient to result in the significant reduction in Rb phosphorylation. The decrease in pRb is more likely to be due to the upregulation of the cell cycle inhibitor p27(Kip), which was notably increased in both the normal and cancer lines. Overexpression of p27 binds to and

prevents the activity of CDK4, inhibiting the phosphorylation of Rb and arresting cells in G1 (321).

It should be noted that within the tumour cells there was a modest halt of cells in G1 rather than a complete halting of cells, and some VIK knockdown cells were still able to progress through to S phase. Aside from CDK4 being downregulated to a much greater extent in the normal breast cells, the other primary difference between normal and tumour cells was upregulation of cyclin E in the tumour cell line only. The upregulation of cyclin E in the tumour cells could suggest the cells are trying to compensate for the other cell cycle changes to continue normal cell cycle progression. The loss of phosphorylated Rb and marked reduction in E2F1, indicates this increase in cyclin E must be independent of the normal Rb/E2F control. It has been shown that over-expression of cyclin E is sufficient to override G1 arrest imposed by CDK4/6 inhibition or lack of pRb (322). Cyclin E transcription can be induced by other signalling pathways such as c-myc, independently of E2F (323). The normal breast cell line had a greater reduction in CDK2 and was unable to upregulate cyclin E. The normal cells were also more sensitive to cell death following VIK knockdown. Potentially, the ability to upregulate cyclin E could assist cell survival following loss of VIK within the tumour cells over non-tumour cells.

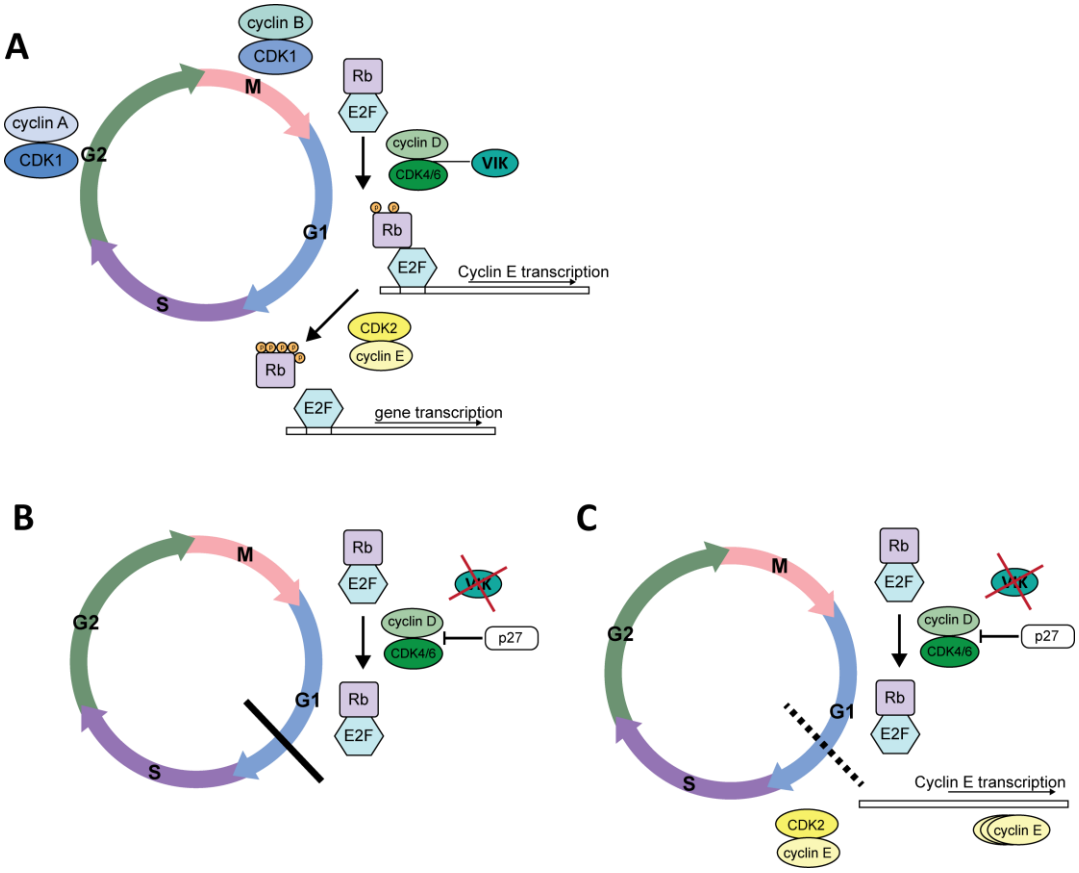

Figure 7.1 Hypothesised schematic of cell cycle regulation in normal breast cells and breast tumour cells upon loss of VIK expression. A) VIK expressing cells with normal cell cycle progression. CDK4/cyclin D complexes phosphorylate Rb. Phosphorylated Rb dissociates from E2F, enabling transcription of cyclin E. CDK2/cyclin E complexes further phosphorylate Rb, leading to complete dissociation from E2F enabling transcription of required S phase genes. B) In non-tumour breast cells loss of VIK causes upregulation of p27, which inhibits CDK4/6 mediated phosphorylation of Rb, therefore inducing cell cycle arrest at G1. C) In breast cancer cells loss of VIK causes upregulation of p27, which inhibits CDK4/6 mediated phosphorylation of Rb, inducing some cell cycle arrest in G1. However, loss of VIK also induces Rb/E2F independent upregulation of cyclin E, allowing some cells to drive cell cycle progression forward.

The marked changes in multiple cell cycle proteins, CDK1, CDK2, p27, cyclin E, E2F1, indicates that VIK has an effect outside of just direct interaction with CDK4. In other cancers, members of the Krüppel-like factor family are known to be involved in cell cycle regulation via their functions as DNA-binding transcriptional regulators. For example in pancreatic cancer, KLF4 results in G1 arrest through induction of the CDK inhibitors p21 and p27, KLF5 has been shown to induce cyclin D in bladder cancer (324), whilst KLF6 activates p21 in prostate cancer (295). Potentially VIK also exerts regulation on the cell cycle via transcriptional activation or repression of cell cycle genes e.g. repression of E2F1, or activation of p27 or cyclin E transcription. To properly examine the transcriptional regulatory role of VIK, chromatin immunoprecipitation would be required to determine regions of DNA the protein binds to. Unfortunately, in part due to the complications with anti-VIK antibodies, this was beyond the scope of this PhD.

The cell cycle data in combination with the induction of apoptosis and cell death, indicates that loss of VIK induces cells cycle arrest at G1, inducing cells to enter apoptosis. It is likely that the role of VIK is more complicated than just the published interaction with CDK4 and VAV1. VIK has zinc finger domains, which could suggest transcriptional regulatory activity but would also aide multiple protein-protein interactions. It is also of interest to note that following IP for VIK multiple proteins were detected. Many of these proteins were all involved within DNA damage response (PARP (243), XRCC5 (325), SSRP1 (326), DDX21 (327), NUCL (328)), suggesting VIK might interact with these proteins and could therefore also be involved in this pathway. It is possible VIK acts as a chaperone or adaptor protein involved in mediating response to DNA damage. Although, further work would be required to investigate this. In response to DNA damage cells can be arrested in G1 to provide time

for cells to repair the damage and proceed into S phase or enter apoptosis if the damage is not repaired (329).

7.8 Potential role for VIK in acquired resistance to CDK4/6 inhibition

CDK4/6 inhibitors are currently one of the most promising novel therapies in ER positive breast cancer, and with increasing clinical use understanding of resistance mechanisms is essential. VIK appears to have a role in resistance to CDK4/6 inhibition in ER positive cell lines. Sensitivity to the selective CDK4/6 inhibitor palbociclib was not linked to baseline VIK expression or methylation. However, in cell lines that are VIK expressing, these results suggest VIK potentially does play a role in resistance to the drug. Whilst over-expression of VIK did not alter sensitivity in the methylated MCF7 cells, siRNA knockdown of VIK in unmethylated cell lines showed a significant shift towards palbociclib resistance. Additionally T47D clones with acquired palbociclib resistance, whose parental cell line is VIK expressing, showed significant downregulation of VIK to barely detectable levels. This demonstrates that in cells that are endogenously expressing VIK, loss of expression might confer resistance to palbociclib. To further confirm the role of VIK in resistance, re-expression of VIK into cells with reduced VIK expression could be utilised to determine if re-expression of VIK resensitises resistant cells to palbociclib. Whilst baseline VIK expression is not an indicative biomarker for resistance to palbociclib, loss of VIK expression over the course of treatment could be a predictive marker for acquired palbociclib resistance.

The decreased VIK mRNA levels in palbociclib resistant cells could either be due to reduced levels of transcription or increased degradation of the mRNA. It would have been interesting to see that the loss of VIK mRNA expression in palbociclib resistant cells is

accompanied by a change in methylation status. However, preliminary results indicate this is not the case, with initial pyrosequencing analysis showing both the sensitive parental T47D cell line and the palbociclib resistant clones are unmethylated (Figure 7.2). Instead, VIK expression in the resistant clones could be altered by other epigenetic changes, such as histone modification. For example, decreased levels of histone acetylation could lead to a more closed chromatin structure. This would limit accessibility of transcription complexes to the DNA, therefore inhibiting transcription of the gene (330). Alternatively, the loss of VIK expression could be due to increased microRNA mediated degradation of the mRNA. microRNAs are increasingly documented to have a role in drug resistance in breast cancer (331). In fact, computational prediction of miRNA binding sites using TargetScan (332) shows the 3'UTR for VIK has multiple conserved miRNA binding sites. For example, miR-181a which has previously been implicated in promoting metastasis (333) and chemotherapeutic resistance (334) in breast cancer. Increased activity of this miRNA in resistant cells could lead to binding within the VIK 3'UTR, promoting mRNA decay.

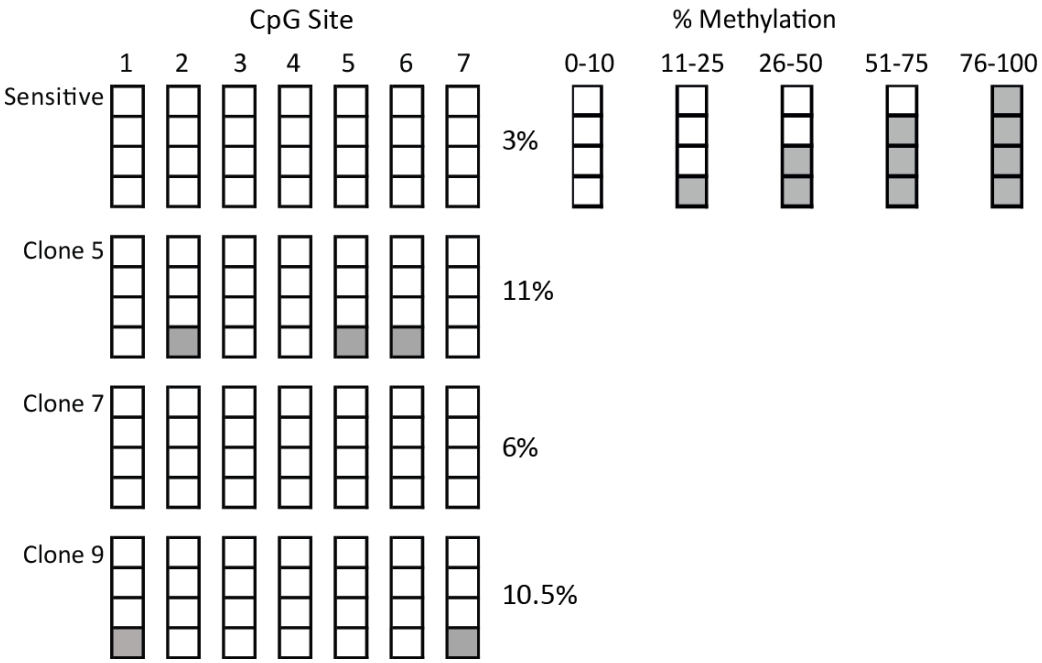

Figure 7.2 Preliminary pyrosequencing analysis of palbociclib resistant T47D clones. Sensitive parental T47D cells and palbociclib resistant clones were analysed for methylation by pyrosequencing. The percentage methylation of 7 individual CpG was assessed and average over 7 all sites calculated to determine percentage methylation for each cell line.

Initially it was hypothesised that VIK could be involved in resistance via the previously published direct interaction between VIK and CDK4 (335). Palbociclib inhibits CDK4/6 by competitively targeting the ATP binding pocket. VIK as a binding partner of CDK4, could potentially alter the drug binding to and inhibiting of CDK4 itself. However, our results argue against this theory. Upon VIK knockdown we observed decreased phosphorylation of Rb. Therefore, cells with knockdown of VIK acquire resistance to palbociclib because the target of the drug is already downregulated as a result of the VIK knockdown. However, the involvement of VIK in palbociclib resistance is unlikely to be simply down to this as we see VIK itself is lost in resistant cells. As discussed above, knockdown of VIK altered multiple cell cycle proteins. Therefore, it is more likely that loss of VIK is involved in upregulation of other cell cycle proteins or other signalling pathways that allow the cells to further escape the CDK4/6 inhibition. As previously discussed, knockdown of VIK upregulated cyclin E. This same upregulation of cyclin E is observed in cell lines with acquired resistance to palbociclib promoting cell cycle entry (336). Therefore, we hypothesise loss of VIK induces upregulation of cyclin E, which is could to contribute to survival of palbociclib resistant cells.

8 Conclusions

This thesis confirms VIK as a novel gene in breast cancer subject to methylation dependent transcriptional silencing. I have shown for the first time that VIK is differentially methylated in breast tumour samples compared to normal breast tissue. Expression of VIK is essential for both normal breast and breast cancer cell survival. Upon downregulation of VIK, VAV1 was upregulated, although this did not appear to rescue cells from cell death. Loss of VIK induces apoptosis through modulation of cell cycle proteins and cell cycle arrest in the G1 phase. Thus demonstrating VIK expression is required for normal cell cycle progression in breast cells. This role of VIK in cell cycle regulation is of particular interest as CDK4/6 inhibitors, such as palbociclib, have been increasingly recognised as effective in combination with endocrine therapy in breast cancer treatment. With increasing clinical use, resistance to palbociclib will become an important clinical issue, an understanding of resistant mechanisms will be crucial. I have demonstrated that loss of VIK is potentially involved in development of acquired resistance to CDK4/6 inhibitors. This would make VIK one of the first novel genes to be linked to resistance to this new class of drug for treatment of breast cancer.

9 References

1. Finn RS, J D, Kalous O, Cohen DJ, Desai AJ, Ginther C, et al. PD 0332991, a selective cyclin D kinase 4/6 inhibitor, preferentially inhibits proliferation of luminal estrogen receptor-positive human breast cancer cell lines in vitro. Breast Cancer Research. 2009;11(5):R77.
2. Sievers F, Wilm A, Dineen D, Gibson T, Karplus K, Li W, et al. Fast, scalable generation of high-quality multiple sequence alignments using Clustal Omega. Molecular systems biology. 2011;7(539).
3. Jemal A, Bray F, Center M, Ferlay J, Ward E, Forman D. Global cancer statistics. Journal Clinical Cancer. 2011;61(69-90).
4. Care BC. Breast Cancer Care Statistics. 2015.
5. Cancer, Research, UK. Cancer incidence statistics http://www.cancerresearchuk.org/health-professional/cancer-statistics/incidence2016 [
6. Ali S, Coombes RC. Endocrine-responsive breast cancer and strategies for combating resistance. Nature Reviews Cancer. 2002;2(2):101-12.
7. Hu M, Yao J, Carroll DK, Weremowicz S, Chen H, Carrasco D, et al. Regulation of In Situ to Invasive Breast Carcinoma Transition. Cancer Cell. 2008;13(5):394-406.
8. Mego M, Mani S, Cristofanilli M. Molecular mechanisms of metastasis in breast cancer--clinical applications. Nature Reviews Clinical Oncology. 2010;7(12):693-701.
9. Schnitt SJ. Classification and prognosis of invasive breast cancer: from morphology to molecular taxonomy. Modern Pathology. 2010;Suppl 2:S60-4.
10. Van Cleef A, Altintas S, Huizing M, Papadimitriou K, Vav Dam P, Tjalma W. Current view on ductal carcinoma in situ and importance of the margin thresholds: A review. Facts Views Vis Obgyn. 2014;6(4):210-8.
11. Rosen P, Harris J, Lippman M, Morrow M, Hellman S. Diseases of the Breast. Philadelphia: Lippincott-Raven; 1996.
12. Warnberg F, Casalini P, Nordgren H, Bergkvist L, Holmberg L, Menard S. Ductal carcinoma in situ of the breast: a new phenotype classification system and its relation to prognosis. Breast Cancer Res Treat. 2002;73:215-21.
13. Cowell C, Weigelt B, Sakr R, Ng C, Hicks J, King T, et al. Progression from ductal carcinoma in situ to invasive breast cancer: revisited. Mol Oncol. 2013;7(5):859-69.
14. Virnig B, Tuttle T, Shamliyan T, Kane R. Ductal Carcinoma In Situ of the Breast: A systematic Review of Incidence, Treatment and Outcomes. JNCI. 2010;102(3):170-8.
15. Yersai O, Barutca S. Biological subtypes of breast cancer: Prognostic and therapeutic implications. World J Clin Oncol. 2014;5(3):412-24.
16. Guedj M, L M, A dR, Orsetti B, Schiappa R, Bibeau F, et al. A refined molecular taxonomy of breast cancer. Oncogene. 2012;31(9):1196-206.
17. Network CGA. Comprehensive molecular portraits of human breast tumours. Nature. 2012;490:61-70.
18. Sorlie T, Tibshirani R, Parker J, Hastie T, Marron S, Nobel A, et al. Repeated observation of breast tumor subtypes in independent gene expression data sets. PNAS. 2003;100:8418-23.
19. Kittaneh M, Monterp A, Gluck S. Molecular Profiling for Breast Cancer: A Comprehensive Review. Biomark Cancer. 2013;5:61-70.

20. Voduc K, Cheang M, Tyldesley S, Galmon K, TO N, Kennecke H. Breast cancer subtypes and the risk of local and regional relapse. J Clin Oncol. 2010;28(10):1684-91.
21. Ignatiadis M, Sotiriou C. Luminal breast cancer: from biology to treatment. Nat Rev Clin Onc. 2013;10:494-506.
22. Sorlie T, Perou C, Tibshirani R, Aas T, Geisler S, Johnsen H, et al. Gene expression patterns of breast carcinomas distinguish tumor subclasses with clinical implications. PNAS. 2001.
23. Révillion F, Bonneterre J, Peyrat J. ERBB2 Oncogene in Human Breast Cancer and its Clinical Significance. Eur J Cancer. 1998;34(6):791-808.
24. Sinna H, Kreipe H. A Brief Overview of the WHO Classification of Breast Tumors, 4th Edition, Focusing on Issues and Updates from the 3rd Edition. Breast Care (Basel). 2013;8(2):149-54.
25. Viale G. The current state of breast cancer classification Annals of Oncology 2012;23(10):207-10.
26. Lehmann B, Bauer J, Chen X, Sanders M, Chakravarthy B, Shyr Y, et al. Identification of human triple-negative breast cancer subtypes and preclinical models for selection of targeted therapies. JCI. 2011;121(7):2750-67.
27. Colditz G. Relationship between estrogen levels, use of hormone replacement therapy, and breast cancer. . J National Cancer Insitute. 1998;90:814-23.
28. Hankinson S, Colditz G, Willett W. Towards an integrated model for breast cancer etiology: the lifelong interplay of genes, lifestyle, and hormones. Breast Cancer Research. 2004;6:213-8.
29. Hart C, Migliaccio I, Malorni L, Guarducci C, Biganzoli L, Leo A. Challenges in the management of advanced, ER-positive, HER2-negative breast cancer. Nat Rev Clin Onc. 2015;12:541-52.
30. Matthews J, Gustafsson J. Estrogen signalling: A subtle balance between ERα and ERβ Mol Interventions. Mol Interventions. 2003;3:281-92.
31. Mosselman S, Polman J, Dijkema R. ERβ: identification and characterization of a novel human estrogen recepto. FEBS Letters. 1996;392:49-53.
32. Hewitt S, Korach K. Estrogen receptors: structure, mechanisms and function. Rev Endocr Metab Disord. 2002;3(3):193-200.
33. MacGregor J, Jordan V. Basic guide to the mechanisms of antiestrogen action. Pharmacol Rev. 1998;50:151-96.
34. McDonnell DP, Norris JD. Connections and regulation of the human estrogen receptor. Science. 2002;296:1642–4.
35. Acconcia F, Kumar R. Signaling regulation of genomic and nongenomic functions of estrogen receptors. Cancer Letters. 2006;238(1):1-14.
36. Lippman M, Monaco M, Bolan G. Effects of Estrone, Estradiol, and Estriol on Hormone responsive Human Breast Cancer in Long-Term Tissue Culture. Cancer REsearch. 1977;37:1901-7.
37. Ruff M, Gangloss M, Wurtz J, Moras S. Estrogen receptor transcription and transactivation Structure-function relationship in DNA- and ligand-binding domains of estrogen receptors. Breast Cancer Res. 2000;2:253-359.
38. Le Romancer M, Poulard C, Cohen P, Sentis S, Renoir J, Corbo L. Cracking the estrogen receptor's posttranslational code in breast tumors. Endocrine Reviews. 2011;32(5):597-622.

39. (EBCTCG). EBCTCG. Effects of chemotherapy and hormonal therapy for early breast cancer on recurrence and 15-year survival: an overview of the randomised trials. Lancet. 2005;365:1687-717.
40. Jorden C. Selective estrogen receptor modulation: Concept and consequences in cancer. Cancer Cell 2002;5:207-13.
41. Miller W. Aromatase inhibitors: mechanism of action and role in the treatment of breast cancer. Semin Oncol. 2003;30(4):3-11.
42. Johnston S. New Strategies in Estrogen Receptor–Positive Breast Cancer. Clin Cancer Res. 2010;16:1979.
43. Ghayad S, Vendress J, Ben Larbi S, Dumontet C, Bieche I, Cohen P. Endocrine resistance associated with activated ErbB system in breast cancer cells is reversed by inhibiting MAPK or PI3K/Akt signaling pathways. Int J Cancer. 2010;126(2):545-62.
44. Goetz M, Knox S, Suman V, Rae J, Safgren S, Ames M, et al. The impact of cytochrome P450 2D6 metabolism in women receiving adjuvant tamoxifen. Breast Cancer Research Treatment. 2007;101(1):113-21.
45. Serrano D, Lazzeroni M, Zambon C, Macis D, Maisonneuve P, Johansson H, et al. Efficacy of tamoxifen based on cytochrome P450 2D6, CYP2C19 and SULT1A1 genotype in the Italian Tamoxifen Prevention Trial. J Pharmacogenomics. 2011;11(2):100-7.
46. Clarke R, Liu MC, Bouker KB, Gu Z, Lee RY, Zhu Y, et al. Antiestrogen resistance in breast cancer and the role of estrogen receptor signaling. Oncogene. 2003;22:7316-39.
47. Stone A, Valdés-Mora F, Gee JMW, Farrow L, McClelland RA, Fiegl H, et al. Tamoxifen-Induced Epigenetic Silencing of Oestrogen-Regulated Genes in Anti-Hormone Resistant Breast Cancer. PLoS ONE. 2012;7(7):e40466.
48. Zhou Y, Yau C, Gray J, Chew K, Dairkee S, Moore D, et al. Enhanced NFκB and AP-1 transcriptional activity associated with antiestrogen resistant breast cancer. BMC Cancer. 2007;7:59.
49. Schiff R, Reddy P, Ahotupa M, Coronado-Heinsohn E, Grim M, Hilsenbeck S, et al. Oxidative stress and AP-1 activity in tamoxifen-resistant breast tumors in vivo. J National Cancer Insitute. 2000;92(21):1926-34.
50. Doisneau-Sixou S, Sergio C, Carroll J, Hui R, Musgrove E, Sutherland R. Estrogen and antiestrogen regulation of cell cycle progression in breast cancer cells. Endocr Relat Cancer. 2003;10(2):179-86.
51. Venditti M, Iwasiouw B, Shiu R. C-myc gene expression alone is sufficient to confer resistance to antiestrogen in human breast cancer cells. Int J Cancer. 2002;99:35-42.
52. Prall O, Rogan E, Musgrove E, Watts C, Sutherland R. c-Myc or cyclin D1 mimics estrogen effects on cyclin E-Cdk2 activation and cell cycle reentry. Molecular Cell Biology. 1998;18(8):4499-508.
53. Rudas M, Lehnert M, Huynh A, Jakesz R, Singer C, Lax S, et al. Cyclin D1 expression in breast cancer patients receiving adjuvant tamoxifen-based therapy. Clinical Cancer Research. 2008;14(6):1767-74.
54. Jirstrom K, Stendahl M, Ryden L, Kronblad A, Bendahl P-O, Stal O, et al. Adverse effect of adjuvant tamoxifen in premenopausal breast cancer with cyclin D1 gene amplification. Cancer Research. 2005;65(17):8009-16.
55. Lundgren K, Brown M, Pineda S, Cuzick J, Salter J, Zabaglo L, et al. Effects of cyclin D1 gene amplification and protein expression on time to recurrence in postmenopausal breast cancer patients treated with anastrozole or tamoxifen: a TransATAC study. Breast Cancer Research. 2012;14(2).

56. Dhillon N, Mudrui M. Ectopic expression of cyclin E in estrogen responsive cells abrogates antiestrogen mediated growth arrest. . Oncogene. 2002;21:4626-34.
57. Carroll J, Prall O, Musgrove E, Sutherland R. A pure estrogen antagonist inhibits cyclin E-Cdk2 activity in MCF-7 breast cancer cells and induces accumulation of p130-E2F4 complexes characteristic of quiescence. J Biol Chem. 2000;275:38221-9.
58. Wang Y, Dean J, Millar E, Tran T, McNeil C, Burd C, et al. Cyclin D1b is aberrantly regulated in response to therapeutic challenge and promotes resistance to estrogen antagonists. Cancer Research. 2008;68(14):5628-38.
59. Cariou S, Donovan J, Flanagan W, Milic A, Bhattacharya N, Slingerland J. Down-regulation of p21WAF1/CIP1 or p27Kip1 abrogates antiestrogen-mediated cell cycle arrest in human breast cancer cells. Proc Natl Acad Sci USA. 2000;97:9042-6.
60. Abukhdeir A, Vitolo M, Argani P, De Marzo A, Karakas B, Konishi H, et al. Tamoxifen-stimulated growth of breast cancer due to p21 loss. Proc Natl Acad Sci USA. 2008;105:288-93.
61. Zwijsen R, Wientjens E, Klompmaker R, van der Sman J, Bernards R, Michalides R. CDK-independent activation of estrogen receptor by cyclin D1. Cell.
62. Sutherland R, Green M, Hall R, Reddel R, Taylor I. Tamoxifen induces accumulation of MCF 7 human mammary carcinoma cells in the G0/G1 phase of the cell cycle. Eur J Cancer Clinical Onocology. 1983;19:615-21.
63. Faridi J, Wang L, Endemann G, Roth R. Expression of constitutively active Akt-3 in MCF-7 breast cancer cells reverses the estrogen and tamoxifen responsivity of these cells in vivo. Clinical Cancer Research. 2003;9:2933-9.
64. deGraffenried L, Friedrichs W, Russell D, Donzis E, Middleton A, Silva J, et al. Inhibition of mTOR activity restores tamoxifen response in breast cancer cells with aberrant Akt activity. Clinical Cancer Research. 2004;10(23):8059-67.
65. McClelland R, Barrow D, Madden T, Dutkowski C, Pamment J, Knowlden J, et al. Enhanced epidermal growth factor receptor signaling in MCF7 breast cancer cells after long-term culture in the presence of the pure antiestrogen ICI 182,780 (Faslodex). Endocrinology. 2001;142(7):2776-88.
66. Zuo T, Wang L, Morrison C, Chang X, Zhang H, Li W, et al. FOXP3 is an X-linked breast cancer suppressor gene and an important repressor of the HER-2/ErbB2 oncogene. Cell. 2007;129:1275-86.
67. Hua G, Zhu B, Rosa F, Deblon N, Adélaïde J, Kahn-Perlès B, et al. A negative feedback regulatory loop associates the tyrosine kinase receptor ERBB2 and the transcription factor GATA4 in breast cancer cells. Molecular Cancer Research. 2009;7:402-14.
68. Hurtado A, Holmes K, Geistlinger T, Hutcheson I, Nicholson R, Brown M, et al. Regulation of ERBB2 by oestrogen receptor-PAX2 determines response to tamoxifen. Nature. 2008;456:663-6.
69. Clark A, West K, Streicher S, Dennis P. Constitutive and inducible Akt activity promotes resistance to chemotherapy, trastuzumab, or tamoxifen in breast cancer cells. Mol Cancer Ther. 2002;1(9):707-17.
70. Miller T, Fox E, Gonzalez-Angulo S. Resistance to endocrine therapy in estrogen receptor-positive (ER+) breast cancer is dependent upon phosphatidylinositol-3 kinase (PI3K) signaling. Cancer Research. 2009;69:24.
71. Riggins R, Bouton A, Liu M, Clarke R. Antiestrogens, aromatase inhibitors, and apoptosis in breast cancer. Vitamins and Hormones. 2005;71:201-37.

72. Paplomata E, O'Regan R. he PI3K/AKT/mTOR pathway in breast cancer: targets, trials and biomarkers. The Adv Med Oncol. 2014;6(4):154-66.
73. Lee J, Loh K, Yap Y. PI3K/Akt/mTOR inhibitors in breast cancer. Cancer Biol Med. 2015;12(4):342-54.
74. Turner B. Defining an epigenetic code. Nature Cell Biology. 2007;9:2-7.
75. Khavari D, Sen D, Rinn J. DNA methylation and epigenetic control of cellular differentiation. Cell Cycle. 2010;9(19):3880-3.
76. Qui J. Epigenetics: unfinished symphony. Nature. 2006;441(7090):143-5.
77. Mattick J. The genetic signatures of noncoding RNAs. PLoS Genetics. 2009;5:e1000459.
78. Dinger M. lncRNAs: Finding the Forest Among the Trees? Molecular Therapy. 2011;19(12):2109-11.
79. Gonzalez I, Munita R, Agirre E, Dittmer T, Gysling K, Misteli T, et al. A lncRNA regulates alternative splicing via establishment of a splicing-specific chromatin signature. Nat Struct Mol Biol. 2015;22(5):370-6.
80. Koerner M, Pauler F, Huang R, Barlow D. The function of non-coding RNAs in genomic imprinting. Development. 2009;136:1771-83.
81. Kanduri C. Long noncoding RNAs: Lessons from genomic imprinting. Biochim Biophys Acta. 2016;1859(1):103-11.
82. Project AET, Project CSHLET. Post-transcriptional processing generates a diversity of 5'-modified long and short RNAs. Nature 2009;457(7232):1028-32.
83. Rinn JL, Kertesz M, Wang K, Squazzo S, Xu X. Functional demarcation of active and silent chromatin domains in human HOX loci by noncoding RNAs. Cell. 2007;129:1311-23.
84. Yu W, Gius D, Onyango P, Muldoon-Jacobs K, Karp J. Epigenetic silencing of tumour suppressor gene p15 by its antisense RNA. Nature. 2008.
85. Nagano T, Mitchell J, Sanz L, Pauler F, Ferguson-Smith A. The Air noncoding RNA epigenetically silences transcription by targeting G9a to chromatin. Science. 2008;322(5908):1717-20.
86. Lai F, Orom UA, Cesaroni M, Beringer M, Taatjes D, Blobel G, et al. Activating RNAs associate with Mediator to enhance chromatin architecture and transcription. Nature. 2013;494(7438):497-501.
87. Ørom U, Derrien T, Beringer M, Gumireddy K, Gardini A, Bussotti G, et al. Long noncoding RNAs with enhancer-like function in human cells. Cell. 2010.
88. Wang K, Yang Y, Liu B, Sanyal A, Croces-Zimmerman R, Chen Y, et al. A long noncoding RNA maintains active chromatin to coordinate homeotic gene expression. Nature. 2011;471:120-4.
89. Mercer T, Mattick J. Structure and function of long noncoding RNAs in epigenetic regulation. Nature Structural & Molecular biology. 2013;20:300-7.
90. Meister G. Argonaute proteins: functional insights and emerging roles. Nat Rev Genet. 2013;14:447-59.
91. Jonas S, Izaurralde E. Towards a molecular understanding of microRNA-mediated gene silencing. Nat Rev Genet. 2015;16:421-33.
92. Carthew R, Sontheimer E. Origins and Mechanisms of miRNAs and siRNAs. Cell. 2009;136(4):642-55.
93. Lee J. Epigenetic Regulation by Long Noncoding RNAs. Science. 2012;338(6113):1435-9.
94. Luger K, Ma A, Richmond R, Sergent D, Richmond T. Crystal structure of the nucleosome core particle at 2.8A˚ resolution. Nature. 1997;389:251-60.

95. Waldmann T, Schneider R. Targeting histone modifications- epigenetics in cancer. Current Opinion in Cell Biology. 2013;25(2):184-9.
96. Venkatesh S, Workman J. Histone exchange , chromatin structure and the regulation of transcription. Nature Reviews Molecular Cell Biology. 2015;16:178-89.
97. Bannister A, Kouzarides T. Regulation of chromatin by histone modifications. Cell Research. 2011;21:381-95.
98. Holliday R. Epigenetics: A historical overview. Epigenetics. 2006;1(2):76-80.
99. Okano M, Bell D, Haber D, Li E. DNA methyltransferases Dnmt3a and Dnmt3b are essential for de novo methylation and mammalian development. Cell. 1999;99(3):247-57.
100. Vinson C, Chatterjee R. CG methylation. Epigenomics. 2013;4(6):655-63.
101. Shen L, Konodo Y, Gua Y, Zhang J, Zhang L, Ahmed S, et al. Genome-Wide Profiling of DNA Methylation Reveals a Class of Normally Methylated CpG Island Promoters. PLoS Genetics. 2007;3(10):e181.
102. Saxonov S, Berg P, Brutlag D. A genome-wide analysis of CpG dinucleotides in the human genome distinguishes two distinct classes of promoters. PNAS. 2006;103:1412-7.
103. Lander E, Linton L, Birren B, Nusbaum C, Zody M, Baldwin J, et al. Initial sequencing and analysis of the human genome. Nature. 2001;409(6822):860-921.
104. Sandoval J, Esteller M. Cancer epigenomics: beyond genomics. Curr Opin Genet Dev. 2012;22(1):50-5.
105. Barrera V, Peinado M. Evaluation of single CpG sites as proxies of CpG island methylation states at the genome scale. Nucleic Acids Research. 2012;40(22):11490-8.
106. Esteller M. Cancer epigenomics: DNA methylomes and histone-modification maps. Nat Rev Genet. 2007;8(4):286-98.
107. Keneda M, Okano N, Hata K, Sado T. Essential role for de novo DNA methyltransferase Dnmt3a in paternal and maternal imprinting. . Nature. 2004;429:2-5.
108. Rodríguez-Paredes M, Esteller M. Cancer epigenetics reaches mainstream oncology. Nature Medicine. 2011:330-9.
109. Herman J, Baylin S. Gene silencing in cancer in association with promoter hypermethylation. New England Journal of Medicine. 2003;349:2042-54.
110. Merlo A, Herman J, Li M, Lee D, Gabrielson E, Burger P, et al. 5' CpG island methylation is associated with transcriptional silencing of the tumour suppressor p16/CDKN2/MTS1 in human cancers. Nature Medicine. 1995;1:686-92.
111. Leone G, Teofili L, Voso M, Lübbert M. DNA methylation and demethylating drugs in myelodysplastic syndromes and secondary leukemias. Haematologica. 2002;87:1324-41.
112. Jones P, Baylin S. The fundamental role of epigenetic events in cancer Nature Reviews Genetics. 2002;3:415-28.
113. Huang T, Laux D, Hamlin P, Tran H, Lubahn D. Identification of DNA methylation markers for human breast carcinomas using the methylation-sensitive restriction fingerprinting technique. Cancer Research. 1997;57(6):1030-4.
114. Chen C, Chen H, Hsiau T, Hasiau A, Brock G. Methylation target array for rapid analysis of CpG island hypermethylation in multiple tissue genomes. American Jounal of Pathology. 2003;16(1):37-45.
115. Szyf M. DNA methylation signatures for breast cancer classification and prognosis. Genome Medicine 2012;4(3):26.
116. Singhal S, Usmani N, Michiels S, Metzger-Filho O, Saini K, Kovalchuk O, et al. Towards understanding the breast cancer epigenome: a comparison of genome-wide DNA methylation and gene expression data. Oncotarget. 2016;7(3):3002-17.

117. Veek J, Esteller M. Breast Cancer Epigenetics: From DNA Methylation to microRNAs. J Mammary Gland Biol Neoplasia. 2010;15(1):5-17.
118. Weigel R, deConinck E. Transcriptional control of estrogen receptor in estrogen receptor-negative breast carcinoma. Cancer Research. 1993;53(15):3472-4.
119. Ferguson A, Lapidus R, Baylin S, Davidson N. Demethylation of the estrogen receptor gene in estrogen receptor-negative breast cancer cells can reactivate estrogen receptor gene expression. Cancer Research. 1995;55(11):2279-83.
120. Zhang W, Chang Z, Shi K, Song L, Cui L, Ma Z, et al. The correlation between DNMT1 and ERα expression and the methylation status of ERα, and its clinical significance in breast cancer. Oncology Letters. 2016;11(3):1995-2000.
121. Stone A, Zotenko E, Locke W, Korbie D, Millar E, Pidsley R, et al. DNA methylation of oestrogen-regulated enchances defines endocrine sensitivity in breast cancer. Nature Communications. 2015;6:1-9.
122. Herman J, Merlo A, Mao L, Lapidus R, Issa J, Davidson N, et al. Inactivation of the CDKN2/p16/MTS1 gene is frequently associated with aberrant DNA methylation in all common human cancers. Cancer Research. 1995;55(20):4525-30.
123. Silva J, Silva J, Domínguez G, García J, Cantos B, Rodríguez R, et al. Concomitant expression of p16INK4a and p14ARF in primary breast cancer and analysis of inactivation mechanisms. Journal of Pathology. 2003;199(3):289-97.
124. Umbricht C, Evron E, Gabrielson E, Ferguson A, Marks J, Sukumar S. Hypermethylation of 14-3-3 sigma (stratifin) is an early event in breast cancer Oncogene. 2001;20(26):3348-53.
125. Ward A, Mello R, Smith S, Kendall S, Just N, Vizeacoumar F, et al. Epigenetic silencing of CREB3L1 by DNA methylation is associated with high-grade metastatic breast cancers with poor prognosis and is prevalent in triple negative breast cancers. Breast Cancer Res. 2016;18(1).
126. Ozturk S, Papageorgis P, Wong C, Lambert A, Abdolmaleky H, Thiagalingam A, et al. SDPR functions as a metastasis suppressor in breast cancer by promoting apoptosis. PNAS. 2016;113(3):638-43.
127. Yongbin Y, Jinghua L, Zhanxue Z, Aimin Z, Youchao J, Yanhong S, et al. TES was epigenetically silenced and suppressed the epithelial-mesenchymal transition in breast cancer. Tumour Biol. 2014;35(11):11381-9.
128. Niwa Y, T O, Nakajima T. BRCA1 expression status in relation to DNA methylation of the BRCA1 promoter region in sporadic breast cancers Japan Journal of Cancer Research. 2000;91(5):519-25.
129. Rice J, Ozcelik H, Maxeiner P, Andrulis I, Futscher B. Methylation of the BRCA1 promoter is associated with decreased BRCA1 mRNA levels in clinical breast cancer specimens. Carcinogenesis. 2000;21(9):1761-5.
130. Esteller M, Silva J, Dominguez G, Bonilla F, Matias-Guiu X, Lerma E, et al. Promoter Hypermethylation and BRCA1 Inactivation in Sporadic Breast and Ovarian Tumors. Journal National Cancer Insitute. 2000;92(7):564-9.
131. Fumagalli C, Pruneri G, Possanzini P, Manzotti M, Barile M, Feroce I, et al. Methylation of O6-methylguanine-DNA methyltransferase (MGMT) promoter gene in triple-negative breast cancer patients. Breast Cancer Research Treatment. 2012;134(1):131-7.
132. Murata H, Khattar N, Kang Y, Gu L, Li G. Genetic and epigenetic modification of mismatch repair genes hMSH2 and hMLH1 in sporadic breast cancer with microsatellite instability. Oncogene. 2002;21(37):5696-703.

133. Pal R, Srivastava N, Chopra R, Gochhait S, Gupta P, Prakash N, et al. Investigation of DNA damage response and apoptotic gene methylation pattern in sporadic breast tumors using high throughput quantitative DNA methylation analysis technology. Molecular Cancer. 2010;23(9):303.
134. Caldon CE, Daly RJ, Sutherland RL, Musgrove EA. Cell cycle control in breast cancer cells. Journal of Cell Biochemistry. 2006;97(2):261-74.
135. Fernández PL, Jares P, Rey MJ, Campo E, Cardesa A. Cell cycle regulators and their abnormalities in breast cancer. Molecular Pathology. 1998;51(6):305-9.
136. Jeffrey P, Russo A, Polyak K, Gibbs E, Hurwitz J, Massague J, et al. Mechanism of CDK activation revealed by the structure of a cyclinA-CDK2 complex Nature. 1995;376(27):313-20.
137. Pavletich N. Mechanisms of cyclin-dependent kinase regulation: structures of CDKs, their cyclin activators, and CIP and INK4 inhibitors. J Mol Biol. 1999;287:821-8.
138. Johnson D, Walker C. Cyclins and cell cycle checkpoints. Annu Rev Pharmacol Toxicol. 1999;39:295-312.
139. Morgan D. Cyclin-dependent kinases: engines, clocks, and microprocessors. Annu Rev Cell Dev Biol. 1997;13.
140. Gopinathan L, Ratnacaram C, Kaldis P. Established and novel Cdk/cyclin complexes regulating the cell cycle and development. Results Probl Cell Differ. 2011;53:365-89.
141. Malumbres M, Barbacid M. Cell cycle, CDKs and cancer: a changing paradigm. Nat Rev Cancer. 2009;9(3):153-66.
142. Hershko A. Mechanisms and regulation of the degradation of cyclin B. Philos Trans R Soc Lond B Biol Sci. 1999;354(1389):1575-6.
143. Diehl J, Cheng M, Roussel M, Sherr C. Glycogen synthase kinase-3β regulates cyclin D1 proteolysis and subcellular localization. . Genes and Development. 1998;12:3499-511.
144. Diehl J, Zindy F, Sherr C. Inhibition of cyclin D1 phosphorylation on threonine-286 prevents its rapid degradation via the ubiquitin-proteasome pathway. Genes and Development. 1997;11.
145. Lin D, Barbash O, KG K, Weber J, Harper J, Klein-Szanto A, et al. Phosphorylation-dependent ubiquitination of cyclin D1 by the SCFFBX4-αBcrystallin complex. Molecular Cell. 2007;24(3):355-66.
146. Jeffrey P, Tong L, Pavletich N. Structural basis of inhibition of CDK-cyclin complexes by INK4 inhibitors. Genes and Development. 2000;14(24):3115-25.
147. Sandhu C, Garbe J, Bhattacharya N, Daksis J, Pan C, Yaswen P, et al. Transforming growth factor beta stabilizes p15INK4B protein, increases p15INK4B-cdk4 complexes, and inhibits cyclin D1-cdk4 association in human mammary epithelial cells. Molecular and Cellular Biology. 1997;17(5):2458-67.
148. Russo A, Tong L, Lee J, Jeffrey P, Pavletich N. Structural basis for inhibition of the cyclin-dependent kinase Cdk6 by the tumour suppressor p16INK4a. Nature. 1998;395(6699):237-43.
149. Franklin D, Xiong Y. Induction of p18INK4c and its predominant association with CDK4 and CDK6 during myogenic differentiation. Molecular Biology of the Cell. 1996;7(10):1587-99.
150. Phelps D, Hsiao K, Li Y, Hu N, Franklin D, Westphal E, et al. Coupled transcriptional and translational control of cyclin-dependent kinase inhibitor p18INK4c expression during myogenesis. Molecular and Cell Biology. 1998;18(4):2334-43.

151. Stepanova L, Leng X, Parker S, Harper J. Mammalian p50Cdc37 is a protein kinase-targeting subunit of Hsp90 that binds and stabilizes Cdk4. Genes and Development. 1996;10:1491-502.
152. Lamphere L, Fiore F, Xu X, Brizuela L, Keezer S, Sardet C, et al. Interaction between Cdc37 and Cdk4 in human cells. Oncogene. 1997;14(1999-2004).
153. Dehay C, Kennedy H. Cell-cycle control and cortical development. Nature Reviews Neuroscience. 2007;8(6):438-50.
154. Denicourt C, Dowdy S. Cip/Kip proteins: more than just CDKs inhibitors. Genes and Development. 2004;18:851-5.
155. Blain S. Switching cyclin D-Cdk4 kinase activity on and off. Cell Cycle. 2008;7:892-8.
156. Reynisdóttir I, Polyak K, Lavarone A, Massagué J. Kip/Cip and Ink4 Cdk inhibitors cooperate to induce cell cycle arrest in response to TGF-beta. Genes and Development. 1995;9(15):1831-45.
157. James M, Ray A, Leznova D, Blain S. Differential modification of p27Kip1 controls its cyclin D-cdk4 inhibitory activity. Molecular and Cellular Biology. 2008;29(1):498-510.
158. Hengst L, Reed S. Translational control of p27Kip1 accumulation during the cell cycle. Science. 1996;271(5257):1861-4.
159. Sherr C, Roberts J. CDK inhibitors: positive andnegative regulators of G1-phase progression. Genes and Development. 1999;13(12):1501-12.
160. Montagnoli A, Fiore F, Eytan E, Carrano A, Draetta G, Hershko A, et al. Ubiquitination of p27 is regulated by Cdk-dependent phosphorylation and trimeric complex formation. Genes and Development. 1999;13(9):1181-9.
161. Blain S, Scher H, Cordon-Cardo C, Koff A. p27 as a target for cancer therapeutics. Cancer Cell. 2003;3(2):111-5.
162. Nurse P. Checkpoint pathways come of age. Cell. 1997;91(7):865-7.
163. Donzelli M, Draetta G. Regulating mammalian checkpoints through Cdc25 inactivation. EMBO reports. 2003;4(7):671-7.
164. Atherton-Fessler S, Parker L, Geahlen R, Piwnica-Worms H. Mechanisms of p34cdc2 regulation. Molecular and Cell Biology. 1993;13(3):1675-85.
165. Draetta G. Cell cycle: Will the real Cdk-activating kinase please stand up Current Biology. 1997;7(1):50-2.
166. Rosenblatt Y, Morgan D. Cell cycle regulation of CDK2 activity by phosphorylation of Thr160 and Tyr15. EMBO J. 1992;11(11):3995-4005.
167. Krajewska M, Heijink A, Bisselink Y, Seinstra R, Silljé H, de Vries E, et al. Forced activation of Cdk1 via wee1 inhibition impairs homologous recombination. Oncogene. 2013;32(24):3001-8.
168. Perry J, Kornbluth S. Cdc25 and Wee1: analogous opposites? Cell Division. 2007;2(12).
169. Trimarchi J, Lees J. Sibling rivalry in the E2F family. . Nature Reviews Molecular Cell Biology. 2002;3:11-20.
170. Ohtani K, DeGregori J, Nevins J. Regulation of the cyclin E gene by transcription factor E2F1. PNAS. 1995;92(26):12146-50.
171. Sutherland RL, Musgrove EA. Cyclins and breast cancer. J Mammary Gland Biol Neoplasia. 2004;9(1):95-104.
172. Di Leonardo A, Linke S, Clarkin K, Wahl G. DNA damage triggers a prolonged p53-dependent G1 arrest and long-term induction of Cip1 in normal human fibroblasts. Genes and Development. 1994;8(21):2540-51.

173. Bertoli C, Skotheim J, de Bruin R. Control of cell cycle transcription during G1 and S phases. Nat Rev Mol Cell Biol. 2013;14(8):518-28.
174. Xu M, Sheppard K, Peng C, Yee A, Piwnica-Worms H. Cyclin A/CDK2 binds directly to E2F-1 and inhibits the DNA-binding activity of E2F-1/DP-1 by phosphorylation. Molecular and Cell Biology. 1994;14(12):8420-31.
175. Marti A, Wirbelauer C, Scheffner M, Krek W. Interaction between ubiquitin-protein ligase SCFSKP2 and E2F-1 underlies the regulation of E2F-1 degradation. Naure Cell Biology. 1999;1(1):14-9.
176. Campanero M, Flemington E. Regulation of E2F through ubiquitin-proteasome-dependent degradation: stabilization by the pRB tumor suppressor protein. PNAS. 1997;94(6):2221-6.
177. Satyanarayana A, Kaldis P. A dual role of Cdk2 in DNA damage response. Cell Division. 2009.
178. Dasika G, Lin S, Zhao S, Sung P, Tompkinson A, Lee E. DNA damage-induced cell cycle checkpoints and DNA strand break repair in development and tumorigenesis. Oncogene. 1999;18(55).
179. Uto K, Inoue D, Shimuta K, Nakajo N, Sagata N. Chk1, but not Chk2, inhibits Cdc25 phosphatases by a novel common mechanism. EMBO J. 2004;23(16):3386-96.
180. Jackman M, Lindon C, Nigg E, Pines J. Active cyclin B1-Cdk1 first appears on centrosomes in prophase. Nature Cell Biology. 2003;5(2):143-8.
181. Abe S, Nagasaka K, Hirayama Y, Kozuka-Hata H, Oyama M, Aoyagi Y, et al. The initial phase of chromosome condensation requires Cdk1-mediated phosphorylation of the CAP-D3 subunit of condensin II. Genes and Development. 2011;25(863-874).
182. Li C, Vassilev A, DePamphilis M. Role for Cdk1 (Cdc2)/Cyclin A in Preventing the Mammalian Origin Recognition Complex's Largest Subunit (Orc1) from Binding to Chromatin during Mitosis. Molecular and Cell Biology. 2004;24(13):5875-86.
183. Tanaka S, Tak Y, Araki H. The role of CDK in the initiation step of DNA replication in eukaryotes. Cell Division. 2007;2(16).
184. Bosco EE, Wang Y, Xu H, Zilfou JT, Knudsen KE, Aronow BJ, et al. The retinoblastoma tumor suppressor modifies the therapeutic response of breast cancer. Journal of Clinical Investigation. 2007;117(1):218-28.
185. Arima Y, Inoue Y, Shibata T, Hayashi H, Nagano O, Saya H, et al. Rb Depletion Results in Deregulation of E-Cadherin and Induction of Cellular Phenotypic Changes that Are Characteristic of the Epithelial-to-Mesenchymal Transition. Cancer Research. 2002;68(13):5104-12.
186. Musgrove E, Sutherland R. RB in breast cancer: differential effects in estrogen receptor-positive and estrogen receptor-negative disease. Cell Cycle. 2010;9(23):4607-15.
187. Buckley MF, Sweeney KJ, Hamilton JA, Sini RL, Manning DL, Nicholson RI, et al. Expression and amplification of cyclin genes in human breast cancer. Oncogene. 1993;8(8):2127-33.
188. Schwartz G, Shah M. Targeting the cell cycle: a new approach to cancer therapy. J Clinical Oncology. 2005;23(36):9408-21.
189. Butt A, McNeil C, Musgrove E, Sutherland R. Downstream targets of growth factor and oestrogen signalling and endocrine resistance: the potential roles of c-Myc, cyclin D1 and cyclin E. Endocr Relat Cancer. 2005;12:S47-S59.
190. van Diest PJ, Michalides RJ, Jannink L, van der Valk P, Peterse HL, de Jong JS, et al. Cyclin D1 expression in invasive breast cancer. Correlations and prognostic value. The American Journal of Pathology. 1997;150(2):705-11.

191. Dickson C, V F, C G, S B, J B, R S, et al. Amplification of chromosome band 11q13 and a role for cyclin D1 in human breast cancer. Cancer Letters. 1995;90(1):43-50.
192. Bartkova J, Lukas J, Müller H, Lützhøt D, Strauss M, Bartek J. Cyclin D1 protein expression and function in human breast cancer. International Journal of Cancer. 1994;57(3):353-61.
193. Gillett C, V F, Smith R, Fisher C, Bartek J, Dickson C, et al. Amplification and overexpression of cyclin D1 in breast cancer detected by immunohistochemical staining. Cancer Research. 1994;54(7):1812-7.
194. Arnold A, Papanikolaou A. Cyclin D1 in breast cancer pathogenesis. J Clin Oncol. 2005;23:4215-24.
195. Yu Q, Sicinska E, Geng Y, Ahnström M, Zagozdzon A, Kong Y. Requirement for CDK4 kinase function in breast cancer. Cancer Cell. 2008;7:892-8.
196. Kenny FS, Hui R, Musgrove EA, Gee JM, Blamey RW, Nicholson RI, et al. Overexpression of cyclin D1 messenger RNA predicts for poor prognosis in estrogen receptor-positive breast cancer. Clinical Cancer Research. 1999;5(8):2069-76.
197. McIntosh GG, Anderson JJ, Milton I, Steward M, Parr AH, Thomas MD, et al. Determination of the prognostic value of cyclin D1 overexpression in breast cancer. Oncogene. 1995;11(5):885-91.
198. Lehn S, Tobin NP, Berglund P, Nilsson K, Sims AH, Jirström K, et al. Down-Regulation of the Oncogene Cyclin D1 Increases Migratory Capacity in Breast Cancer and Is Linked to Unfavorable Prognostic Features. The American Journal of Pathology. 2010;177(6):2886-97.
199. Millar E, Dean J, McNeil C, O'Toole S, Henshall S, Tran T, et al. Cyclin D1b protein expression in breast cancer is independent of cyclin D1a and associated with poor disease outcome. Oncogene. 2011;28(15):1812-20.
200. Nair B, Vadlamudi R. Regulation of hormonal therapy resistance by cell cycle machinery. Gene Ther Mol Biol. 2008;12.
201. Thangavel C, Dean Jl Fau - Ertel A, Ertel A Fau - Knudsen KE, Knudsen Ke Fau - Aldaz CM, Aldaz Cm Fau - Witkiewicz AK, Witkiewicz Ak Fau - Clarke R, et al. Therapeutically activating RB: reestablishing cell cycle control in endocrine therapy-resistant breast cancer. Endocr Relat Cancer. 2011;18(3):333-45.
202. Brenner A, Paladugu A, Wang H, Olopade O, Dreyling M, Aldaz C. Preferential loss of expression of p16(INK4a) rather than p19(ARF) in breast cancer. Clinical Cancer Research. 1996;2(12):1993-8.
203. Lee J, Ko E, Cho J, Park H, Lee J, Nam S, et al. Methylation and immunoexpression of p16(INK4a) tumor suppressor gene in primary breast cancer tissue and their quantitative p16(INK4a) hypermethylation in plasma by real-time PCR. Korean J Pathol. 2012;46(6):554-61.
204. Alkarain A, Jordan R, Slingerland J. p27 deregulation in breast cancer: prognostic significance and implications for therapy. J Mammary Gland Biol Neoplasia. 2004;9(1):67-80.
205. Chiarle R, Pagano M, Inghirami G. The cyclin dependent kinase inhibitor p27 and its prognostic role in breast cancer. Breast Cancer Research. 2001;3:91-4.
206. Chu I, Hengst L, Silingerland J. The Cdk inhibitor p27 in human cancer: prognostic potential and relevance to anticancer therapy. 2008;8:253-67.
207. Tsutsui T, Hesabi B, Moons D, Pandolfi P, Hansel K, Koff A, et al. Targeted disruption of CDK4 delays cell cycle entry with enhanced p27(Kip1) activity. Molecular Cell Biology. 1999;19(10):7011-9.

208. Senderowicz A. Small molecule modulators of cyclin-dependent kinases for cancer therapy. Oncogene. 2000;19(56):6600-6.
209. Whittaker S, Walton M, Garrett M, Workman P. The Cyclin-dependent kinase inhibitor CYC202 (R-roscovitine) inhibits retinoblastoma protein phosphorylation, causes loss of Cyclin D1, and activates the mitogen-activated protein kinase pathway. Cancer Research. 2004;64(1):262-72.
210. Shapiro G. Preclinical and clinical development of the cyclin-dependent kinase inhibitor flavopiridol. Clinical Cancer Research. 2004;10(12 Pt 2):4270s-5s.
211. Kaur G, Stetler-Stevenson M, Sebers S, Worland P, Sedlacek H, Myers C, et al. Growth inhibition with reversible cell cycle arrest of carcinoma cells by flavone L86-8275. J National Cancer Insitute. 1992;84(22):1736-40.
212. Parker B, Kaur G, Nieves-Neira W, Taimi M, Kohlhagen G, Shimizu T, et al. Early induction of apoptosis in hematopoietic cell lines after exposure to flavopiridol. Blood. 1998;91(2):458-65.
213. Li Y, Bhuiyan M, Alhasan S, Senderowicz A, Sarkar F. Induction of apoptosis and inhibition of c-erbB-2 in breast cancer cells by flavopiridol. Clinical Cancer Research. 2000;6(1):223-9.
214. Sadler W, Vogelzang N, Amato R, Sosman J, Taber D, Liebowitz D, et al. Flavopiridol, A Novel Cyclin-Dependent Kinase Inhibitor, in Metastatic Renal Cancer: A University of Chicago Phase II Consortium Study. Journal of Clinical Oncology. 2000;18(2):371-.
215. Ang C, O'Reilly E, Carvajal R, Capanu M, Gonen M, Doyle L, et al. A Nonrandomized, Phase II Study of Sequential Irinotecan and Flavopiridol in Patients With Advanced Hepatocellular Carcinoma. Gastrointestinal Cancer Research. 2012;5(6):185-9.
216. Bible K, Peethambaram P, Oberg A, Maples W, Groteluschen D, Boente M, et al. A phase 2 trial of flavopiridol (Alvocidib) and cisplatin in platin-resistant ovarian and primary peritoneal carcinoma: MC0261. Gynecolo Oncol. 2012;127(1):55-62.
217. Carvajal R, Tse A, Shah M, Lefkowitz R, Gonen M, Gilman-Rosen L, et al. A phase II study of flavopiridol (Alvocidib) in combination with docetaxel in refractory, metastatic pancreatic cancer. Pancreatology. 2009;9(4):404-9.
218. Liu G, Gandara D, Lara P, Raghavan D, Doroshow J, Twardowsk iP, et al. A Phase II trial of flavopiridol (NSC #649890) in patients with previously untreated metastatic androgen-independent prostate cancer. Clinical Cancer Research. 2004;10(3):924-8.
219. Fornier M, Rathkopf D, Shah M, Patil S, O'Reilly E, Tse A. Phase I dose-finding study of weekly docetaxel followed by flavopiridol for patients with advanced solid tumors. Clinical Cancer Research. 2007;13:5841-6.
220. Parry D, Guzi T, Shanahan F, N D, D P, Wiswell D, et al. Dinaciclib (SCH 727965), a novel and potent cyclin-dependent kinase inhibitor. Mol Cancer Ther. 2010;9(8):2344-53.
221. Mitri Z, Karakas C, Wei C, Briones B, Simmons H, Ibrahim N, et al. A phase 1 study with dose expansion of the CDK inhibitor dinaciclib (SCH 727965) in combination with epirubicin in patients with metastatic triple negative breast cancer. Invest New Drugs. 2015;33(4):890-4.
222. Mita M, Joy A, Mita A, Sankhala K, Jou Y, Zhang D, et al. Randomized phase II trial of the cyclin-dependent kinase inhibitor dinaciclib (MK-7965) versus capecitabine in patients with advanced breast cancer. Clin Breast Cancer. 2014;14(3):169-76.
223. Johnson N, Shapiro G. Cyclin-dependent kinases (cdks) and the DNA damage response: rationale for cdk inhibitor–chemotherapy combinations as an anticancer strategy for solid tumors. Expert Opin Ther Targets. 2014;14(11):1199-212.

224. Xia Q, Cai Y, Peng R, Wu G, Shi Y, Jiang W. The CDK1 inhibitor RO3306 improves the response of BRCA-proficient breast cancer cells to PARP inhibition. Int J Oncol. 2014;44(3):735-44.
225. Barvian M, Boschelli D, Cossrow J, Dobrusin E, Fattaey A, Fritsch A, et al. Pyrido[2,3-d]pyrimidin-7-one inhibitors of cyclin-dependent kinases. J Medicinal Chemistry. 2000;43(24):4606-16.
226. Asghar U, Witkiewicz A, Turner N, Knudsen E. The history and future of targeting cyclin-dependent kinases in cancer therapy. Nature Reviews Drug Discovery. 2015;14(2):130-46.
227. Gelbert L, Cai S, Lin X, Sanchex-Martinez C, Del Prado M, Leallena M, et al. Preclinical characterisation of CDK4/6 inhibitor LY2835219: in vivo cell cycle-dependent/independent tumour activities alone/in combination with gemcitabine. Invest New Drugs. 2014;32(5):825-37.
228. Fry D, Harvey P, Keller P, Elliott W, Meade M, Trachet E, et al. Specific inhibition of cyclin-dependent kinase 4/6 by PD 0332991 and associated antitumor activity in human tumor xenografts. Mol Cancer Ther. 2004;3(11):1427-38.
229. Toogood P. Cyclin-dependent kinase inhibitors for treating cancer. Medicinal Research Reviews. 2001;21(6):487-98.
230. Dean J, Thangavel C, McClendon A, Reed C, Knudsen E. Therapeutic CDK4/6 inhibition in breast cancer: key mechanisms of response and failure. Oncogene. 2010;29(28):4018-32.
231. DeMichele A, Clark AS, Tan KS, Heitjan DF, Gramlich K, Gallagher M, et al. CDK 4/6 inhibitor palbociclib (PD0332991) in Rb+ advanced breast cancer: phase II activity, safety, and predictive biomarker assessment. Clinical Cancer Research. 2014;21(5):995-1001.
232. Slamon D, Hurvitz S, Applebaum S, Glaspy J, Allison K, DiCarlo B, et al. Phase I study of PD 0332991, cyclin-D kinase (CDK) 4/6 inhibitor in combination with letrozole for first-line treatment of patients with ER-positive, HER2-negative breast cancer. J Clin Oncol. 2010;28(15s).
233. Juric D, Hamilton E, Estevex L, De Boer R, Mayer I, Campone M, et al. Phase Ib/II study of LEE011 and BYL719 and letrozole in ER+, HER2– breast cancer: Safety, preliminary efficacy and molecular analysis. Cancer Reserarch. 2015;75:P5-19-24.
234. Patnaik A, Tosen L, Tolaney S, Tolcher A, Goldman J, Gandhi L, et al. Efficacy and Safety of Abemaciclib, an inhibitor of CDK4 and CDK6, for patients with breast cancer, non-small cell lung cancer and other solid tumours. Cancer Discovery. 2016;6(7):1-14.
235. Finn RS, Crown JP, Lang I, Boer K, Bondarenko IM, Kulyk SO, et al. The cyclin-dependent kinase 4/6 inhibitor palbociclib in combination with letrozole versus letrozole alone as first-line treatment of oestrogen receptor-positive, HER2-negative, advanced breast cancer (PALOMA-1/TRIO-18): a randomised phase 2 study. The Lancet Oncology. 2014;16(1):25-35.
236. Turner NC, Ro J, André F, Loi S, Verma S, Iwata H, et al. Palbociclib in Hormone-Receptor–Positive Advanced Breast Cancer. New England Journal of Medicine. 2015;373(3):209-19.
237. Cristofanilli M, Turner N, Bondarenko I, Ro J, Im S, Masuda N, et al. Fulvestrant plus palbociclib versus fulvestrant plus placebo for treatment of hormone-receptor-positive, HER2-negative metastatic breast cancer that progressed on previous endocrine therapy (PALOMA-3): final analysis of the multicentre, double-blind, phase 3 randomised controlled trial. Lancet. 2016;15:pii: S1470-2045.

238. McConnell BB, Yang VW. Mammalian Kruppel-like factors in health and diseases. Physiol Rev. 2010;90(4):1337-81.
239. Huebner K, Druck T, Croce C, Thiesen H. Twenty-seven nonoverlapping zinc finger cDNAs from human T cells map to nine different chromosomes with apparent clustering. Am J Hum Genetics. 1991;48(4):726-40.
240. Limame R, Op de Beeck K, Lardon F, De Wever O, Pauwels P. Krüppel-like factors in cancer progression: three fingers on the steering wheel. Oncotarget. 2014;5(1):29-48.
241. Tetreault M-P, Yang Y, Katz JP. Kruppel-like factors in cancer. Nat Rev Cancer. 2013;13(10):701-13.
242. Wei D, Kanai M, Jia Z, Le X, Xie K. Kruppel-like factor 4 induces p27Kip1 expression in and suppresses the growth and metastasis of human pancreatic cancer cells. Cancer Research. 2008;68(12):4631-19.
243. Chen C, S BM, Sun X, Otto KB, Guo P, Dong X-Y, et al. KLF5 promotes cell proliferation and tumorigenesis through gene regulation and the TSU-Pr1 human bladder cancer cell line. Int J Cancer. 2006;118(6):1346-55.
244. Dong JT, Chen C. Essential role of KLF5 transcription factor in cell proliferation and differentiation and its implications for human diseases. Cell Mol Life Sci. 2009;66(16):2691-706.
245. DiFeo A, A MJ, Narla G. The role of KLF6 and its splice variants in cancer therapy. Drug Resistant Update. 2009;2(1-7).
246. Lahiri S, Zhao J. Krüppel-like factor 8 emerges as an important regulator of cancer. Am J Transl Res. 2012;4(3):357-63.
247. Wang X, Zheng M, Liu G, Xia W, McKeown-Longo P, Hung M, et al. Kruppel-like factor 8 induces epithelial to mesenchymal transition and epithelial cell invasion. Cancer Research. 2007;67(15):7184-93.
248. Wang X, Zhao J. KLF8 transcription factor participates in oncogenic transformation. Oncogene. 2007;26(3):456-61.
249. Sachdeva M, Dodd R, Huang Z, Grenier C, Ma Y, Lev D, et al. Epigenetic silencing of Kruppel like factor-3 increases expression of pro-metastatic miR-182. Cancer Letters. 2015;369(1):202-11.
250. Zhou S, Tang X, Tang F. Krüppel-like factor 17, a novel tumor suppressor: its low expression is involved in cancer metastasis. Tumour Biology. 2015.
251. Dong P, Kaneuchi M, Xiong Y, Cao L, Cai M, Liu X, et al. Identification of KLF17 as a novel epithelial to mesenchymal transition inducer via direct activation of TWIST1 in endometrioid endometrial cancer. Carcinogenesis. 2014;35(4):760-8.
252. Ghaleb AM, Jp K, Kaestner KH, Du JX, Yang VW. Kruppel-like factor 4 exhibits antiapoptotic activity following gamma-radiation-induced DNA damage. Oncogene. 2007;26(16):2365-73.
253. Wang B, Zhao M, Cui N, Lin D, Zang A, Qin Y, et al. Krüppel-like factor 4 induces apoptosis and inhibits tumorigenic progression in SK-BR-3 breast cancer cells. FEBS Open Bio. 2015;5:147-54.
254. Zhao Y, Hamza M, Leong HS, Lim CB, Pan YF, Cheung E, et al. Kruppel-like factor 5 modulates p53-independent apoptosis through Pim1 survival kinase in cancer cells. Oncogene. 2007;3(27):1-8.
255. Liu R, Zheng Hq Fau - Zhou Z, Zhou Z Fau - Dong J-T, Dong Jt Fau - Chen C, Chen C. KLF5 promotes breast cell survival partially through fibroblast growth factor-binding protein 1-pERK-mediated dual specificity MKP-1 protein phosphorylation and stabilization. Journal of Biological Chemistry. 2009;284(25):16791-8.

256. Shi Q, Gao Y, Xu S, Du C, Li F, Tang X, et al. Krüppel-like factor 5 promotes apoptosis triggered by tumor necrosis factor α in LNCaP prostate cancer cells via up-regulation of mitogen-activated protein kinase kinase 7. Urologic Oncology. 2015:S1078-439(15)00447-0.
257. Ghaleb A, Nandan M, Chanchevalap S, Dalton W, Hisamuddin I, Yang V. Krüppel-like factors 4 and 5: the yin and yang regulators of cellular proliferation. Cell Research. 2005;15:92-6.
258. Farrugia M, Sharma S, Lin C, McLaughlin S, Vanderbilt D, Ammer A, et al. Regulation of anti-apoptotic signaling by Kruppel-like factors 4 and 5 mediates lapatinib resistance in breast cancer Cell Death and Disease. 2015;6:e1699.
259. Shen P, Sun J, Xu G, Zhang L, Yang Z, Xia S, et al. KLF9, a transcription factor induced in flutamide-caused cell apoptosis, inhibits AKT activation and suppresses tumor growth of prostate cancer cells. Prostate. 2014;74(9):946-58.
260. Simmen RC, Pabona J, Velarde MC, Simmons C, Rahal O, Simmen FA. The emerging role of Kruppel-like factors in endocrine-responsive cancers of female reproductive tissues. Journal of Endocrinology. 2010;204(3):223-31.
261. Ray S, Pollard J. KLF15 negatively regulates estrogen-induced epithelial cell proliferation by inhibition of DNA replication licensing. Proc Natl Acad Sci USA. 2012;109(21):1334-243.
262. Katzav S, Martin-Zanca D, Barbacid M. Vav, a novel human oncogene derived from a locus ubiquitously expressed in hematopoietic cells. EMBO J. 1989;8:2283-90.
263. Bustello X. Vav proteins, adaptors and cell signaling. Oncogene. 2001;20(44):6372-81.
264. Crespo P, Schuebel K, Ostrom A, Gutkind J, Bustelo X. Phosphotyrosine-dependent activation of Rac-1 GDP/GTP exchange by the vav proto-oncogene product. Nature. 1997;385(6612):169-72.
265. Schuebel K, Movilla N, Rosa J, Bustelo X. Phosphorylation-dependent and constitutive activation of Rho proteins by wild-type and oncogenic Vav-2. EMBO J. 1998;17(22):6608-21.
266. Hornstein I, Alcover A, Katzav S. Vav proteins, masters of the world of cytoskeleton organization. Cell Signalling. 2004;16(1):1-11.
267. Katzav S, Martin-Zanca D, Barbacid M. vav, a novel human oncogene derived from a locus ubiquitously expressed in hematopoietic cells. 8. 1989;8(0261-4189):2283-90.
268. Tybulewicz V. Vav-family proteins in T-cell signalling. Curr Opin Immunol. 2005;17(3):267-74.
269. Hornstein I, Pikarsky E, Groysman M, Amir G, Peylan- Ramu N, Katzav S. The haematopoietic specific signal transducer Vav1 is expressed in a subset of human neuroblastomas. Journal of Pathology. 2003;199:526-33.
270. Fernandez-Zapico ME, Gonzalez-Paz Nc Fau - Weiss E, Weiss E Fau - Savoy DN, Savoy Dn Fau - Molina JR, Molina Jr Fau - Fonseca R, Fonseca R Fau - Smyrk TC, et al. Ectopic expression of VAV1 reveals an unexpected role in pancreatic cancer tumorigenesis. Cancer Cell. 2005;1:39-49.
271. Lazer G, Idelchuk Y, Schapira V, Pikarsky E, Katzav S. The haematopoietic specific signal transducer Vav1 is aber- rantly expressed in lung cancer and plays a role in tumourigenesis. Journal of Pathology. 2009;219:25-34.
272. Qi Y, Kong F, Deng Q, Li J, Cui R, Pu Y, et al. Clinical significance and prognostic value of Vav1 expression in Non-small cell lung cancer. American Jounal of Cancer Research. 2015;5(8):2491-17.

273. Lazer G, Katzav S. Guanine nucleotide exchange factors for RhoGTPases: Good therapeutic targets for cancer therapy? Cell Signalling. 2011;23(6):969-79.
274. Sebban S, Farago M, Gashai D, Ilan L, Pikarsky E, Ben-Porath I, et al. Vav1 fine tunes p53 control of apoptosis versus proliferation in breast cancer. PLoS One. 2013;8(1932-6203 (Electronic)).
275. Grassilli S, Brugnoli F, Lattanzio R, Rossi C, Perracchio L, Mottolese M, et al. High nuclear level of Vav1 is a positive prognostic factor in early invasive breast tumors: a role in modulating genes related to the efficiency of metastatic process. Oncotarget. 2014;5:4320-36.
276. Du M, Chen X, Zhou X, Wan Y, Lan B, Zhang C, et al. Estrogen induces Vav1 expression in human breast cancer cells. PLoS ONE. 2014;9(6):e99052.
277. Houlard M, Romero-Portillo F, Germani A, Depaux A, Regnier-Ricard F, Gisselbrecht S, et al. Characterization of VIK-1: a new Vav-interacting Kruppel-like protein. Oncogene. 2005;6(24):28-38.
278. Urrutia R. KRAB-containing zinc-finger repressor proteins. Genome Biol. 2003;4(10):231.
279. Morgan A, Rubenstein E. Proline: The Distribution, Frequency, Positioning, and Common Functional Roles of Proline and Polyproline Sequences in the Human Proteome. PLoS ONE. 2013.
280. Crook T. Unpublished data.
281. Livak K, Schmittgen T. Analysis of relative gene expression data using real-time quantitative PCR and the 2(-Delta Delat C(T)) Method. Methods. 2001;25(4):402-8.
282. Bustin S, Benes V, Garson J, Hellemans J, Huggett J, Kubista M, et al. The MIQE Guidelines: Minimum Information for Publication of Quantitative Real-Time PCR experiments. Clinical Chemistry. 2009;55(4):611-22.
283. Trapnell C, Pachter L, Salzberg S. Top-Hat: discovering splice junctions with RNA-seq. Bioinformatics. 2009;25(9):1105-11.
284. Anders S, Pyl P, Huber W. HTSeq- a python framework to work with high-throughput sequencing data. Bioinformatics. 2015;31(2):166-9.
285. Ritchie M, Phipson B, Wu D, Law C, Shi W, Smyth G. Limma powers differential expression analyses for RNA-sequencing and microarray studies. Nucleic Acids Research 2015;43(7):e47.
286. Benjamini Y, Hochberg Y. Controling the false discovery rate: a practical and powerful approach to multiple testing. Stat Soc Ser B. 1995;57:289-300.
287. Biosystems A. Methylation Analysis by Bisulfite Sequencing: Chemistry, Products and Protocols from Applied Biosystems. 2007.
288. Brünner N, Boysen B, Jirus S, Skaar T, Holst-Hansen C, Lippman J, et al. MCF7/LCC9: an antiestrogen-resistant MCF-7 variant in which acquired resistance to the steroidal antiestrogen ICI 182,780 confers an early cross-resistance to the nonsteroidal antiestrogen tamoxifen. Cancer Research. 1997;57(16):3486-93.
289. Tolhurst R, Thomas R, Kyle F, Patel H, Periyasamy M, Photiou A, et al. Transient over-expression of estrogen receptor-α in breast cancer cells promotes cell survival and estrogen-independent growth. Breast Cancer Res Treat. 2011;128(2):357-68.
290. TCGA Research Network. [Available from: http://cancergenome.nih.gov/.
291. Quandt K, Frech K, Karas H, Wingender E, Werner T. MatInd and MatInspector: new fast and versatile tools for detection of consensus matches in nucleotide sequence data. Nucleic Acids Research. 1995;23:4878-84.

292. Suzuki J, Imansishi E, Nagata S. Exposure of phosphatidylserine by Xk-related protein family members during apoptosis. J Biol Chem. 2014;289(44):30257-67.
293. Chaitanya G, Alexander J, Babu P. PARP-1 cleavage fragments: signatures of cell-death proteases in neurodegeneration. Cell Commu Signal. 2010;8(31).
294. Gamsjaeger R, Liew C, Loughlin F, Crossley M, Mackay J. Sticky fingers: zinc-fingers as protein-recognition motifs. Trends in Biochemiscal Sciences. 2007;32(2):63-70.
295. .
296. Yang K, Hitomi M, Stacey D. Variations in cyclin D1 levels through the cell cycle determine the proliferative fate of a cell. Cell Division. 2006;1(32).
297. Maier T, Guell M, Serrano L. Correlation of mRNA and protein in complex biological samples. FEBS Letters. 2009;583(24):3966-73.
298. Vogel C, Marcotte E. Insights into the regulation of protein abundance from proteomic and transcriptomic analyses. Nature Reviews Genetics. 2013;13(4):227-32.
299. Cooper S, Shedden K. Microarrays and the relationship of mRNA variation to protein variation during the cell cycle. Journal of Theoretical Biology. 2007;249(3):574-81.
300. Tanguay R, Gallie D. Translational efficiency is regulated by the length of the 3' untranslated region. Molecular Cell Biology. 1996;16(1):146-56.
301. Sandberg R, Neilson J, Sama A, Sharp P, Burge C. Proliferating cells express mRNAs with shortened 3' untranslated regions and fewer microRNA target sites. Science. 2008;320(5883):1643-7.
302. Han L, Witmer P, Casey E, Valle D, Sukumar S. DNA methylation regulates microRNA expression. Cancer Biology & Therapy. 2007;6(8):1284-8.
303. Wu L, Zhaou H, Zhang Q, Zang J, Ni F, Liu C, et al. DNA Methylation Mediated by a MicroRNA Pathway. Molecular Cell. 2010;38(3):465-74.
304. Huang J, Wang Y, Guo Y, Sun S. Down-regulated microRNA-152 induces aberrant DNA methylation in hepatitis B virus-related hepatocellular carcinoma by targeting DNA methyltransferase Hepatology. 2010;52(1):60-70.
305. Sinha D, Adler A, Field Y, Chang H, Segal E. Systematic functional characterization of cisregulatory motifs in human core promoters. Genome Research. 2008;18(3):477-88.
306. Boosani C, Agrawal D. Methylation and microRNA-mediated epigenetic regulation of SOCS3. Mol Biol Rep. 2015;42:853-72.
307. Barclay J, Anderson S, Waters M, Curlewis J. SOCS3 as a tumor suppressor in breast cancer cells, and its regulation by PRL. Int J Cancer. 2009;124(8):1756-66.
308. Akaogi K, Nakajima Y, Ito I, Kawasaki S, Oie Sh, Murayama A, et al. KLF4 suppresses estrogen-dependent breast cancer growth by inhibiting the transcriptional activity of ERalpha. Oncogene. 2009;13(28):2894-902.
309. Guo P, Dong X, Zhao K, Sun X, Li Q, Dong J. Estrogen-induced interaction between KLF5 and estrogen receptor (ER) suppresses the function of ER in ER-positive breast cancer cells. Int J Cancer. 2010;126(1):8189.
310. Hu D, Zhou Z, Davidson N, Huang Y, Wan Y. Novel insight into KLF4 proteolytic regulation in estrogen receptor signaling and breast carcinogenesis. . J Biol Chem. 2012;287:13584-97.
311. Carroll J, Meyer C, Song J, Li W, Geislinger T, Eeckhoute J, et al. Genome-wide analysis of estrogen receptor binding sites. Nature Genetics. 2006;38(11).
312. Ross-Innes C, Stark R, Teschendorff A, Holmes K, Ali R, Dunning M, et al. Differential oestrogen receptor binding is associated with clinical outcome in breast cancer. Nature. 2012;481:389-93.

313. Hurtado A, Holmes K, Ross-Innes C, Schmidt D, Carroll J. FoxA1 is a key determinant of estrogen receptor function and endocrine response. Nature Genetics. 2011;43(1):27-33.
314. Tong D, Czerwenka K, Heinze G, Ryffel M, Schuster E, Witt A, et al. Expression of KLF5 is a prognostic factor for disease-free survival and overall survival in patients with breast cancer. Clinical Cancer Research. 2006;12(8):2442-8.
315. Meyer S, Hasenstein J, Baktula A, Velu C, Xu Y, Wan H, et al. Kruppel-like factor 5 is not required for K-RasG12D lung tumorigenesis, but represses ABCG2 expression and is associated with better disease-specific survival. Americal Journal of Pathology. 2010;177:1503-13.
316. Wei D, Gong W, Kanai M, Schlunk C, Wang L, Yao J, et al. Drastic down-regulation of Kruppel-like factor 4 expression Is critical in human gastric cancer development and progression. Cancer Research. 2005;65(7):2746-54.
317. Zammarch iF, Morelli M, Menicagli M, Di Cristofano C, K Z, Paolucci A, et al. KLF4 is a novel candidate tumor suppressor gene in pancreatic ductal carcinoma. Americal Journal of Pathology. 2011;178(1):361-72.
318. Foster K, Liu Z, Nail C, Li X, Fitzgerald T, Bailey S, et al. Induction of KLF4 in basal keratinocytes blocks the proliferation-differentiation switch and initiates squamous epithelial dysplasia. Oncogene. 2005;24(9):1491-500.
319. Foster K, Frost A, McKie-Bell P, Lin C, Engler J, Grizzle W, et al. Increase of GKLF messenger RNA and protein expression during progression of breast cancer. Cancer Research. 2000;60:6488-95.
320. Rowland B, Bernards R, Peeper D. Nuclear localization of KLF4 is associated with an aggressive phenotype in early-stage breast cancer. Nature Cell Biology. 2005;7(11):1074-82.
321. Pandya A, Talley L, Frost A, Fitzgerald T, Trivedi V, Chakravarthy M, et al. Nuclear localization of KLF4 is associated with an aggressive phenotype in early-stage breast cancer. . Clinical Cancer Research. 2004;10:2709-19.
322. Ray A, James M, Larochelle S, Fisher R, Blain S. p27Kip1 Inhibits Cyclin D-Cyclin-Dependent Kinase 4 by Two Independent Modes. Molecular and Cellular Biologys. 2009;29(4):986-99.
323. Lukas J, Herzinger T, Hansen K, Moroni M, Resnitzky D, Helin K, et al. Cyclin E-induced S phase without activation of the pRb/E2F pathway. Genes and Development. 1997;11:1479-92.
324. Beier R, Bürgin A, Kiermaier A, Fero M, Karsunky H, Saffrich R, et al. Induction of cyclin E–cdk2 kinase activity, E2F-dependent transcription and cell growth by Myc are genetically separable events. EMBO J. 2000;19(21):5813-23.
325. Narla G, Heath KE-, Reeves H, Li D, Giono LE, Kimmelman AC, et al. KLF6, a candidate tumor suppressor gene mutated in prostate cancer. Science. 2001;294(5551):2563-6.
326. Javle M, Curtin N. The role of PARP in DNA repair and its therapeutic exploitation. British Journal of Cancer. 2011;105:1114-22.
327. Martinez-Marignac V, Rodrigue A, Davidson D, Couillard M, Al-Moustafa A, Abramovitz M, et al. The Effect of a DNA Repair Gene on Cellular Invasiveness: Xrcc3 Over-Expression in Breast Cancer Cells. PLoS ONE. 2011;6(1).
328. Sand-Dejmek J, Adelmant G, Sobhian B, Calkins A, Marto J, Iglehart D, et al. Concordant and opposite roles of DNA-PK and the "facilitator of chromatin transcription" (FACT) in DNA repair, apoptosis and necrosis after cisplatin. Molecular Cancer. 2011;10(74):2-11.

329. Calo E, Flynn R, Martin L, Spitale R, Chang H, Wysocka J. RNA helicase DDX21 coordinates transcription and ribosomal RNA processing. Nature. 2015;518:249-53.
330. Goldsteina M, Derheimera F, Tait-Muldera J, Kastana M. Nucleolin mediates nucleosome disruption critical for DNA double-strand break repair. PNAS. 2013;110(42):16874-9.
331. Norbury C, Zhivotovsky B. DNA damage-induced apoptosis. Oncogene. 2004;2797-2808.
332. Eberharter A, Becker P. Histone acetylation: a switch between repressive and permissive chromatin. EMBO reports. 2002;3(3):224-9.
333. Hayes E, Lewis-Wanbi J. Mechanisms of endocrine resistance in breast cancer: an overview of the proposed roles of noncoding RNA. Breast Cancer Research. 2015;17(1):40-53.
334. Agarwal V, Bell G, Nam J, Bartel D. Predicting effective microRNA target sites in mammalian mRNAs. eLIFE. 2015;4(e05005).
335. Taylor M, Sossey-Alaoui K, hompson C, Danielpour D, Schiemann W. TGF-β upregulates miR-181a expression to promote breast cancer metastasis. Journal of Clinical Investigation. 2013;123(1):150-63.
336. Niu J, Xue A, Chi Y, Xue J, Wang W, Zhao Z, et al. Induction of miRNA-181a by genotoxic treatments promotes chemotherapeutic resistance and metastasis in breast cancer. Oncogene. 2016;35:1302-13.